DESIGN OF A REGENERATIVE BRAKING SYSTEM FOR RETROFITTED ELECTRIC VEHICLES

E076514

SAHARAT CHANTHANUMATAPORN

เลขหมู่.....
เลขทะเบียน 76514
วัน เดือน ปี 25 ส.ค. 2557
.b.....
.i.....

A THESIS SUBMITTED IN PARTIAL FULFILLMENT

OF THE REQUIREMENT FOR THE DEGREE OF

MASTER OF ENGINEERING IN AUTOMOTIVE ENGINEERING

(INTERNATIONAL PROGRAM)

INTERNATIONAL COLLEGE

KING MONGKUT'S INSTITUTE OF TECHNOLOGY LADKRABANG

2013

KMITL-2013-IC-M-004-003

This material is reserved for educational use only, not allowed for commercial use.
Forbidden to modify the content, and cite the document when use.

COPYRIGHT 2013

INTERNATIONAL COLLGE

KING MONGKUT'S INSTITUTE OF TECHNOLOGY LADKRABANG

NATIONAL SCIENCE AND TECHNOLOGY DEVELOPMENT AGENCY

This material is reserved for educational use only, not allowed for commercial use.

Forbidden to modify the content, and cite the document when use.

APPROVAL SHEET

This material is reserved for educational use only, not allowed for commercial use.

Thesis	Design of a Regenerative Braking System for Retrofitted Electric Vehicles
Student	Mr.Saharat Chanthanumataporn
Student ID.	53600902
Degree	Master of Engineering
Program	Automotive Engineering (International Program)
Year	2013
Thesis Advisor	Asst. Prof. Dr. Monsak Pimsarn Dr. Sarawut Lerspalungsanti Assoc. Prof. Masaki YAMAKITA Dr. Sittikorn Lapapong

ABSTRACT

A problem of retrofitted electric vehicles is the limitation of co-performing a regenerative brake with the conventional system. To solve this, a brake force management system is required. In the previous studies, there primarily are two concepts, which are series and parallel regenerative braking scheme. The disadvantages of series scheme are that it is suitable only for a front-rear split brake layout and it requires a great deal of modification effort. The drawbacks of parallel scheme are an insufficient energy recovery efficiency, a low level of ride comfort during braking, and a risk of wheel-locking situation.

Therefore, this thesis proposes the innovative scheme that can resolve the former problems. The working principle is to perform the regenerative brake at its full capacity and to maintain the overall braking force to be similar to the driver's brake demand by utilizing a unique feature of an anti-lock braking system (ABS). To achieve this during a brake situation, an emulated "wheel lock-up" signal is sent to the ABS control unit to decrease the mechanical brake force until the amount of reduced force is equal to the provided regenerative one.

This material is reserved for educational use only, not allowed for commercial use.
Forbidden to modify the content, and cite the document when use.

The idea of the proposed scheme is verified by means of field tests. The emulated "wheel lock-up" signal is sent into the ABS control unit to investigate brake pressure characteristics. The results show the ABS capability of controlling the brake pressure. Based on the results, the feasibility of the proposed scheme is confirmed.

Computational analysis is adopted to predict the performance of the proposed scheme. The reference criteria are recovery efficiency, safety, and ride comfort during braking. The proposed scheme is benchmarked against the ABS-equipped conventional braking system, the parallel scheme, and the modified parallel scheme. The mathematical modeling of this study is formulated in MATLAB/Simulink and its accuracy is verified by field experiments.

In conclusion, the proposed scheme can solve the disadvantages of the previous studies. As for the problems of the series scheme, the proposed scheme can be used for both the cross-link brake layout and the front-rear split one. Moreover, it requires only minor modification. Compared with the parallel schemes, it provides the higher recovery efficiency, the greater brake force distribution, and the better passenger ride comfort during braking.

King Mongkut's Institute of Technology Ladkrabang

This material is reserved for educational use only, not allowed for commercial use.
Forbidden to modify the content, and cite the document when use.

ACKNOWLEDGEMENT

The study was a scholarship in automotive engineering program under Thailand Advanced Institute of Science and Technology, Tokyo Institute of Technology (TAIST-Tokyo Tech), and Thailand Graduate Institute of Science and Technology (TGIST). This program is a collaboration of National Science and Technology Development Agency (NSTDA), Thailand, Tokyo Institute of Technology (Tokyo Tech), Japan, and King Mongkut's Institute of Technology Ladkrabang (KMITL), Thailand. This study has been conducted during the year 2010-2013 as a part of a research project in the Automotive Laboratory, National Metal and Materials Technology Center (MTEC), Thailand.

I would like to express my sincerest thanks and appreciation to my major advisors, Dr. Sarawut Lerspalungsanti and Dr. Sittikorn Lapapong, Automotive Laboratory MTEC, Assistant Professor Dr. Monsak Pimsarn, department of Mechanical Engineering, KMITL and Associate Professor Dr. Masaki Yamakita, department of Mechanical and Control Engineering, Tokyo Tech, for his generous support, technical guidance, and encouragement all the time during the research. I would like to thank Mr. Sikharin Sorachot and all members in Automotive Laboratory for their technical support, guidance, and equipment. In addition, I would like to extend my appreciation to Mr. Suphakrit Koocharoenprasit, Mr. Dittapoom Shinabuth, Mr. Mahassajun Suwancharoen, Mr. Chatchawan Lakkhananukun, Mr. Ronnachai Sutthisung, Mr. Paran Chuvichit, Mr. Teetiwachara Ngiumsa-nga, and all TAIST-Tokyo Tech members for their technical supports and helps.

Finally, I would like to give this success to my mother and my father who always stand by me with encouragement and financial support.

Saharat Chanthanumataporn

July 2013

This material is reserved for educational use only, not allowed for commercial use.
Forbidden to modify the content, and cite the document when use.

TABLE OF CONTENTS

This material is reserved for educational use only, not allowed for commercial use.
Forbidden to modify the content, and cite the document when use.

TABLE OF CONTENTS (CONT.)

This material is reserved for educational use only, not allowed for commercial use.
Forbidden to modify the content, and cite the document when use.

TABLE OF CONTENTS (CONT.)

This material is reserved for educational use only, not allowed for commercial use.
Forbidden to modify the content, and cite the document when use.

LIST OF TABLES

Table Page

King Mongkut's Institute of Technology Ladkrabang

This material is reserved for educational use only, not allowed for commercial use.
Forbidden to modify the content, and cite the document when use.

LIST OF FIGURES

Figure Page

This material is reserved for educational use only, not allowed for commercial use.
Forbidden to modify the content, and cite the document when use.

LIST OF FIGURES (CONT.)

This material is reserved for educational use only, not allowed for commercial use.
Forbidden to modify the content, and cite the document when use.

LIST OF FIGURES (CONT.)

Figure Page

This material is reserved for educational use only, not allowed for commercial use.
Forbidden to modify the content, and cite the document when use.

LIST OF FIGURES (CONT.)

Figure Page

This material is reserved for educational use only, not allowed for commercial use.
Forbidden to modify the content, and cite the document when use.

CHAPTER 1

INTRODUCTION

1.1 Background

As currently known, the global warming has increasingly become an important worldwide issue. It is believed that its cause is the increase of concentrations of greenhouse gases in the Earth's atmosphere. Examples of the greenhouse gases are carbon dioxide, nitrous oxide, etc. From the examples, one can obviously determine that one of the primary sources of these greenhouse gas emissions is the burning of fossil fuels, particularly automobile emissions. Thus, one way to mitigate this global-warming issue is to reduce the amount of the greenhouse gases emitted to the atmosphere. Changes of use from Combustion-Engine (CE) vehicles to electrical ones may be one of the possible solutions to help alleviating this issue, since an Electric Vehicle (EV) virtually has zero emission.

Typically, a production EV is manufactured with a braking system that not only provides a braking force but also can recover some energy during braking, and this system is called a regenerative braking system. In this system, a propelling motor of an EV can function as an electrical generator converting braking energy into electrical one that can be stored in an energy storage device or used in electrical applications [1]. It can be concluded that regenerative braking systems are able to make EVs more efficient. Past researches show that by using recovered energy, an EV can extend its working or drivable range in a single charging. Further, a Hybrid Electric Vehicle (HEV) can improve its fuel economy, especially for the vehicle that mainly runs in traffic jam areas or frequently start/stop driving conditions [2]. Moreover, past researches suggested that an EV's driving range in urban could be extended between 14 and 40% by adding the regenerative brake [3], [4].

This material is reserved for educational use only, not allowed for commercial use.
Forbidden to modify the content, and cite the document when use.

1.2 Problem Statement

In some countries, especially developing countries, the use of EVs is still not widespread and not affordable due to its high cost. Therefore, there is an idea to study the retrofit of a combustion-engine production car to be an electric one. However, conventional braking systems of retrofitted EVs, conventional hydraulic, are not designed for co-working with a regenerative brake. Further, it is not possible to remove the conventional braking system and use only the regenerative brake with the following reasons. In emergent braking situation, only a regenerative brake cannot provide the enough brake force to stop a car. In addition, the regenerative braking system cannot operate all times since it is necessary to stop working in some situation, for instance during high battery voltage and/or temperature. To solve the above problems, a brake force management system is required. In previous studies, there primarily are two brake force management concepts, series regenerative scheme and parallel regenerative scheme. The disadvantages of series scheme are that it requires a great deal of modification effort and it is suitable only for a front-rear split brake layout. However, more modern passenger cars are equipped with the cross-link circuit brake layout. The drawbacks of parallel scheme are an insufficient energy recovery efficiency, a low level of ride comfort during braking, and a risk of wheel-locking situation. Consequently, it is necessary to develop a brake force control scheme for retrofitted EVs, which is free from the disadvantages of the previous studies.

1.3 Objectives

- To develop a reliable regenerative braking system for retrofitted Electric Vehicles (EVs), which allows
    - simplification of vehicle modification
    - enhancement of regenerative energy efficiency
    - compatibility with both cross-link and front-rear split circuit brake layout
- To validate, investigate, and analyze the performance of the proposed regenerative braking system

This material is reserved for educational use only, not allowed for commercial use.
Forbidden to modify the content, and cite the document when use.

1.4 Scopes

- To introduce a regenerative braking system for retrofitted EVs. In this thesis, the retrofitted EV is developed from a conventional car, Toyota Vios/Honda Jazz model year 2009
- To verify the feasibility of the proposed concept by field experiments
- To develop a mathematical model of the proposed regenerative braking system by using MATLAB/Simulink
- To investigate and validate the mathematical model by field experiments
- To investigate and analyze the performance of the proposed system by the verified mathematical model

1.5 Overview of Regenerative Design Procedure

The procedure of regenerative design is organized into six processes as shown in Figure 1.1 and summarized as followed:

Literature review

The fundamentals of the conventional braking systems and the regenerative braking systems are studied and concluded. Moreover, the concepts of the previous studies are reviewed. This review focuses on the integration approaches of the regenerative brake on retrofitted EVs and the verification methodologies for the regenerative braking systems.

Proposing regenerative braking system

The proposed regenerative braking system is developed and proposed. This process focuses on developing the regenerative integration approaches and the brake force management algorithm. The design criteria of proposed scheme are effective performance, compatibility with both cross-link and front-rear split circuit brake layout, and simplification of vehicle modification.

Proof of concept

The feasibility of the proposed scheme is verified by field tests. The emulated "wheel lock-up" signal is sent into the ABS to investigate the characteristics of brake pressure. The test

This material is reserved for educational use only, not allowed for commercial use.
Forbidden to modify the content, and cite the document when use.

conditions are set at various initial velocities and brake force demands to verify the feasibility of the proposed scheme at all braking conditions.

Mathematical modeling and verification

The mathematical modeling of the proposed regenerative braking scheme, the ABS-equipped conventional braking system, the parallel regenerative scheme, and the modified parallel regenerative scheme are formulated in MATLAB/Simulink. In addition, the accuracy of the mathematical model is verified by the results obtained from field tests.

Performance prediction

The proposed scheme is benchmarked against the ABS-equipped conventional brake, the parallel scheme, and the modified parallel scheme. The reference criteria are recovery efficiency, safety, and ride comfort during braking.

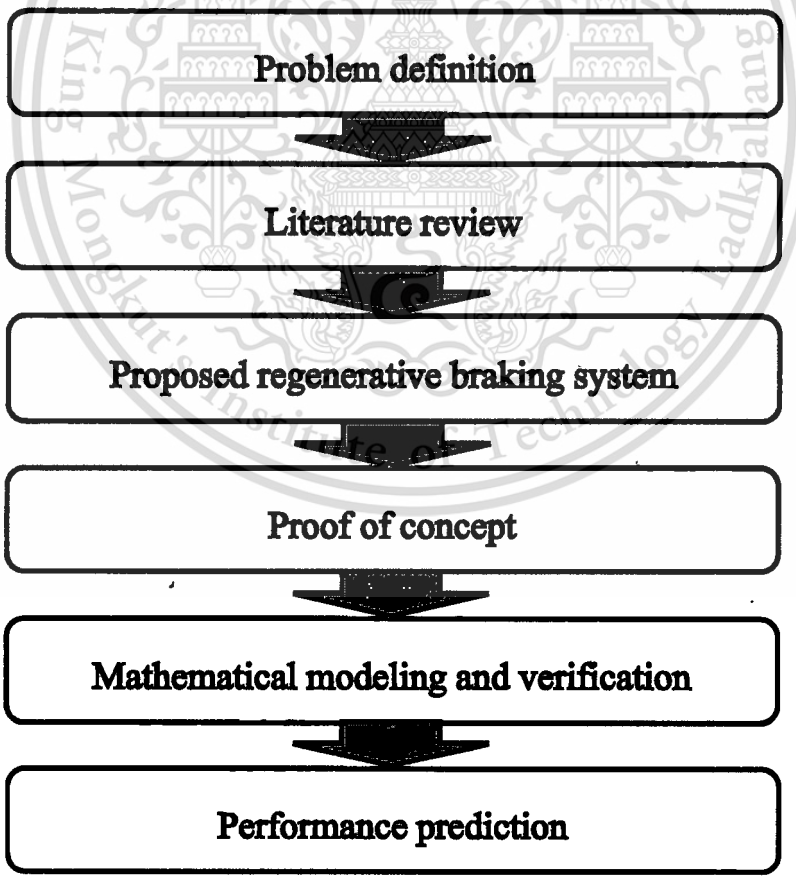

Figure 1.1 Systematic procedure of regenerative braking design

This material is reserved for educational use only, not allowed for commercial use.
Forbidden to modify the content, and cite the document when use.

1.6 Thesis Outlines

This thesis is divided into 5 Chapters. The contents are summarized as followed:

Chapter 1: Introduction

This chapter introduces the general background of regenerative braking system, the problem statement, the objectives, the scopes, and the design procedure.

Chapter 2: Literature Reviews

This chapter reviews the idea used for designing and investigating the proposed system. It is divided into 4 main headings, the fundamental of conventional braking systems, the fundamental of regenerative braking systems, the integration scheme for the regenerative braking systems in retrofitted EV, and the verification methodologies for regenerative braking system.

Chapter 3: Modeling and Verification

This chapter explains the details of the proposed regenerative scheme, the proof of concept, the experimental setup, the mathematical modeling, and the verification of mathematical model.

Chapter 4: Results and Discussions

This chapter presents the reliable simulation results and discussions. The characteristic of regenerative braking scheme, the braking distance, the regenerative efficiency, and the longitudinal load transfer of the proposed scheme is compared with those of the ABS-equipped conventional braking system, the parallel scheme, and the modified parallel scheme.

Chapter 6: Conclusions and Suggestions

This chapter provides the comprehensive conclusions of this thesis and some beneficial suggestions for further research.

This material is reserved for educational use only, not allowed for commercial use.
Forbidden to modify the content, and cite the document when use.

CHAPTER 2

LITERATURE REVIEWS

2.1 Fundamental of Conventional Braking Systems

Retrospectively around eighty years ago, the braking systems of passenger cars do not show more progress than they should be [22] since they were well trusted that the most efficient approach is to utilize the hydraulic systems for transmitting the driver foot-pedal force to the brake module of each wheel. The principle of hydraulic brake system is to convert a driver force into a hydraulic pressure. Then, this pressure is transferred into each braking generator. A caliper brake and a drum brake, a braking generator, are responsible for transforming the hydraulic pressure into brake torque to retard the wheels rotation [20].

2.1.1 Brake Circuit Layout

To solve the malfunction problem of the hydraulic brake force transmission system in a conventional braking system, the modern hydraulic brake force transmission systems is dual-circuit brake system in order to have a spare one in case of one circuit failure. For passenger cars, there are two common types of brake circuit layout, front-rear split and cross-link circuit as shown in Figure 2.1. The disadvantage of front-rear split circuit is the insufficiency of provided brake force if the front circuit fails. Generally, the brake force distribution between front and rear wheels is the ratio 2:1. Thus, if the front circuit is malfunction, the rear brake can provide only one-third of the original braking capacity [22]. For the cross-link circuit type, the diagonal split design is done to enable the brake force to be equally shared between each hydraulic circuit. Therefore, each circuit has the same braking capacity and the ratio of front-real brake force distribution does not influence the ability to stop [22].

This material is reserved for educational use only, not allowed for commercial use.
Forbidden to modify the content, and cite the document when use.

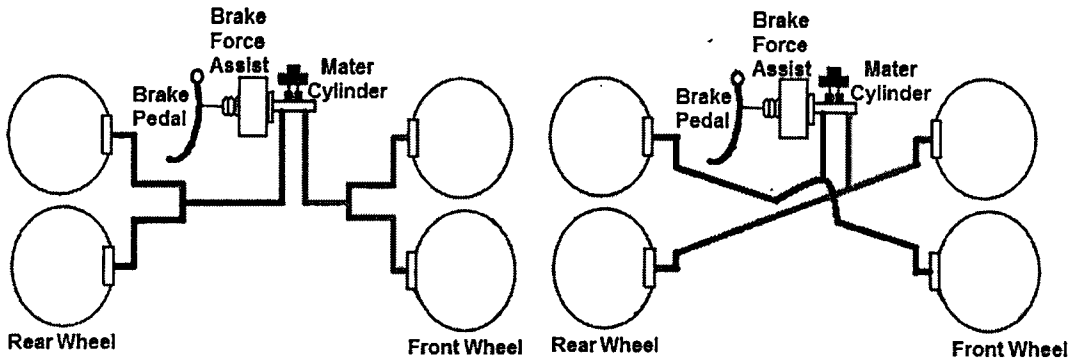

Figure 2.1 Brake circuit layout, front-rear split circuit (Left) and cross-link circuit (Right)

2.1.2 Antilock Brake Systems (ABS)

The noticeable function of the braking systems is to reduce the vehicle speed or stop the vehicle. In addition, the brake braking systems must maintain the vehicle's directional stability simultaneously with performing its function. The braking systems must avoid the wheel locking up situation that causes two negative effects. Firstly, a braking distance increases if a wheel is locked with the reason that the longitudinal coefficient of friction is lower, thus decreasing the generated braking force. Secondly, the locked wheel cannot generate much lateral force. Therefore, the steering on the locked front wheels cannot be controlled. Furthermore, the locked rear wheels make the vehicle unstable for the reason that the locked rear wheels cannot resist the rapid change in the yaw velocity induced by steering inputs [23].

Once a driver presses the brake pedal, the rotating wheel is decelerated in relation with the road surface. This deceleration causes a slip between road and tire, and this slip generates the braking forces on the vehicle. As the driver increases the brake requirement, the slip increases and thus the higher braking force is generated. However, this increment is restricted by the static friction coefficient between road and tire. If slip is beyond the stable range of friction coefficient, it uncontrollably increases. At 100% slip, the wheel locking up occurs and the friction coefficient between tire and road is in unstable zone [23]. The wheel slip's behavior is shown in Figure 2.2. Wheel slip generally is defined as a non-unit percentage and is given by

This material is reserved for educational use only, not allowed for commercial use.
Forbidden to modify the content, and cite the document when use.

$$\text{Slip}(\%) = \frac{v - r\omega}{v} \times 100 \qquad (2.1)$$

Where V = vehicle velocity (m/s)

r = wheel radius (m)

ω = angular velocity of wheel (rad/s)

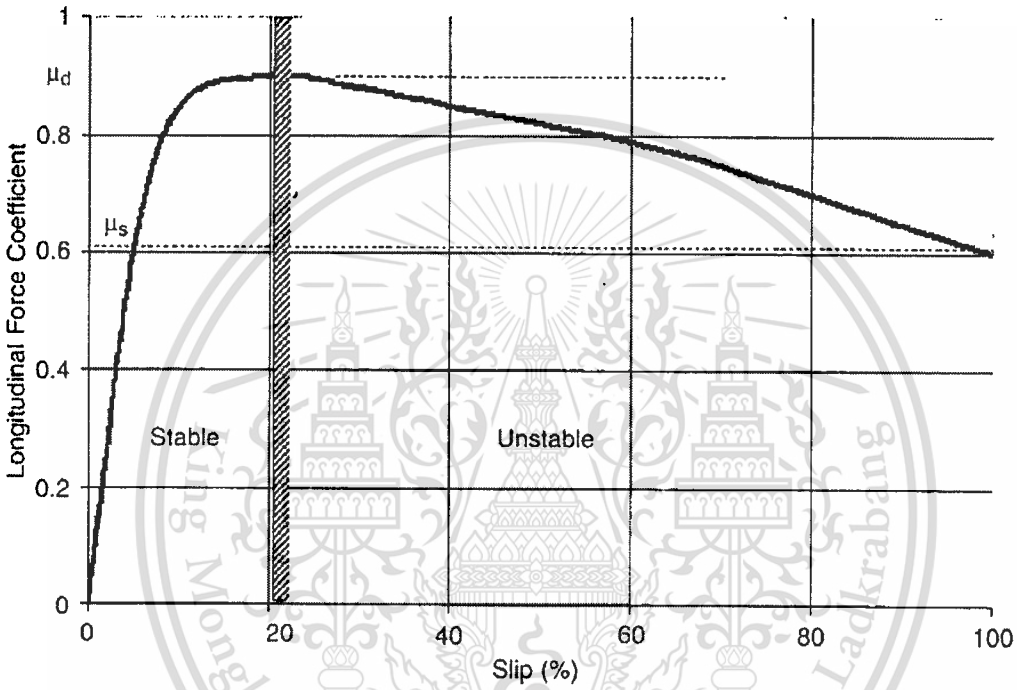

Figure 2.2 Longitudinal coefficient of friction vs. Slip (%) [SAE J2246 (1992)]

The function of antilock brake systems (ABS) is to maintain the tractive contact of the braking wheel with road surface. The ABS monitors the wheel locking-up and immediately diminishes braking pressure of the affected wheel. Under most circumstances, The ABS can shorten stopping distance by retaining the tire-road interaction at the maximum friction coefficient. Moreover, the significant advantage of preventing wheel locking is that the vehicle can keep its maneuverability throughout braking. Figure 2.3 shows a plot of brake pressure, wheel velocity, and slip for a wheel while The ABS is operated. As shown in Figure 2.3, the wheel slip increases linearly with the brake pressure until the coefficient of friction exceeds the static range,

This material is reserved for educational use only, not allowed for commercial use.
Forbidden to modify the content, and cite the document when use.

after which the wheel slip then swiftly increases. At that time, The ABS senses this increase and reduces the brake pressure making the wheel speed increases to prevent the wheel lock-up. As soon as the system detects that the wheel is rolling again, brake pressure is reapplied, and the process repeats itself [23].

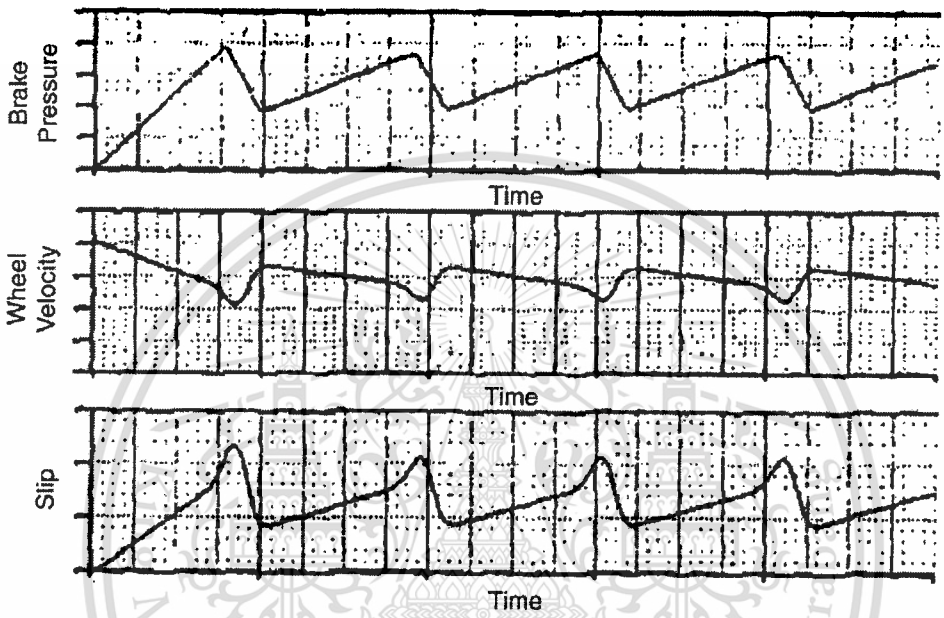

Figure 2.3 Antilock brake system (ABS) response for a single wheel [SAE J2246 (1992)]

Typically, The ABS composes of three mains components; wheel speed sensor, control unit, and modulator. The ABS control unit monitors the wheel locking-up by acquiring the signal of wheel speed sensors and sends a control signal to the modulator. The ABS modulator is responsible for regulating the brake fluid pressure. It is normally installed between the master cylinder and the braking generator as illustrated in Figure 2.4. The brake pressure of each wheel is independently controlled; one channel for each wheel. The main components of the ABS modulator are inlet solenoid valve, outlet solenoid valve, reservoir, motor pump, and damping chamber. The ABS modulator can operate in three modes; pressure intensifying, pressure retaining, and pressure reducing by controlling the solenoid valves and the motor pump as shown in Table 2.1.

This material is reserved for educational use only, not allowed for commercial use.
Forbidden to modify the content, and cite the document when use.

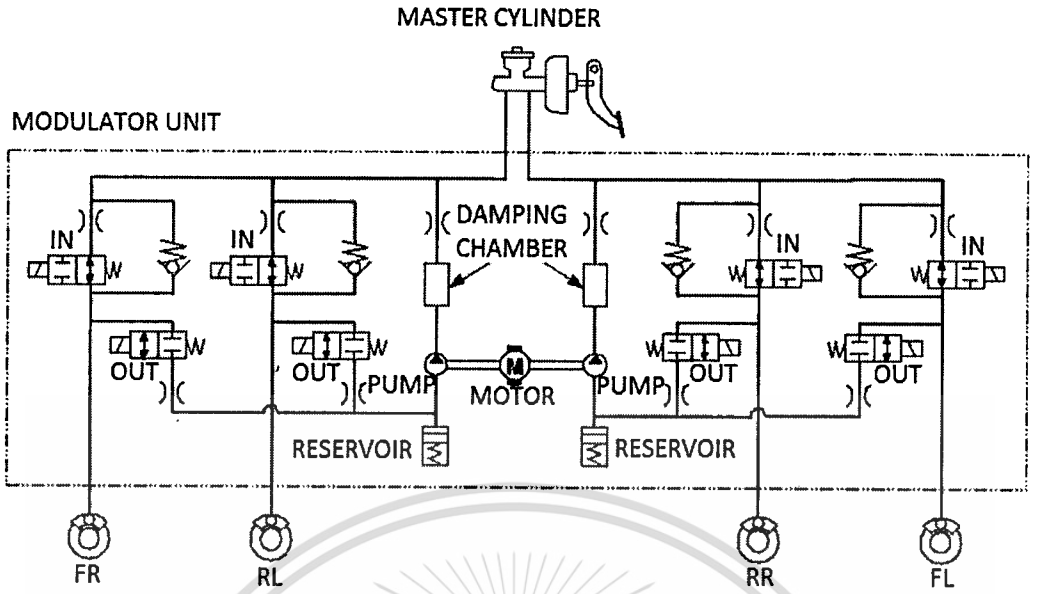

Figure 2.4 ABS modulator [26]

Table 2.1 Solenoid valve and brake fluid status of each ABS mode [26]

Mode	Inlet Solenoid Valve	Outlet Solenoid Valve	Brake Fluid
Pressure intensifying mode	Open	Closed	Master cylinder fluid is pumped out to the caliper.
Pressure retaining mode	Closed	Closed	Caliper fluid is retained by the inlet and outlet valves.
Pressure reducing mode	Closed	Open	● Caliper fluid flows through the outlet valve to the reservoir. ● The motor pumps the reservoir fluid through the damping chamber to the master cylinder

This material is reserved for educational use only, not allowed for commercial use.
Forbidden to modify the content, and cite the document when use.

2.1.3 Vehicle Dynamics during Braking

The dynamics as a vehicle is braking can be considered by using the dynamic free-body diagram shown in Figure 2.5. Starting from the static weight distribution of a car is given by equation 2.2 and 2.3.

$$\text{Weight on the front axle} = W_f = \frac{mgd}{c+d} \tag{2.2}$$

$$\text{Weight on the rear axle} = W_r = \frac{mgc}{c+d} \tag{2.3}$$

Where m is vehicle mass, g is gravitational constant, and c, d, and h are distance of the center of gravity from front axle, rear axle, and center of gravity height. If a car is braked under steady-state condition, the knowledge of Newton's law can analyze the vehicle dynamics as following equations.

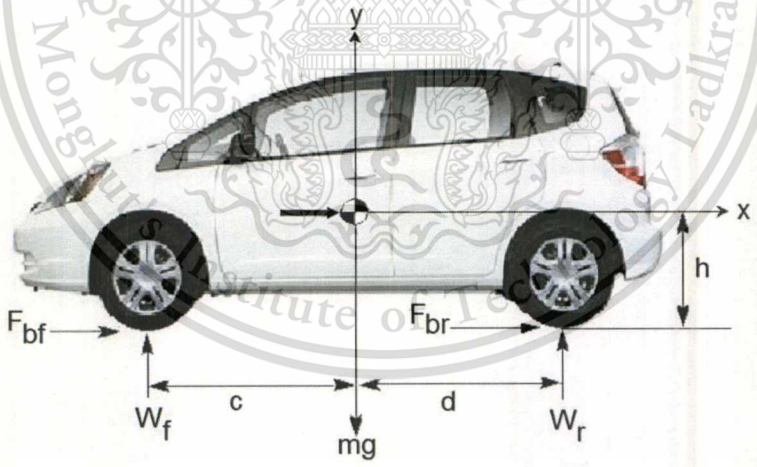

Figure 2.5 Free-body diagram of a car during braking

$$\sum F_x = ma_x = F_{bf} + F_{br} \tag{2.4}$$

$$\sum F_y = 0 = W_f' + W_r' - mg \tag{2.5}$$

This material is reserved for educational use only, not allowed for commercial use.
Forbidden to modify the content, and cite the document when use.

Where a_x is longitudinal deceleration, F_{bf} and F_{br} tire force or braking force of front and rear tires respectively, and W_f' and W_r' are dynamic vertical weight of front and rear axle respectively.

Therefore $$W_r' = mg - W_f' \tag{2.6}$$

$$\sum M_{CG} = 0 = h(F_{bf} + F_{br}) + W_r'(d) - W_f'(c) \tag{2.7}$$

Therefore $$\sum M_{CG} = 0 = ma_x h + W_r'(d) - W_f'(c) \tag{2.8}$$

Equations (2.6) and (2.8) can be merged to determine the dynamic weight on front and rear axle while a car is braking respectively in equation 2.9 and 2.10. In these equations, the first terms on the right sides are the static weight and the second terms are the dynamic weight. In another word, while a vehicle is braking, the weight on front axle increases according to the reducing weight on rear axle due to dynamic principle.

$$W_f' = \frac{mgd}{c+d} + \frac{ma_x h}{c+d} \tag{2.9}$$

$$W_r' = \frac{mgc}{c+d} - \frac{ma_x h}{c+d} \tag{2.10}$$

2.2 Fundamental of Regenerative Braking Systems

One of the most important features of electric vehicles (EVs) and hybrid electric vehicles (HEVs) is their ability to recuperate the significant amounts of braking energy. For regenerative braking, the goal is to recover as much vehicle kinetic/potential energy as possible. The regenerative braking system is not a new concept. The hybrid vehicles of the 1900s used the regenerative braking system. The regenerative braking has been used in trolleys for 100 years; the generated power goes back into the power line. The electric motors in EVs and HEVs can be switched to be the generators to convert the kinetic and potential energy into the electric energy

This material is reserved for educational use only, not allowed for commercial use.
Forbidden to modify the content, and cite the document when use.

that can be stored in the energy storage and used to propel the vehicle again. The comparison of an EV motor/generator function and power flow direction is shown in Figure 2.6.

Different from a regenerative braking system, a conventional braking system is generally a friction braking system, by which braking energy is converted into unrecovered heat. Figure 2.7 shows the comparison between a regenerative braking system and a friction one. Both braking systems do the same function, providing braking force, but they are different in energy converting capability.

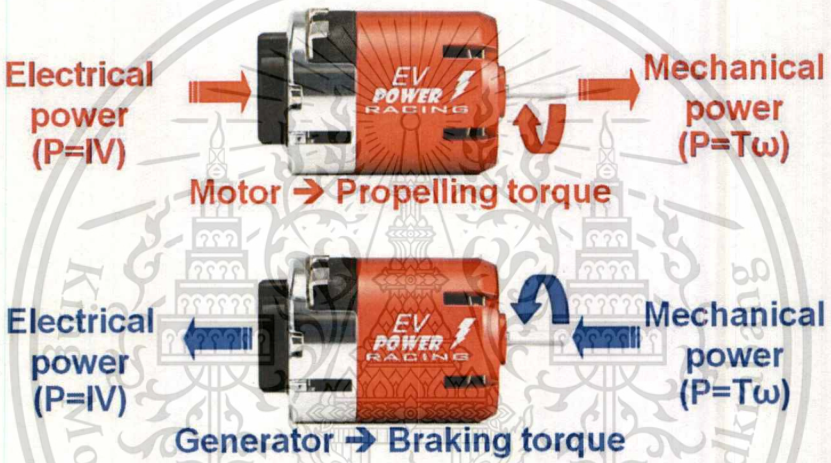

Figure 2.6 Comparison of an EV motor/generator function and power-flow direction

This material is reserved for educational use only, not allowed for commercial use.
Forbidden to modify the content, and cite the document when use.

Figure 2.7 Comparison of regenerative and friction braking system

2.2.1 Potential of Regenerative Energy

Most amount of energy is taken out from a vehicle to stop it. Based on equation 2.11, in the situation of braking a car having 1500 kg from 100 km/h speed until it stops, the braking system consumes energy about 0.16 kWh and dissipates it in heat form. In case of using a braking system, the braking distance is limited about ten meters. However, if this amount of energy is not consumed by the braking system but only by rolling resistance and aerodynamic drag, the vehicle will continuously travel around 2 km as shown in Figure 2.8 [16].

$$E = \frac{1}{2}mv^2 \tag{2.11}$$

In case of the vehicle driving in chronic stop-and-go traffic situation such as urban area, the majority of energy is lost by braking process, resulting in high fuel consumption. Figure 2.9 shows the comparison of overall traction energy, drag and rolling resistance lost energy, and braking energy of 1500 kg passenger car in an FTB 75 urban drive cycle. Table 2.2 presents the lists of Maximum speed, average speed, total traction energy, and energy consumed by drags and

This material is reserved for educational use only, not allowed for commercial use.
Forbidden to modify the content, and cite the document when use.

braking of the 1500 kg passenger car, traveling 100 km in different drive cycles. From Figure 2.9 and Table 2.2, these data show that in the typical urban driving condition a braking energy may reach more than 25 % of total traction energy. In large cities like New York may extend to 70%. Therefore, it would be deserved to recover this lost energy by adopting the effective regenerative brake, which leads to improvement of fuel economy in HEVs and prolongation of driving range in EVs [16].

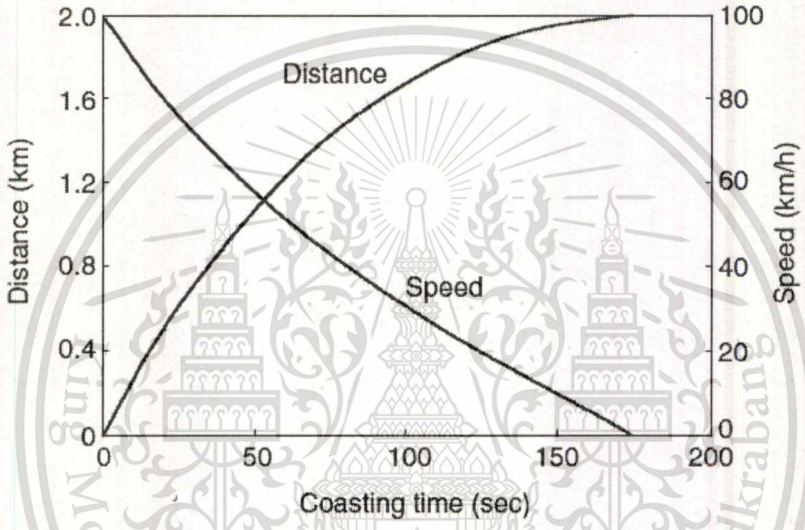

Figure 2.8 Coasting speed and distance [16]

This material is reserved for educational use only, not allowed for commercial use.
Forbidden to modify the content, and cite the document when use.

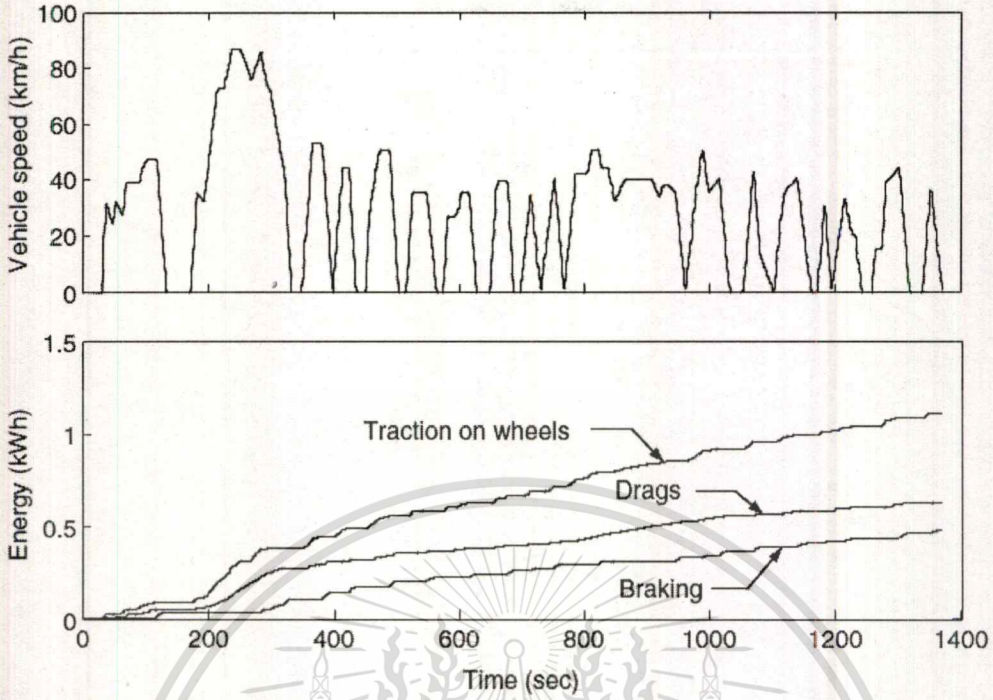

Figure 2.9 Total traction energy and energies consumed by drags and braking in an FTB 75 urban drive cycle [16]

Table 2.2 Maximum speed, average speed, total traction energy, and energies consumed by drags and braking per 100 km traveling distance in different drive cycles [16]

	FTP 75 Urban	FTP 75 Highway	US06	ECE-1	New York City
Maximum speed (km/h)	86.4	97.7	128.5	120	44.6
Average speed (km/h)	27.9	79.3	77.5	49.9	12.2
Total traction energy[a] (kWh)	10.47	10.45	17.03	11.79	15.51
Total energy consumed by drags[a] (kWh)	5.95	9.47	11.73	8.74	4.69
Total energy consumed by braking[a] (kWh)	4.52	0.98	5.30	3.05	10.82
Percentage of braking energy to total traction energy (%)	43.17	9.38	31.12	25.87	69.76

[a]Measured on driven wheels.

This material is reserved for educational use only, not allowed for commercial use.
Forbidden to modify the content, and cite the document when use.

สำนักหอสมุดกลาง พระจอมเกล้าลาดกระบัง

2.2.2 Mechanical/Regenerative Brake Force Management Concept

Generally, it is impossible to use a regenerative brake without the conventional brake in EVs and HEVs. In emergent braking situation, the brake torque demand is much more than the torque that an electric motor can produce. Further, a regenerative braking system cannot operate all times. It is necessary to stop working in some situation, for instance during high battery voltage and/or temperature. In EVs and HEVs, the conventional friction braking systems must coexist with the regenerative braking system. Thus, the proper design for co-operating between friction brake and regenerative brake is a major concern [16], [19]. In the regenerative design process, two significant points have been considered. The first point is a proportion between the regenerative brake and friction bake that can recover the regenerative energy as much as possible. The second matter is the brake force distribution between front and rear wheels that keep the vehicle stable. In the present day, the friction and regenerative brake force management concepts can be mainly classified as series scheme and parallel scheme. Each strategies makes up of pros and cons that will be given more details in next paragraph.

In **Series Regenerative Braking Scheme**, the regenerative brake force is primarily provided at full capacity during all braking process. The friction brake force is flexibly supplied for the rest of brake force demand when the brake force demand exceeds the regenerative capacity or/and when the motor or energy storage can no longer accept more recovered energy [21]. Figure 2.10 shows the distribution between regenerative and friction brake force of series scheme The regenerative brake force increases according to the brake pedal pressure, representing the brake demand, until the limitation of motor or energy storage capacity is reached. After this limitation, the friction brake supplies the rest of brake force demand. The advantage of this scheme is the satisfied regenerative efficiency. However, this scheme must install the addition system for controlling the amount of friction brake force. Since the friction brake force of this scheme is provided by considering the capability of motor and energy storage. This requirement is the disadvantage making this scheme expensive and complicated. In general, the addition friction-

This material is reserved for educational use only, not allowed for commercial use.
Forbidden to modify the content and cite the document when use.
76514

brake-force control system is the brake-by-wire system such as an electro-hydraulic brake (EHB) or an electro-mechanical brake (EMB). Because the brake-by-wire system is a semi-electrical system, many components have to be redesigned, replaced, and inserted in original system. This system also requires more sensors, processors and wiring; all of these increase the cost and complexity of the regenerative system. The details of these systems will be explained in the next section.

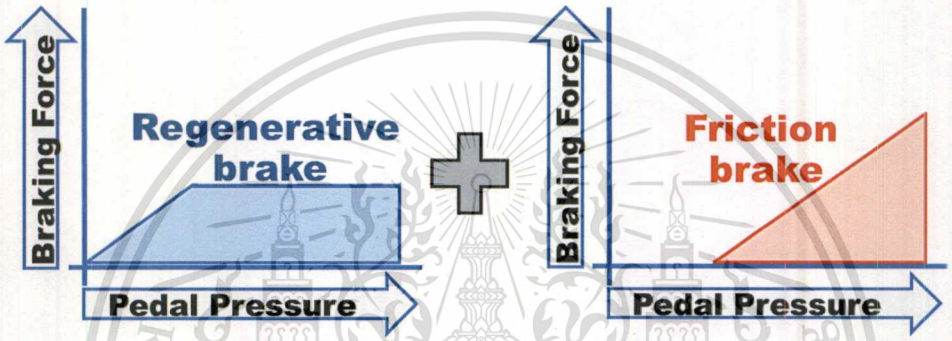

Figure 2.10 Regenerative and friction brake force distribution of series strategy

In **Parallel Regenerative Braking Scheme,** the regenerative brake force is provided in parallel with the friction brake force. The brake force distribution diagram of this scheme is shown in Figure 2.11. The amount of the friction brake force and the regenerative brake force depends on the brake pedal demand. The friction brake force and the regenerative brake force are independent. The main provided brake force is the friction brake force. Therefore, more braking energy of this scheme is lost as heat by friction brake. This scheme offers lower regenerative efficiency than the parallel scheme. Nonetheless, the surpassing advantages are the cost effective and unsophisticated system because this scheme needs only the simple motor controller for the regenerative brake force management [20].

This material is reserved for educational use only, not allowed for commercial use.
Forbidden to modify the content, and cite the document when use.

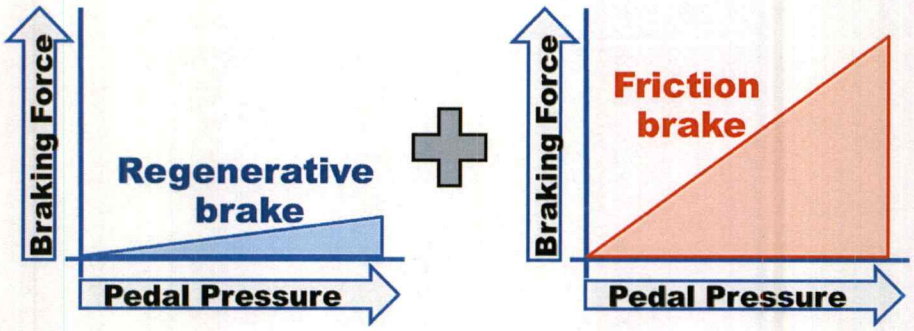

Figure 2.11 Parallel regenerative braking strategy

2.3 Integration Scheme for Regenerative Braking Systems in Retrofitted EVs

This section explained about how to integrate a regenerative brake with the conventional braking system of retrofitted EVs. In this study, the integration methodology is classified by the type of brake force management and the name of integration scheme is called by the name of the brake force management scheme. Generally, there are two main brake force management schemes, parallel and series scheme, as explain in the previous section. However, there are some systems improved from the main schemes for example the modified parallel scheme. The improvement objective of the modified parallel scheme is to enhance the regenerative efficiency. An overview of integration schemes is shown in Table 2.3. This overview presents the comparison of the series scheme, the parallel scheme, and the modified parallel scheme. The comparison criteria are the examples of previous researches, modification effort, regenerative efficiency, braking distance, and wheel-locking prevention. The details of each integration scheme are presented in the next subsection.

This material is reserved for educational use only, not allowed for commercial use.
Forbidden to modify the content, and cite the document when use.

Table 2.3 Comparison of integration schemes

Regenerative Brake management scheme	Series scheme	Parallel scheme	Modified parallel scheme
Example of previous research	Feng et al. [5], Gao et al. [6], Pabagiotidis et al. [7], Jang et al. [8], Yeo et al. [9], J.K. Ahn et al. [13], and Ehsani et al. [16],	Ehsani et al.[16]	Chanthanumataporn et al. [31]
Modification effort	Modified by installing EHB or EMB	N/A	Modified by installing Solenoid valves and controller
Regenerative efficiency	High	Low	Low
Braking distance	Good	Good	Good
Wheel-locking prevention	Good	Poor	Poor

2.3.1 Series Regenerative Scheme

The main purpose of this section is to describe the details of integrating the series regenerative scheme into the conventional brake of retrofitted EVs. As explained in the previous section, the regenerative brake force of series scheme is primarily provided at full capacity during all braking process. The friction brake force is responsible for the rest of brake force demand. This friction brake force is provided independently from the master cylinder. Therefore, the additional brake force controller is required for this scheme. The integration schemes of the previous studies use the Hydraulic Brake (EHB) and Electro Mechanic Brake (EMB) for controlling the amount of friction brake force. However, the limitation of the previous integration schemes is that they are compatible with only the front-rear split brake layout.

This material is reserved for educational use only, not allowed for commercial use.
Forbidden to modify the content, and cite the document when use.

The EHB is the system that can control the amount of friction brake independently from brake pedal. The EHB can be divided into driven wheels EHB and all wheels EHB. In the driven wheels EHB, the friction brake circuit of driven wheels is separated from the master cylinder and supported by the EHB. For the all wheels EHB, non-driven wheels are also controlled by the EHB and do not connect to the master cylinder. The advantage of all wheels EHB is that it can maximize the recovered energy by stopping all friction brakes and providing only the regenerative brake. However, this system also has some disadvantage. In the case that the EHB and the regenerative brake simultaneously failure, there is no any back-up braking system, which is so dangerous. In the previous studies, Feng et al. [5], Jang et al. [8], and Yeo et al. [9] introduce the driven wheel EHB in their regenerative braking systems that can be applied only to the front-rear split brake layout. Figure 2.12 displays the schematic diagram of conventional braking system (front-rear split brake layout). The hydraulic brake module of the previous study is shown in Figure 2.13. This module is modified by cutting the front braking circuit and then installing the EHB at the front wheel side and installing the stroke simulator at the master cylinder side. Thus the hydraulic brake force generated at the front wheels is independent from the master cylinder pressure but depends on the regenerative control unit that controls the EHB.

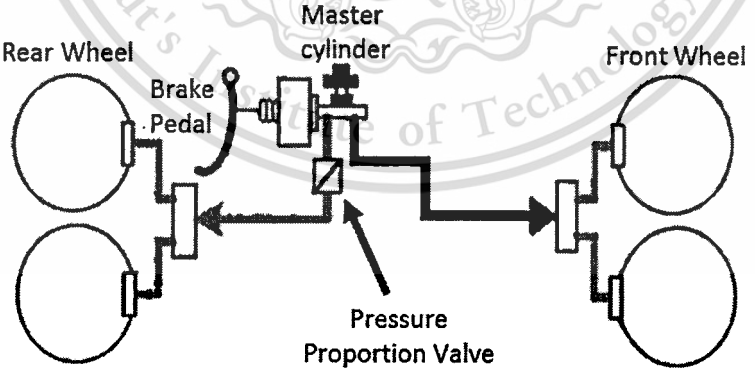

Figure 2.12 Schematic diagram of conventional braking system (front-rear split brake layout)

This material is reserved for educational use only, not allowed for commercial use.
Forbidden to modify the content, and cite the document when use.

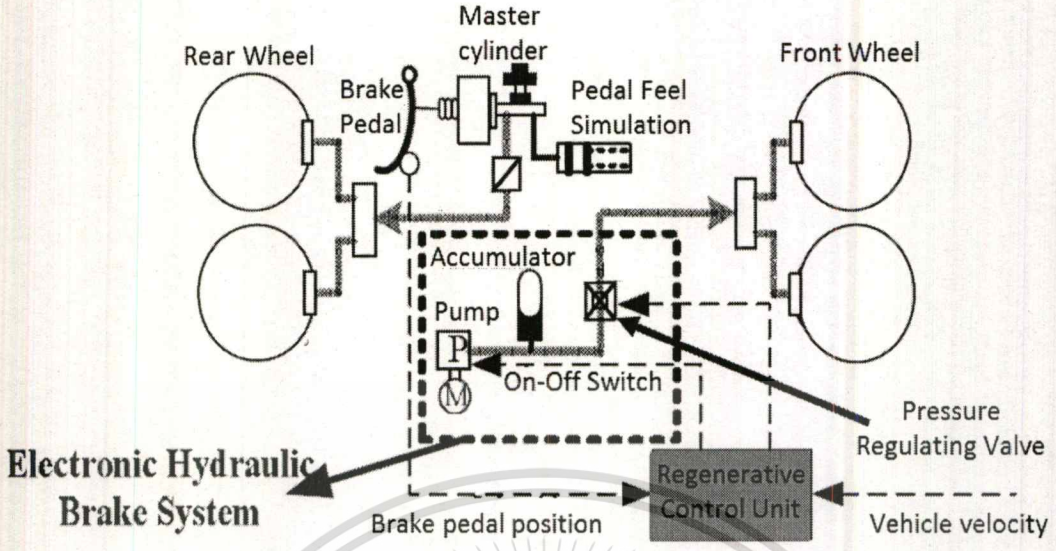

Figure 2.13 Electro-Hydraulic Brake (EHB) for series scheme [5]

The EMB is 100% brake-by-wire; thus, the conventional hydraulic braking parts are replaced by electrical components. The EMB can also be classified into driven wheel EMB and all wheels EMB as similar as the EHB system. Figure 2.14 shows the driven wheels EMB system for the series scheme. J.K. Ahn et al. [13] use this system in their regenerative braking system. For this system, the conventional hydraulic brake actuator is replaced by the electrical brake actuator. Compared to the EHB, the EMB is less complicated. However, this braking system is still under research and development. More reliability and details must be improved.

Most integration methodologies for series scheme are suitable for a car that equips with a front-rear split brake layout. Examples are the work of Gao et al. [6] that presents the regenerative braking system for controlling the front and rear brake forces of EVs and hybrid EVs and the work of Pabagiotidis et al. [7] that proposes the regenerative braking algorithm for allocating the front-rear brake forces based on a look-up table. However, more braking systems of modern sub-compact and compact production cars are the cross-link brake layout; thus, the previously proposed modification schemes are not compatible with them. Besides, these schemes require

This material is reserved for educational use only, not allowed for commercial use.
Forbidden to modify the content, and cite the document when use.

major modification of the conventional braking systems and the high-cost equipment. Most of the braking components must be replaced with specifically designed parts.

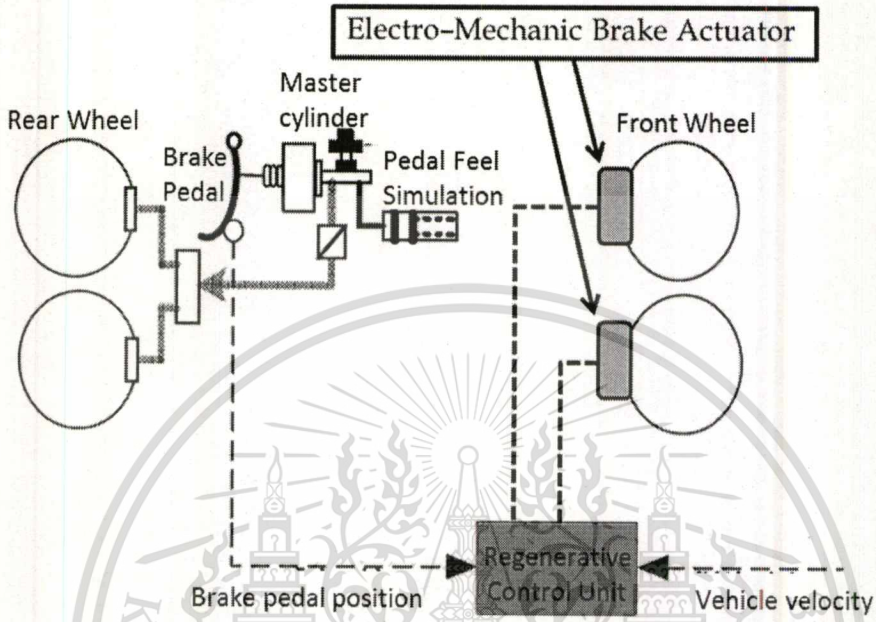

Figure 2.14 Electro-Mechanic Brake (EMB) for series scheme

2.3.2 Parallel Regenerative Scheme

This part provides the details of integrating the parallel regenerative scheme into the conventional braking system of retrofitted EVs. According to the details explained in section 2.2.2, the principle of this scheme is to provide the regenerative brake force in parallel with friction brake force. The regenerative brake force and the friction brake force are independent. Thus, the modification on the conventional braking system is not required. Figure 2.15 shows the schematic diagram of conventional braking system before the modification. The schematic diagram of parallel regenerative scheme is shown in Figure 2.16. An additional position sensor is installed at the brake pedal to measure the brake force demand. When the regenerative control unit completely receives three signals, battery's state of charge (SOC), motor's angular speed (RPM) and brake force requirement, it can calculate a regenerative brake torque command and

This material is reserved for educational use only, not allowed for commercial use.
Forbidden to modify the content, and cite the document when use.

then send this command into the inverter. After the inverter receives the command, it generates a regenerative brake torque corresponding to this signal. At the same time, a friction brake force is applied according to the brake demand. The friction brake force of this scheme is similar to that of the conventional braking system. As a result, the total brake force at the front wheels is over demand. Therefore, the regenerative brake torque is limited to make the total brake force of this scheme not too different from that of conventional braking system. Consequently, low energy efficiency can be achieved due to the regenerative brake force limitation.

The algorithm of parallel regenerative scheme is displayed in Figure 2.17. This flowchart concludes the working process of the regenerative brake torque controller. The system starts when the brake pedal is activated. The regenerative braking control unit acquires the brake pedal position, the motor RPM, the regenerative braking torque limit, and the battery SOC. Then, the motor RPM and battery SOC are used for calculating the available regenerative torque (T_{Reg_Avb}) by equation 2.12. The braking pedal position is used for estimating the regenerative torque demand by equation 2.13.

$$T_{Reg\_Avb} = T(RPM) \times W(SOC) \tag{2.12}$$

$$T_{Reg\_Demand} = T(\text{Brake pedal position}) \tag{2.13}$$

where T(RPM) is the current motor torque estimated from the motor torque/speed characteristics curve and the motor's angular speed. The weight factor (W), which is the function of battery SOC, is illustrated in Figure 2.18. The weight factor is assigned to be one from SOC = 0% to SOC = 80%, meaning the battery is fully capable for charging. In the SOC range of 80%-90%, the weight factor is linearly decreased from one to zero. From SOC = 90% onwards, the weight factor is set to be zero to protect the battery from overcharging.

This material is reserved for educational use only, not allowed for commercial use.
Forbidden to modify the content, and cite the document when use.

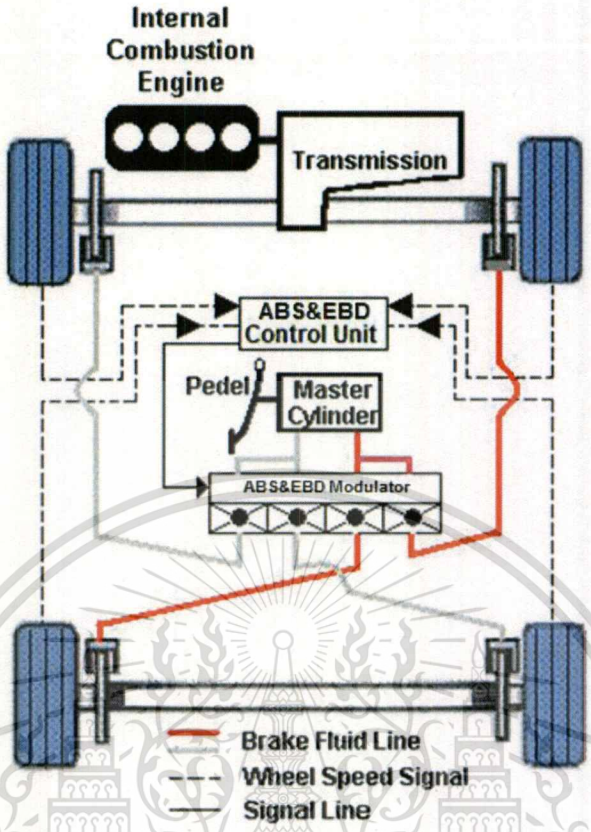

Figure 2.15 Schematic diagram of ABS-quipped conventional braking system

In the next process, the available regenerative torque is regulated not to exceed the regenerative torque limit by condition in equation 2.14. Similarly, the regenerative torque has to be controlled by the condition in equation 2.15 not to exceed the braking torque requirement. Finally, when the regenerative torque is completely determined, the regenerative control unit sends the regenerative torque command to the inverter.

$$T_{Reg\_Lim} = \begin{cases} T(Limit) & if\ T_{Reg\_Avb} > T(Limit) \\ T_{Reg\_Avb} & if\ T_{Reg\_Avb} \leq T(Limit) \end{cases} \quad (2.14)$$

$$T_{Reg\_Motor} = \begin{cases} T_{Reg\_Lim} & if\ T_{Reg\_Demand} > T_{Reg\_Lim} \\ T_{Reg\_Demand} & if\ T_{Reg\_Demand} \leq T_{Reg\_Lim} \end{cases} \quad (2.15)$$

This material is reserved for educational use only, not allowed for commercial use.
Forbidden to modify the content, and cite the document when use.

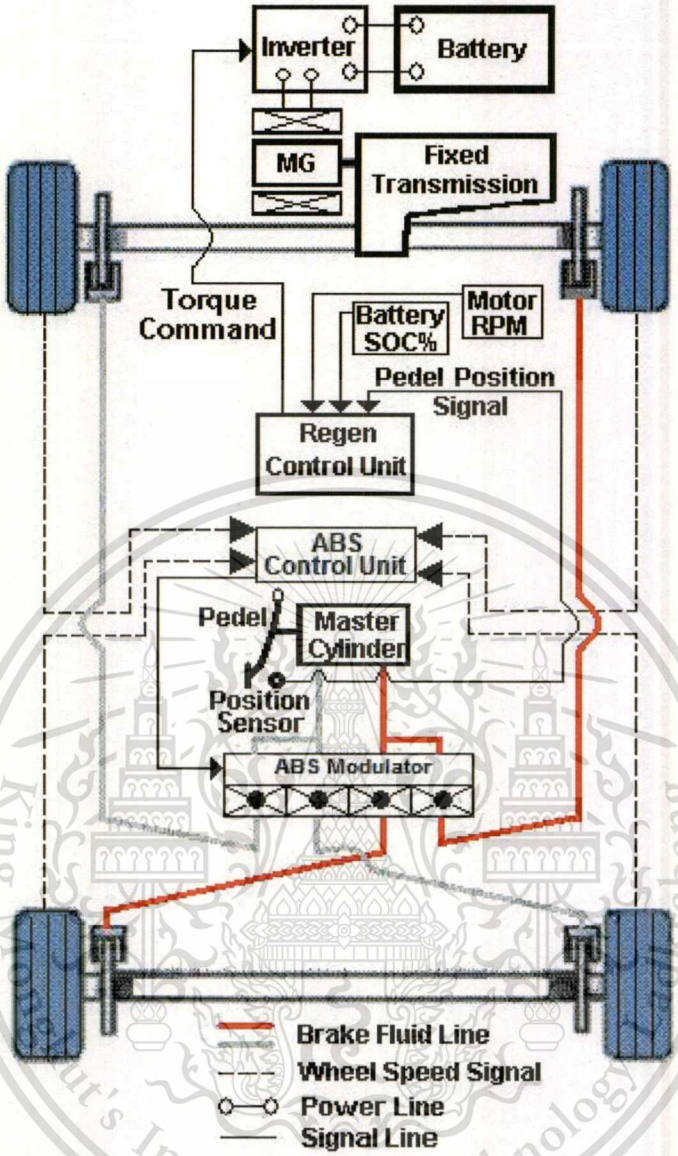

Figure 2.16 Schematic diagram of parallel regenerative scheme

This material is reserved for educational use only, not allowed for commercial use.
Forbidden to modify the content, and cite the document when use.

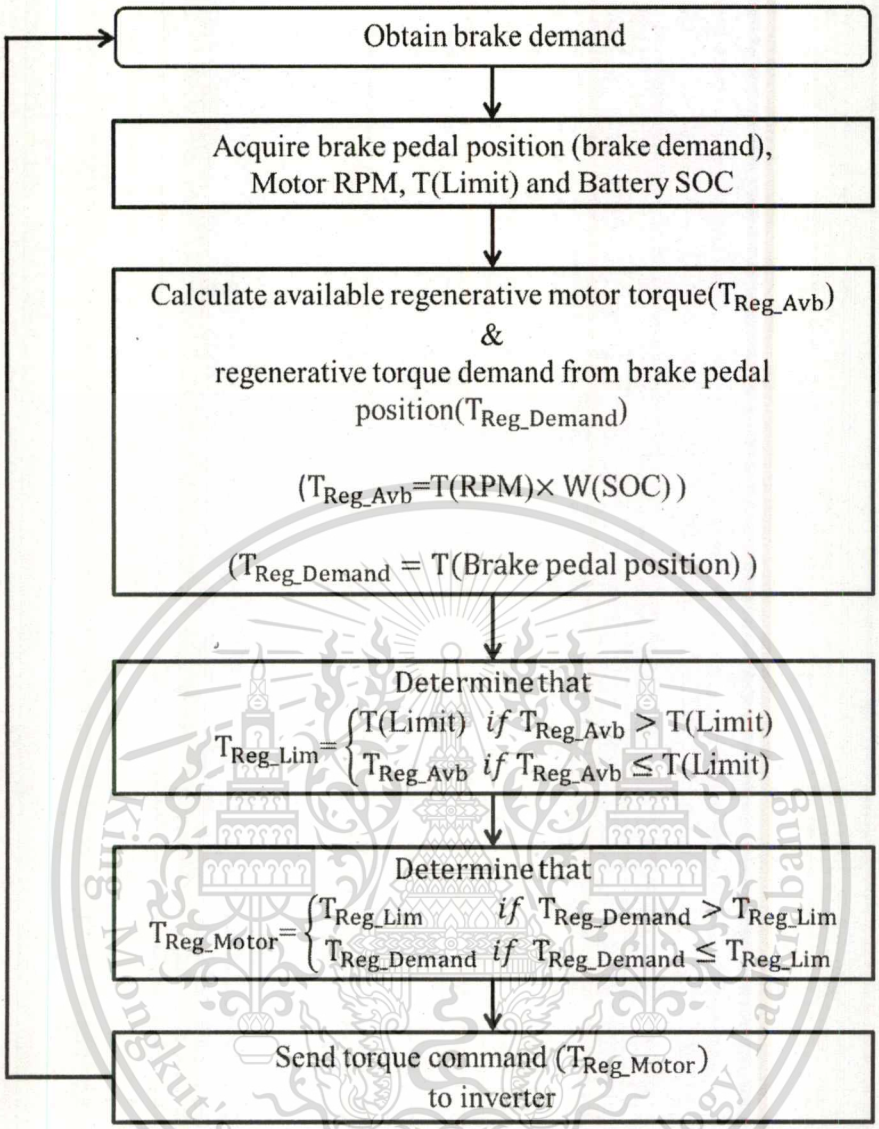

Figure 2.17 Flowchart of parallel regenerative braking algorithm

This material is reserved for educational use only, not allowed for commercial use.
Forbidden to modify the content, and cite the document when use.

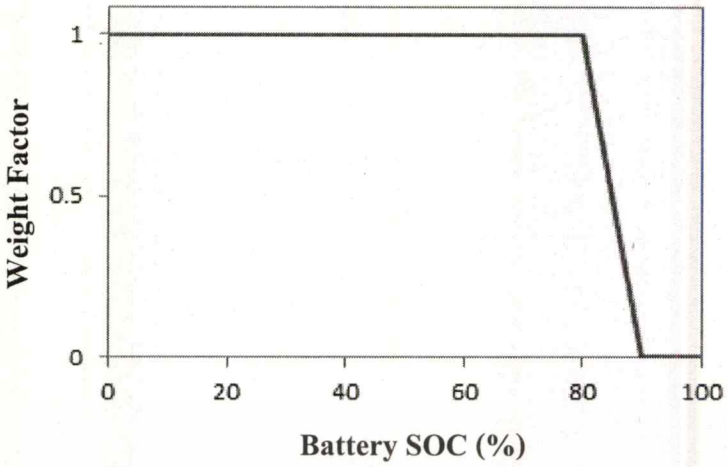

Figure 2.18 Weight Factor vs. Battery SOC (%)

2.3.3 Modified Parallel Regenerative Scheme

This section presents the details of the modified parallel scheme. This scheme is developed from the parallel scheme, explained in the previous section. The improvement objective is to enhance the regenerative efficiency of the conventional parallel scheme. Required for this improvement, the solenoid valve unit is installed between the master cylinder and the ABS modulator. The idea of this add-on feature is to control the solenoid valve to pause the brake fluid pressure until the brake force requirement of all wheels is greater than the capability of regenerative brake force. This scheme can increase the recovered energy since it allows only the regenerative brake to perform during the initial period of braking. The system diagram is shown in Figure 2.19. The modification at the conventional braking system is done by installing the additional regenerative control unit, the pressure sensor, and the solenoid valve unit between the master cylinder and the ABS modulator. Figure 2.20 shows the algorithm flowchart of this scheme. When the brake pedal is activated, the regenerative braking control unit measures the brake pressure in the master cylinder to determine the brake demand requested by a driver. The master cylinder pressure is converted to be the brake torque demand of front-rear wheels by equation 2.16.

This material is reserved for educational use only, not allowed for commercial use.
Forbidden to modify the content, and cite the document when use.

$$T_{Demand} = P_{master} \times ((A_{wcf} \times r_f) + (A_{wcr} \times r_r)) \times \mu \times 4 \quad (2.16)$$

P_{master} is the brake pressure in the master cylinder, A_{wcf} is the cylinder area of front caliper, A_{wcr} is the cylinder area of rear caliper, μ is the friction coefficient of brake pad, r_f is the effective radius of front brake disk and r_r is the effective radius of rear brake disk. Number four is derived from two brake pads per caliper and two brake circuits, left and right. Simultaneously with the process of acquiring the master cylinder pressure, the control unit receives the motor angular speed, the regenerative braking torque limit value (T(Limit)), and the battery's state of charge (SOC). The motor angular speed and the battery SOC are used to calculate the available regenerative torque by equation 2.12 as same as the first scheme. Moreover, the pressure at master cylinder is converted to be the regenerative brake torque demand, T(Reg_Demand), by using equation 2.17.

$$T_{Reg\_Demand} = \frac{P_{master} \times ((A_{wcf} \times r_f) + (A_{wcr} \times r_r)) \times \mu \times 4}{i \times N_d} \quad (2.17)$$

where i is the gear ratio and N_d is the differential gear ratio. After getting each torque values, the regenerative control unit regulates the available regenerative torque as same as the equation 2.14 of the parallel scheme. Similarly, the regenerative control unit also controls the regenerative torque not to exceed the brake torque demand by condition in equation 2.15. Subsequently, when the regenerative brake torque is completely determined, the regenerative control unit sends the regenerative torque command to the inverter and estimates the regenerative braking torque, generated at front wheel to compare with the brake torque demand. In the final stage, the regenerative control unit checks that the front-rear wheels brake torque requirement is greater than the provided regenerative braking force or not. In the case that the condition is false, the regenerative control unit pauses the brake fluid pressure. At this time, only the regenerative brake is operated, all braking energy is entirely recovered. On the contrary, it terminates pausing brake

This material is reserved for educational use only, not allowed for commercial use.
Forbidden to modify the content, and cite the document when use.

fluid pressure. The brake force distribution of this condition is as identical as that of parallel scheme.

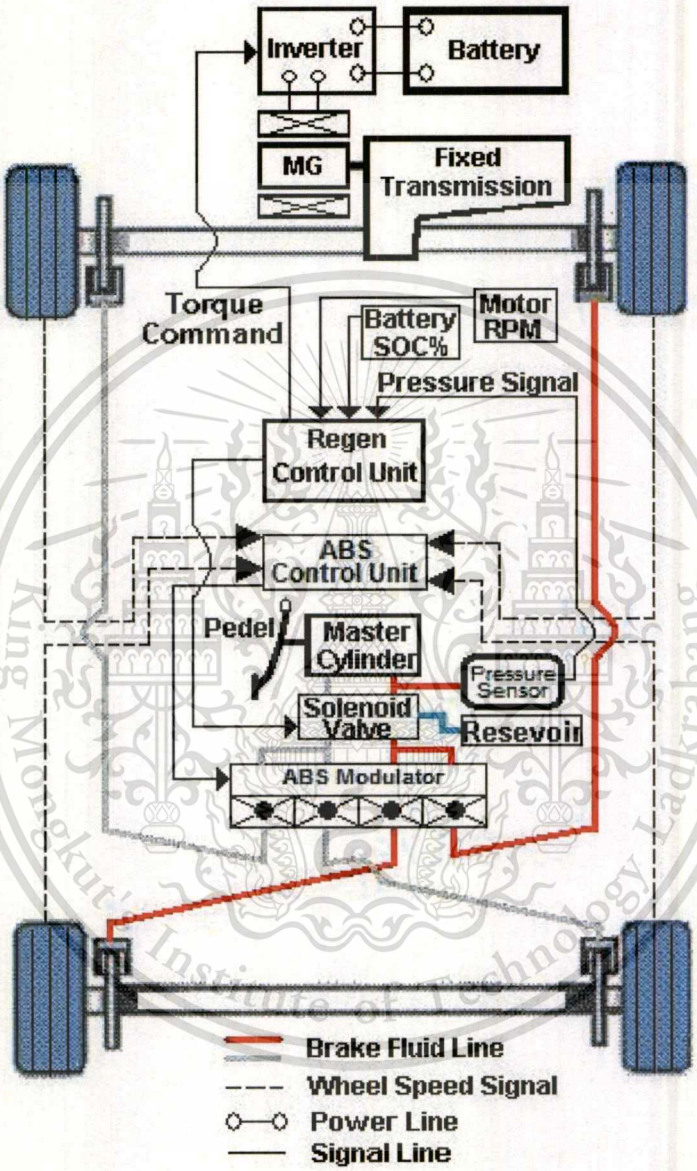

Figure 2.19 Schematic diagram of modified parallel regenerative scheme

This material is reserved for educational use only, not allowed for commercial use.
Forbidden to modify the content, and cite the document when use.

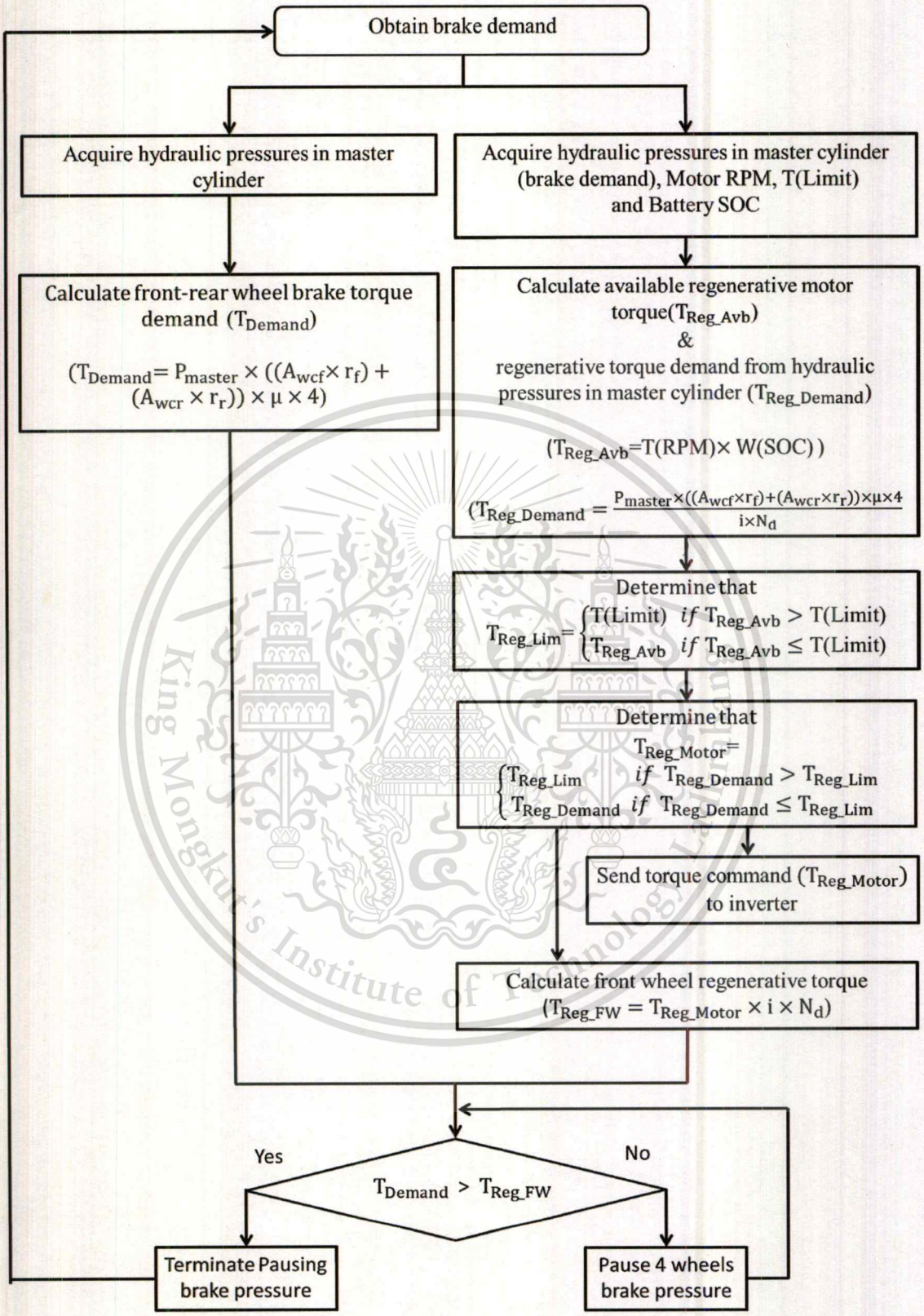

Figure 2.20 Flowchart of modified parallel regenerative braking algorithm

This material is reserved for educational use only, not allowed for commercial use.
Forbidden to modify the content, and cite the document when use.

2.4 Verification Methodologies for Regenerative Braking Systems

Generally, there have been various methodologies for evaluating the performances of regenerative braking systems. It can be mainly divided into mathematical analysis and experimental investigation. The mathematical analysis is the most effective means since it can be effortlessly adapted the parameters, platforms, and algorithms. There are many examples such as the work of Gao et al. [6] and Peng et al. [11] that use the mathematical analysis to investigate the effectiveness of the regenerative braking system. However, these works do not notify the name of modeling software. In addition, Feng et al. [5], Panagiotidis et al. [7], Yeo et al. [9], Ahn et al. [13], Zhang et al. [14], and Tehrani et al. [15], develop the mathematical models to evaluate the performance of their proposed regenerative braking systems by using MATLAB/Simulink. Jang et al. [8] use AMESim (advanced modeling environment for performing simulation of engineering) for modeling their hydraulic system and dynamic powertrain. Selim et al. [25] use MATLAB/Simulink for modeling their brake force controller, Dymola for modeling their motor, engine, friction brake, and battery and IPG CarMaker for medeling road features, vehicle dynamics, and suspension systems. However, the mathematical analyses are sometimes in concern of their accuracy. Thus, to verify their precision and reliability, some mathematical models are sometimes validated by experiments. Moreover, the experimental investigation is used not only for the mathematical analysis verification but also used for the proof of proposed brake force control scheme. Examples are the works of Peng et al. [11] and Zhang et al. [14] that experimentally verify and examine their proposed brake force control scheme in real vehicle. Further, Jang et al. [8] set up a regenerative test-bench to assess the performance of their regenerative hydraulic system. In conclusion, the mathematical modeling in MATLAB/Simulink is the most popular and reliable. The knowledge of modeling by MATLAB/Simulink can be used for my work. The experimental verification should be done to prove the possibility of the regenerative scheme and to verify the reliability of the mathematical model.

This material is reserved for educational use only, not allowed for commercial use.
Forbidden to modify the content, and cite the document when use.

CHAPTER 3

MODELING AND VERIFICATION

3.1 Proposed Integration Scheme for Retrofitted Regenerative Braking System

As explained in chapter 2, there are two brake-force management concepts, series scheme and parallel scheme. Series scheme is more accepted since it provides the greater brake force distribution and the higher recovery efficiency. However, in previous the studies, the integration scheme of series one is not compatible with the cross-link circuit brake layout. Furthermore, it also needs many major modifications and cost-intensive components. Therefore, to resolve the previous troubles, the design criteria of proposed scheme are effective performance, compatibility with both cross-link and front-rear split circuit brake layout, and simplification of vehicle modification.

The diagram of a conventional braking system called the cross-link circuit layout is shown in Figure 2.15. This layout is commonly used in modern passenger cars. To convert this conventional system into a regenerative braking system used in a retrofitted EV, the schematic, shown in Figure 3.1, is proposed. In a retrofitted EV, an engine is replaced by a propelling motor that perform as a generator during braking. An additional regenerative control unit is required to manage the proper brake forces among the conventional braking system and the regenerative one. A pressure sensor is installed to acquire the hydraulic pressure in the master cylinder, and the other two are used to obtain the pressures in both front brake calipers. The signals from the pressure sensors are then given to the regenerative control unit, and so are those of the motor's angular speed and battery's state of charge (SOC). In addition, the signals transmitted from the front wheel-speed sensors are rerouted to the regenerative braking control unit instead of the ABS control unit.

In a standard braking system of modern passenger cars, there commonly are an ABS and its control unit that regulates the braking forces. The ABS inherits a unique feature that can

This material is reserved for educational use only, not allowed for commercial use.
Forbidden to modify the content, and cite the document when use.

automatically release the brake pressure while the wheels are being locked up during braking. In this study, the proposed scheme utilizes this feature of the ABS. To recover some energy during braking, an emulated "wheel lock-up" signal is sent by the additional regenerative control unit to the ABS control unit to perform the reduction of brake pressure at mechanical braking system, resulting in the reduced friction brake force. The amount of this reduced brake force is then replaced by that of the regenerative one. In this concept, total braking energy is as same as that of conventional braking system but frictional braking energy is reduced. Figure 3.2 summarizes this novel concept of the proposed scheme.

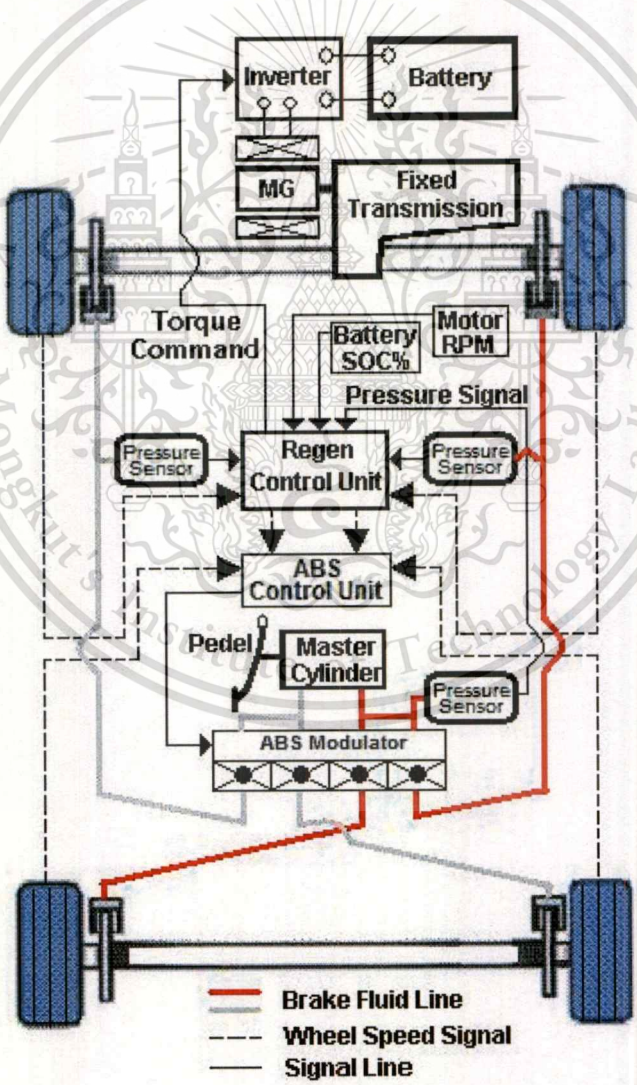

Figure 3.1 Schematic of retrofitted EV and proposed regenerative braking system

This material is reserved for educational use only, not allowed for commercial use.
Forbidden to modify the content, and cite the document when use.

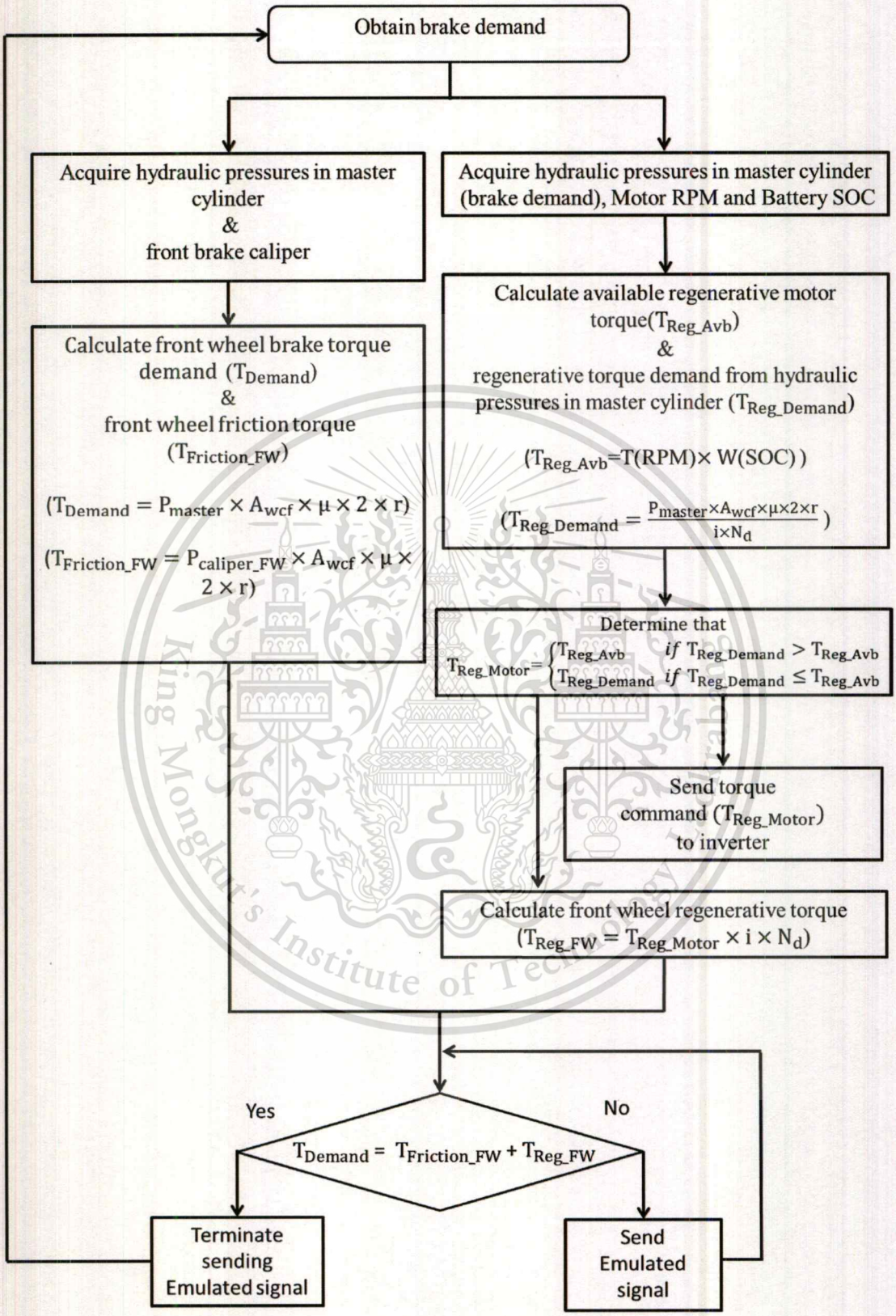

Figure 3.2 Flowchart of proposed regenerative braking algorithm

This material is reserved for educational use only, not allowed for commercial use.
Forbidden to modify the content, and cite the document when use.

The scheme starts working once the brake pedal is activated. The regenerative braking control unit determines the pressure in the master cylinder to calculate the brake demand requested by a driver. Besides, the pressures in the front brake calipers are measured to calculate the friction brake torque at the front wheels. By measuring the pressures in the master cylinder and the brake calipers, the demanded torque (T_{Demand}) and the friction brake torque of the front wheels ($T_{Friction\_FW}$) are calculated according to equation 3.1 and equation 3.2, respectively.

$$T_{Demand} = P_{master} \times A_{wcf} \times \mu \times 2 \times r \tag{3.1}$$

$$T_{Friction\_FW} = P_{caliper\_FW} \times A_{wcf} \times \mu \times 2 \times r \tag{3.2}$$

P_{master} denotes the brake pressure in the master cylinder, $P_{caliper}$ describes the pressure in the brake caliper, A_{wcf} is the cylinder area of front caliper, μ is the friction coefficient of brake pad, and r is the effective radius of brake disk.

Concurrently with the process described above, the control unit captures the motor angular speed and the battery state of charge (SOC) to calculate the available regenerative motor brake torque (T_{Reg_Avb}) according to the following equation:

$$T_{Reg\_Avb} = T(RPM) \times W(SOC) \tag{3.3}$$

T(RPM) denotes the current motor torque estimated from the motor characteristic curve and the motor's angular speed. The weight factor (W), which is the function of battery SOC, is illustrated in Figure 2.18. The weight factor is assigned to be one from SOC = 0% to SOC = 80%, meaning the battery is fully capable of charging. In the SOC range of 80%-90%, the weight factor is linearly decreased from one to zero. From SOC of 90% onwards, the weight factor is set to be zero to protect the battery from overcharging. Based on equation 3.4, the pressure in the master cylinder is converted to the regenerative torque demand (T_{Reg_Demand}).

This material is reserved for educational use only, not allowed for commercial use.
Forbidden to modify the content, and cite the document when use.

$$T_{Reg\_Demand} = \frac{P_{master} \times A_{wcf} \times \mu \times 2 \times r}{i \times N_d} \quad (3.4)$$

Where, i is the gear ratio and N_d is the differential gear ratio. In the case that the regenerative torque demand is less than the available regenerative motor torque, it is necessary to regulate the motor torque not to exceed the demand. Thus, the condition in equation 3.5 is defined:

$$T_{Reg\_Motor} = \begin{cases} T_{Reg\_Avb} \ if \ T_{Reg\_Demand} > T_{Reg\_Avb} \\ T_{Reg\_Demand} \ if \ T_{Reg\_Demand} \leq T_{Reg\_Avb} \end{cases} \quad (3.5)$$

As a command, this torque is also sent to the inverter. Based on this torque, the gear ratio (i), and the differential gear ratio (N_d), the front wheel regenerative torque (T_{Reg_FW}) is calculated by using equation 3.6.

$$T_{Reg\_FW} = T_{Reg\_Motor} \times i \times N_d \quad (3.6)$$

After obtaining the brake torque demand of the front wheels (T_{Demand}), the friction brake torque at the front wheels ($T_{Friction\_FW}$), and the regenerative brake torque at the front wheels (T_{Reg_FW}), the regenerative brake control unit assesses if the demanded torque given by the driver equals to the summation of the front wheel frictional brake torque and the front wheel regenerative torque. In the case that the condition is false, the control unit feeds the emulated "wheel lock-up" signal to the ABS control unit to decrease the braking force of the frictional braking system such that the reduced braking force is similar to that provided by the regenerative system.

3.2 Proof of Concept

Since the proposed integration scheme for retrofitted regenerative braking system is firstly introduced in the automotive field, the proof of concept is set up to verify the feasibility of the proposed scheme. The emulated "wheel lock-up" signal is sent to the ABS to investigate the

This material is reserved for educational use only, not allowed for commercial use.
Forbidden to modify the content, and cite the document when use.

characteristic of brake pressure. The expect results are the brake fluid pressure reductions at various testing conditions, which vary the brake demands and the initial speeds. In addition, the braking energy of each condition is calculated by the experimental brake pressure to evaluate the potentiality of recovered energy. This experiment is carried out at a proving ground with a conventional passenger car. A gasoline engine car, Toyota Vios shown in Figure 3.3 is used as the experimental vehicle. Since this experiment is done on the engine vehicle, it does not provide any regenerative braking torque. However, the lack of real regenerative brake torque does not cause any problem because this experiment focuses on the feasibility of controlling the brake fluid pressure by sending the emulated "wheel lock-up" signal to the ABS.

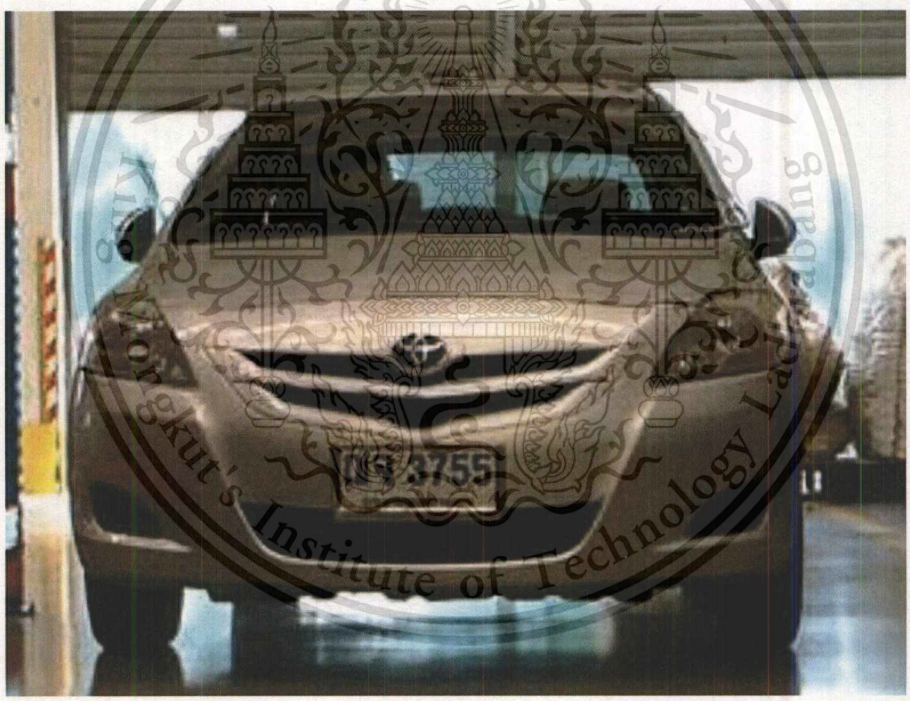

Figure 3.3 Toyota Vios, experimental vehicle

The testing outline for the proof of concept is shown in Figure 3.4. The testing track is organized into three sections. The first section is prepared for maintaining the car velocity at any test speeds. The prepared distance of this section is calculated by using equation 3.7, a basic

This material is reserved for educational use only, not allowed for commercial use.
Forbidden to modify the content, and cite the document when use.

equation of linear motion. To keep in reserve, the calculation condition is set at worst cases, starting from 0 km/h, maintain vehicle speed at 80 km/h, and acceleration 0.1g. The second one is set to inform the driver to be ready to depress the brake pedal. The third one is arranged to fully depress the brake pedal until the car stops. The distance of this section is also calculated by using equation 3.7 and worst conditions, deceleration 0.1 g and vehicle speed 80 km/h, to keep in reserve. The calculation distance is 83.7 meters. However, for the safety concern, the prepared distance of the first section and this section is determined for 200 meters.

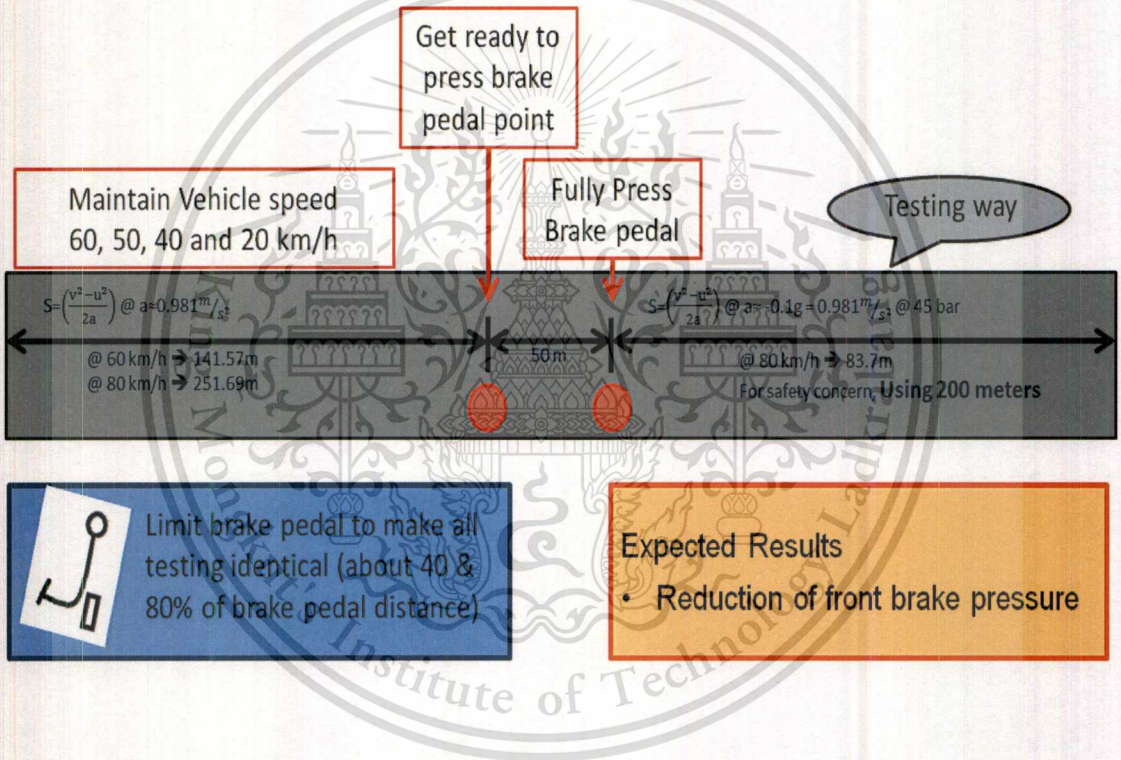

Figure 3.4 Proof of concept outline

$$S = \left(\frac{v^2-u^2}{2a}\right) \tag{3.7}$$

To verify the feasibility of the proposed scheme at all braking conditions, test conditions are set at various working velocities and brake force demands. Eight conditions are determined at brake

This material is reserved for educational use only, not allowed for commercial use.
Forbidden to modify the content, and cite the document when use.

pedal 40% and 80% of car speed 20, 40, 50, 60 km/h. Each condition is repeated 3 times so overall test number is 24 times as shown in Table 3.1.

Table 3.1 Test conditions for proof of concept

Testing Number	% Brake Pedal	Testing Velocity (km/h)	Number of times
1	40%	20	1
2			2
3			3
4		40	1
5			2
6			3
7		50	1
8			2
9			3
10		60	1
11			2
12			3
13	80%	20	1
14			2
15			3
16		40	1
17			2
18			3
19		50	1
20			2
21			3
22		60	1
23			2
24			3

3.2.1 Experimental Setup

The interested parameters of the experimental field test are the brake fluid pressure, the vehicle speed, and the emulated ABS signal. The testing equipment and the wiring outline is shown in Figure 3.5. A pressure sensor is installed at the master cylinder, the front right wheel caliper, the front left wheel caliper, and the rear left wheel drum to detect the brake fluid pressure of each point. The VBOX Global Positioning System (GPS) is set up at the center of gravity of the car to measure vehicle speed. To design an interface among the testing equipment, the laptop

This material is reserved for educational use only, not allowed for commercial use.
Forbidden to modify the content, and cite the document when use.

computer, and the NI DAQ device, LabVIEW is used for creating the communication protocol. The communication protocol can be used for real-time monitoring, data logging, and signal generating.

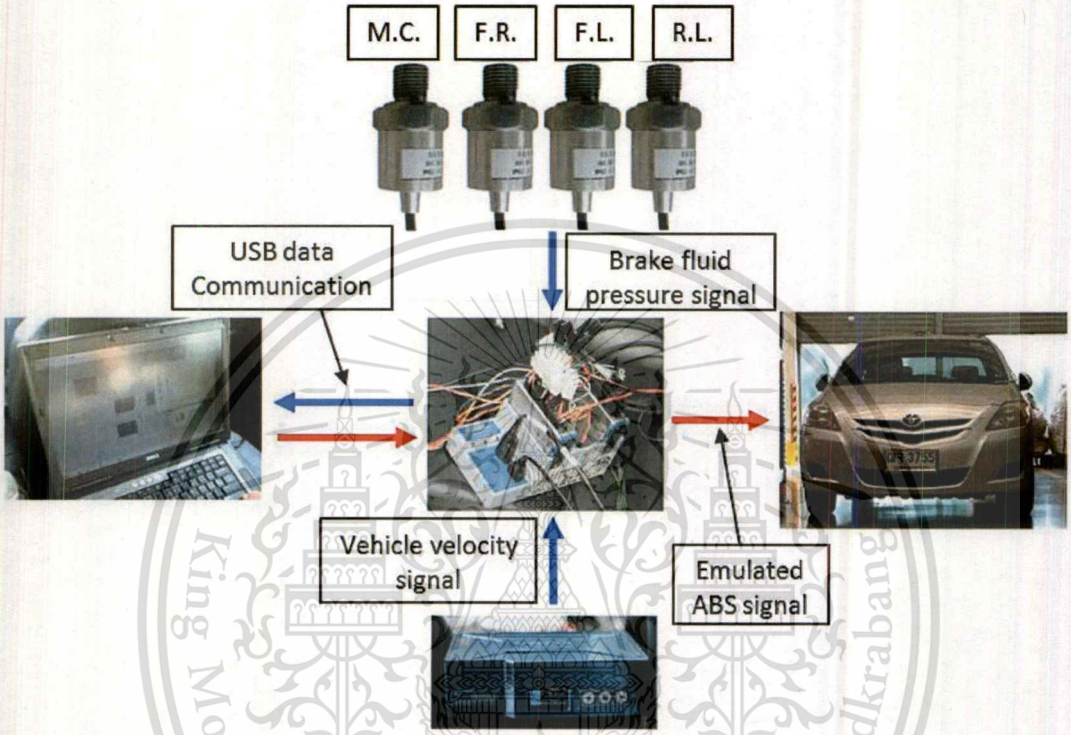

Figure 3.5 Test equipment and wiring outline

3.2.1.1 Pressure Sensor

To measure the brake fluid pressure of relevant points, four pressure sensors are required. The first point is at the master cylinder to determine the brake force requirement. The second one is at the front-left wheel brake to sense the existed friction brake force. The third one is at the front-right wheel brake. The forth one is at the left rear wheel brake. Figure 3.6 shows the installation of the pressure sensor at the master cylinder. The three-way fitting is additionally installed between the master cylinder and the ABS modulator to give a way for connecting the pressure sensor. For measuring the brake fluid pressure at the wheel brake calipers, the special

This material is reserved for educational use only, not allowed for commercial use.
Forbidden to modify the content, and cite the document when use.

equipment is required to connect the pressure sensor at the brake fluid bleeding valve as shown in Figure 3.7.

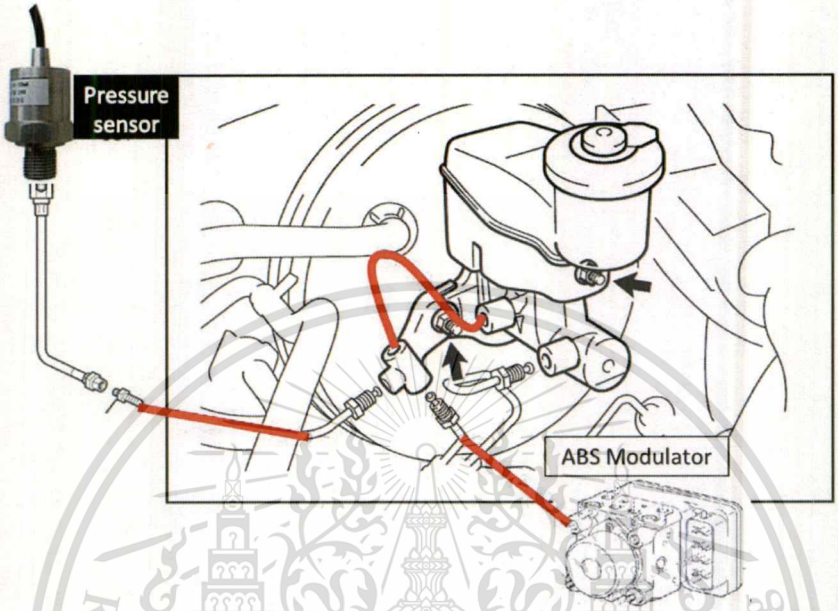

Figure 3.6 Installation of pressure sensor at master cylinder

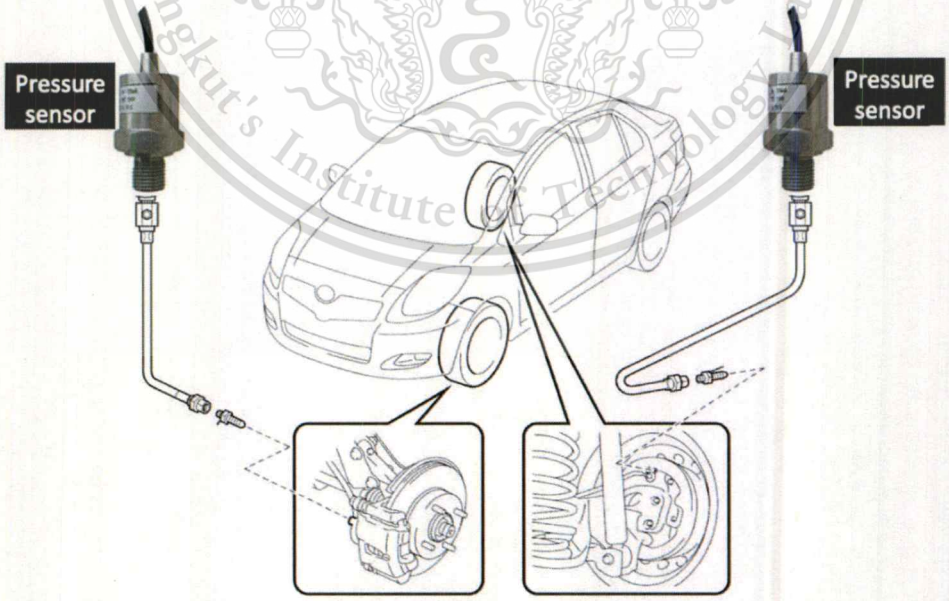

Figure 3.7 Installation of pressure sensor at brake actuators [27]

This material is reserved for educational use only, not allowed for commercial use.
Forbidden to modify the content, and cite the document when use.

Figure 3.8 shows the brake fluid pressure sensor, used in this study. Figure 3.9 presents the brake fluid pressure sensors, installed at the front wheel (left) and the rear wheel (right). Moreover, the pressure sensors of this study were tested before being installed in the experimental car to verify their sensitivity by concurrently comparing with pressure gauge as shown in Figure 3.10 and their sensitivity results are identical as shown in Figure 3.11. In addition, the output of the pressure sensors is analog output. This output is measured by NI module 9205 that give more detail in next section.

Figure 3.8 Brake fluid pressure sensor[28]

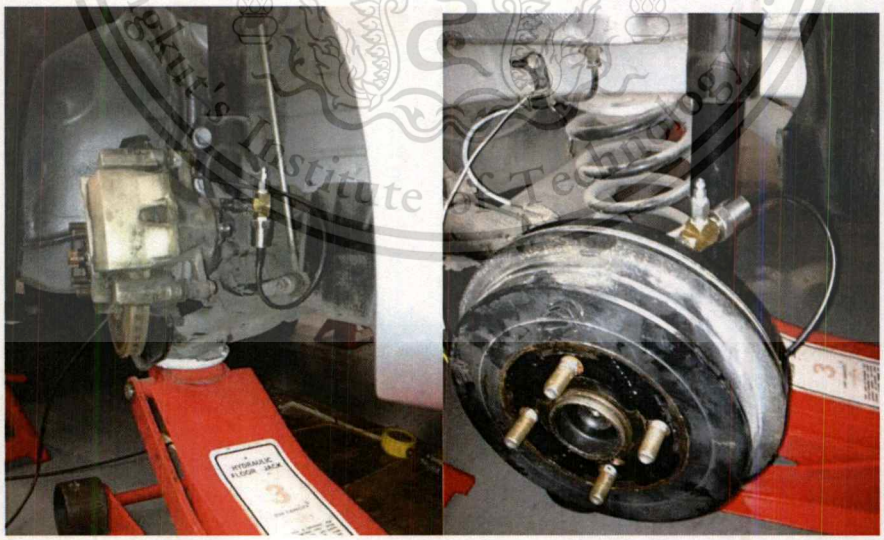

Figure 3.9 Brake fluid pressure sensor installed at front wheel (left) and rear wheel (right)

This material is reserved for educational use only, not allowed for commercial use.
Forbidden to modify the content, and cite the document when use.

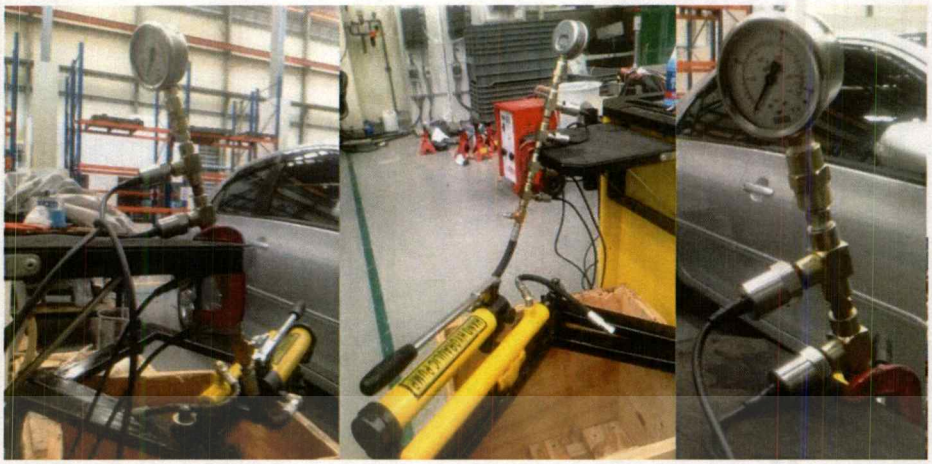

Figure 3.10 Pressure sensors sensitivity verification

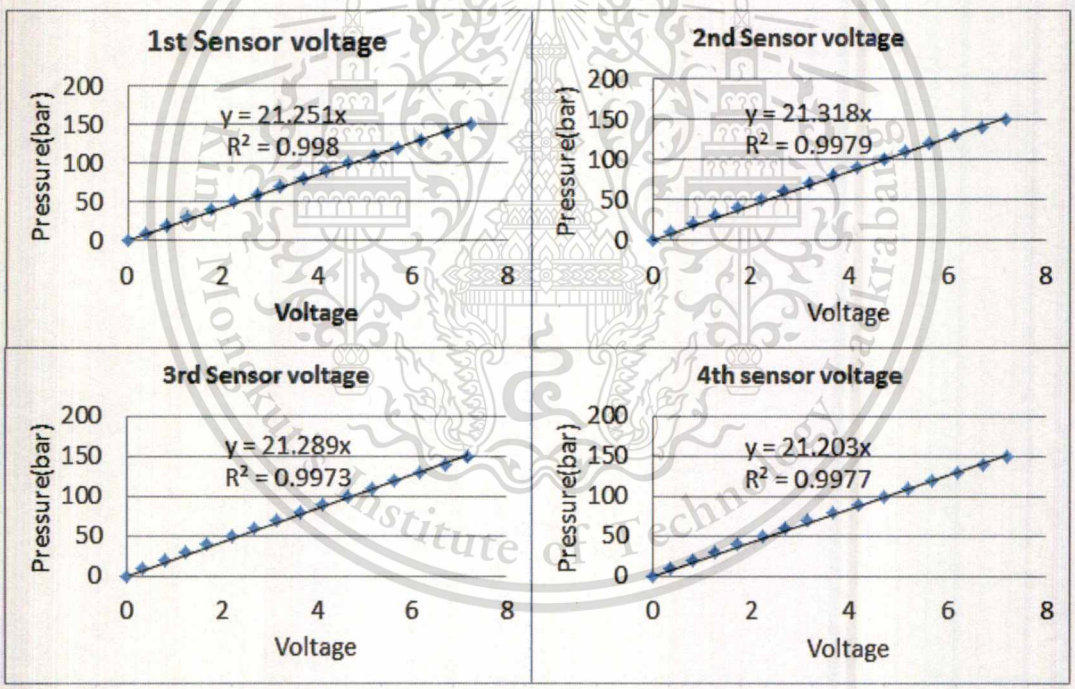

Figure 3.11 Pressure sensors sensitivity

3.2.1.2 VBOX Global Positioning System (GPS)

During field test, the vehicle speed is measured by using VBOX GPS model:VB20SL3 shown in Figure 3.12. This system is accurate and convenient since it is independent of the wheel

This material is reserved for educational use only, not allowed for commercial use.
Forbidden to modify the content, and cite the document when use.

sizes and the on-board speed sensors of the tested car. The model of VBOX GPS, used in this study, is VB20SL3, a multi-purpose non-contact speed sensor. By using two advanced dual antenna GPS engines, the VB20SL3 can calculate the vehicle speed and the vehicle direction. In this work, the selected output of this GPS is analog output. This output is measured by NI module 9205 as same as the pressure sensor. Figure 3.13 displays the GPS antennas, which are installed on the roof of the experiment car.

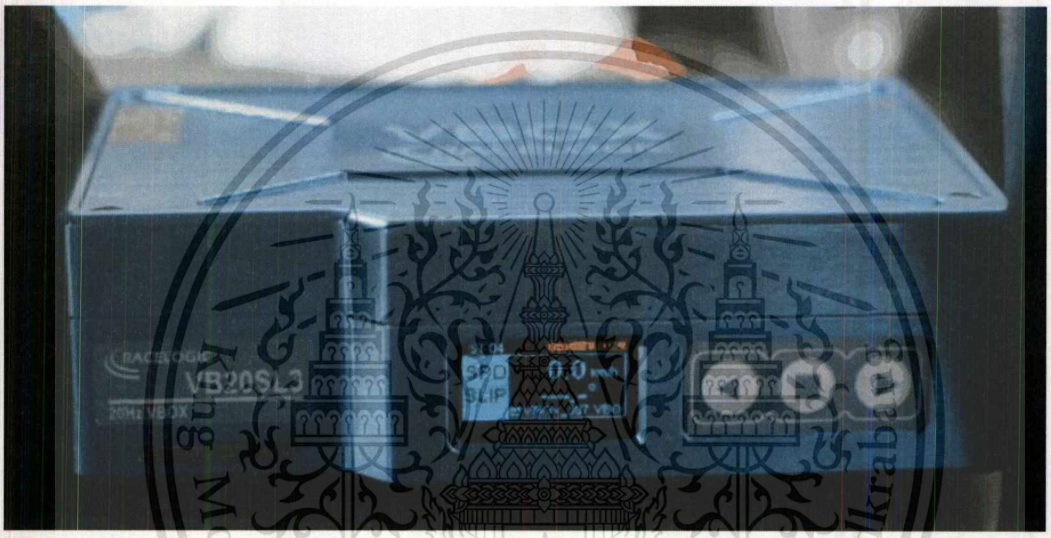

Figure 3.12 VBOX GPS model:VB20SL3

Figure 3.13 VBOX GPS antennas

This material is reserved for educational use only, not allowed for commercial use.
Forbidden to modify the content, and cite the document when use.

3.2.1.3 NI DAQ Device

Data Acquisition (DAQ) is an automatic process of reading and holding electrical signals to measure, log, or display the signals by using software. However, the capability of DAQ hardware is beyond reading the signals. The main responsibility of DAQ hardware could be concluded as follow:

- Analog input → acquiring electrical signal
- Analog output → providing measurable electrical signal for controlled device
- Digital I/O → acquiring and generating digital signal
- Counter I/O → measuring recoder signal and generating pulse signal [30].

In the field test of this study, the data acquisition of National Instruments (NI DAQ), shown in Figure 3.14, is used as regenerative control unit in the proof of concept. The NI DAQ is a computer-based hardware with programmable software, which can provide various input and output supports depending on equipped module. Two NI modules are adopted. NI 9205 module, shown Figure 3.15, is used to measure the output signals of the brake fluid pressure sensors and the GPS system. Then, NI 9485 module, shown Figure 3.16, is applied to generate the emulated ABS wheel speed signal and to switch between the real ABS signal and the emulated one. The detail of generating the emulated ABS one is explained in the next heading.

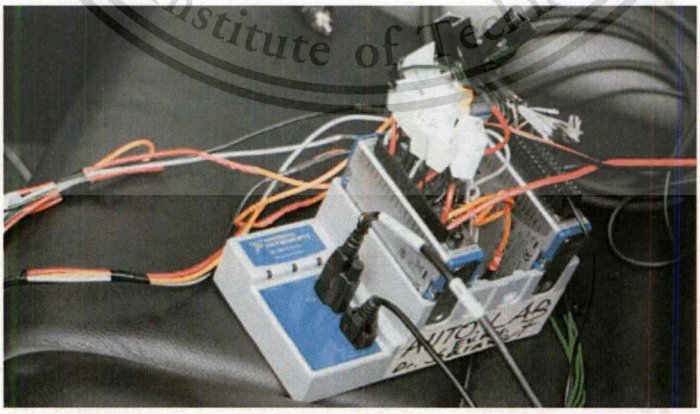

Figure 3.14 The example of National Instruments (NI) data acquisition device [24]

This material is reserved for educational use only, not allowed for commercial use.
Forbidden to modify the content, and cite the document when use.

Figure 3.15 NI 9205 [24]

Figure 3.16 NI 9485 [24]

3.2.1.4 ABS Signal Generator

As already mentioned, the NI 9485 module is adopted for generating and switching the ABS signal. The NI 9485 is the module of 8 channel solid state relay outputs. The wiring diagram between the NI 9485 and the vehicle's wheel speed sensor is shown in Figure 3.17. To switch and generate the wheel speed signal, three channels of relay are required. In case that the real wheel speed signal is sent from the sensor to the ABS controller, the circuit of first contact is closed but those of second and third contact is opened. In case of generating the emulated wheel speed

This material is reserved for educational use only, not allowed for commercial use.
Forbidden to modify the content, and cite the document when use.

signal, the first contact's circuit is opened; the second contact's circuit is closed but the third contact is switched between on and off according to the frequency command. From the document of Toyota, the signal of ABS wheel speed is a different-step pulse of electric current between 7 and 14 mA as illustrated in Figure 3.18. The bandwidth of square wave depends on rotational wheel speed.

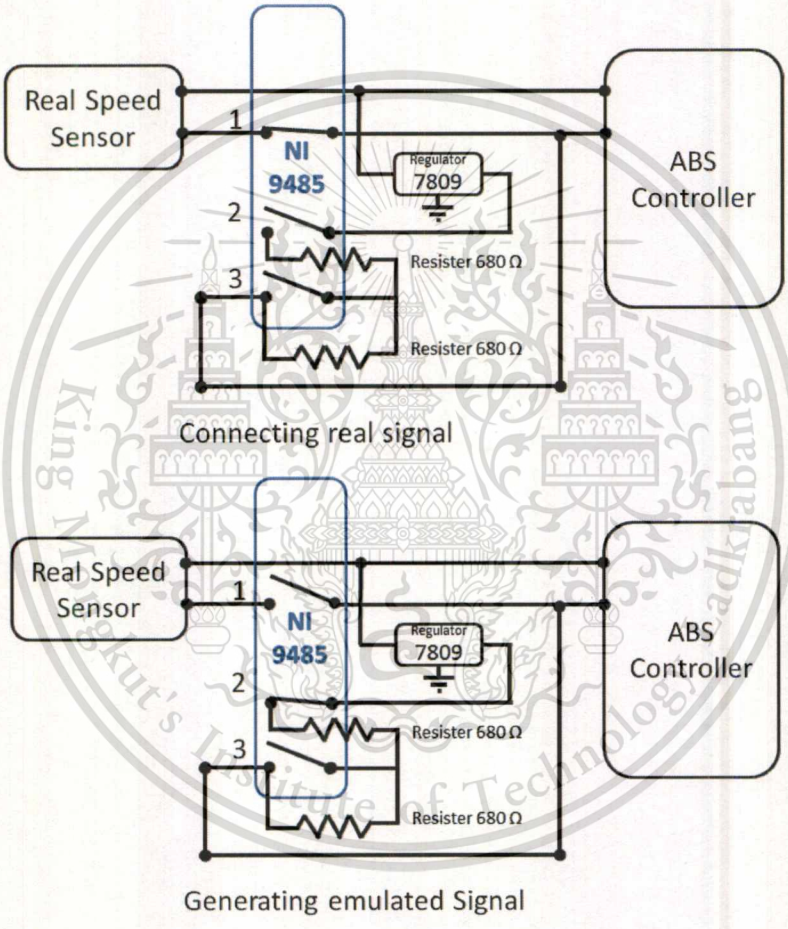

Figure 3.17 NI 9485 wiring diagram

The data of this ABS signal is proofed by the mini experiment focusing on current and voltage during an operating of wheel speed sensor. The experimental outline is shown in Figure 3.19. From measuring the voltage and the current of the wheel speed sensor, it could be conclude

This material is reserved for educational use only, not allowed for commercial use.
Forbidden to modify the content, and cite the document when use.

that the output current signal is always between 7 mA and 14 mA when the wheel is rotated, although its voltage is fluctuated. Therefore, to fully imitate the real ABS wheel speed signal, the integrated circuit (IC) regulator LM7809 is adopted in order to regulate the voltage drop across resister, about 9.6 volts (measured data). From the basic electrical formula, V=IR, if a voltage drop and resistance are constant, a current is also constant. By calculation, I=V/R, I=14 mA if V=9.6 volt and R=680 ohm. I=7 mA if V=9.6 volt and R=1360 ohm. The IC regulator and resister, installed on the NI 9485, are shown in Figure 3.20.

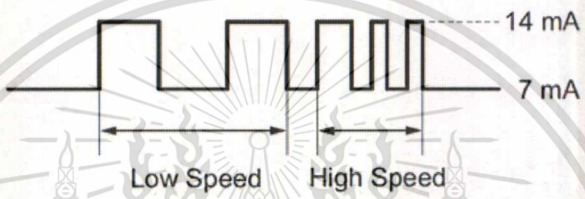

Figure 3.18 Pulse signal of wheel speed [27]

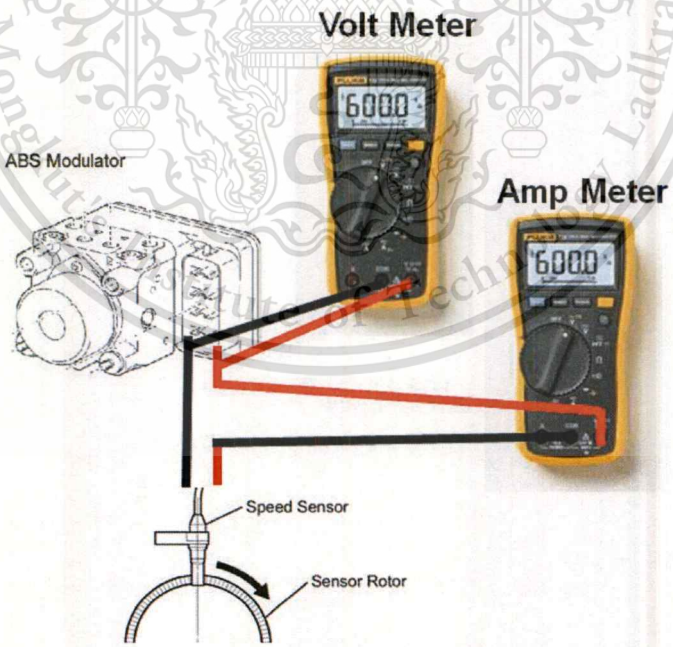

Figure 3.19 Experimental outline of proofing ABS wheel speed signal

This material is reserved for educational use only, not allowed for commercial use.
Forbidden to modify the content, and cite the document when use.

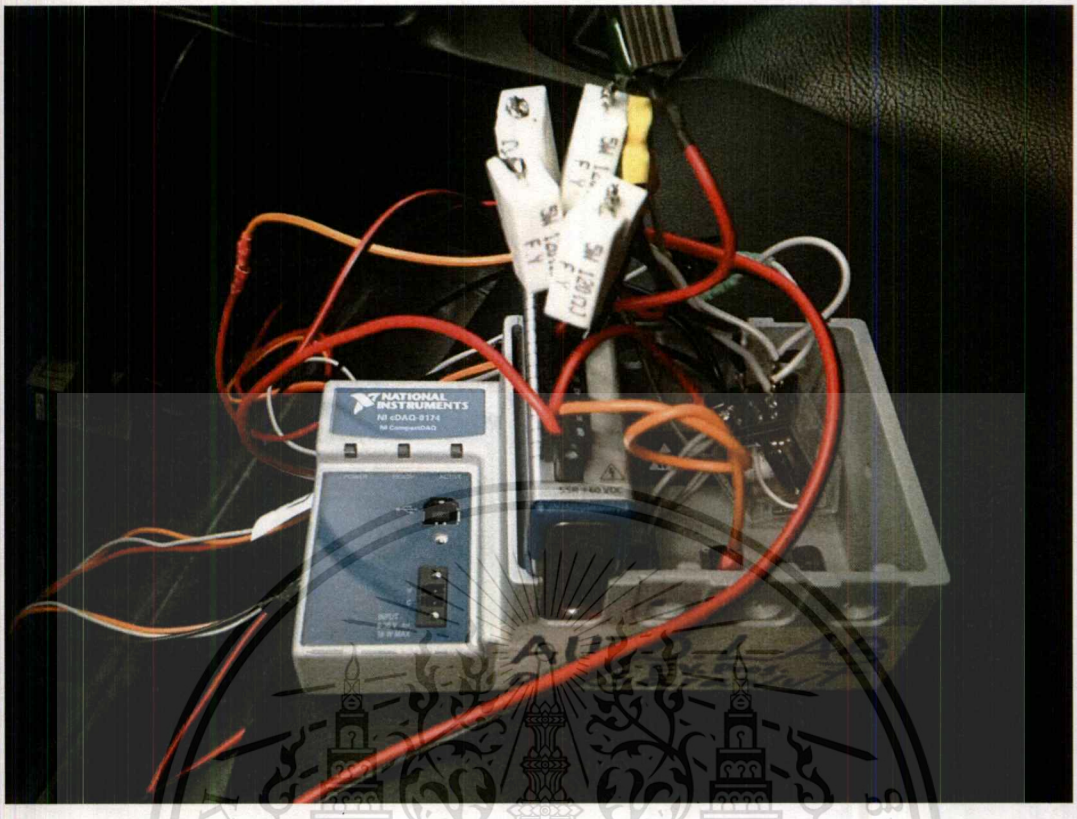

Figure 3.20 IC regulator and resister installed on NI 9485

3.2.1.5 LabVIEW Graphical Programing

LabVIEW is a graphical programming software that uses the data flow programming language to support NI DAQ devices. In this study, the LabVIEW is used to measure, display, and log data of brake pressure and vehicle speed, which are transferred from the NI9205. Moreover, it is used for controlling the NI9485, solid-state relay to generate the emulated ABS signal. Figure 3.21 shows the block diagrams of graphic source codes. The DAQ assistant 2-5 are used for controlling the NI9485 to switch between the real signal and the emulated signal. DAQ assistant 6-7 are used to generate the emulated signal. It acquires the control signal from simulate signal block. In dash frame, the data transferred from NI9205 is read by the DAQ assistant and distributed to each unit-converter and each display block diagram. After that, all displayed data

This material is reserved for educational use only, not allowed for commercial use.
Forbidden to modify the content, and cite the document when use.

are recorded by Write to measurement block. Figure 3.22 illustrated LabVIEW front panel, which is used to display the measured signal and to control the emulated ABS signal.

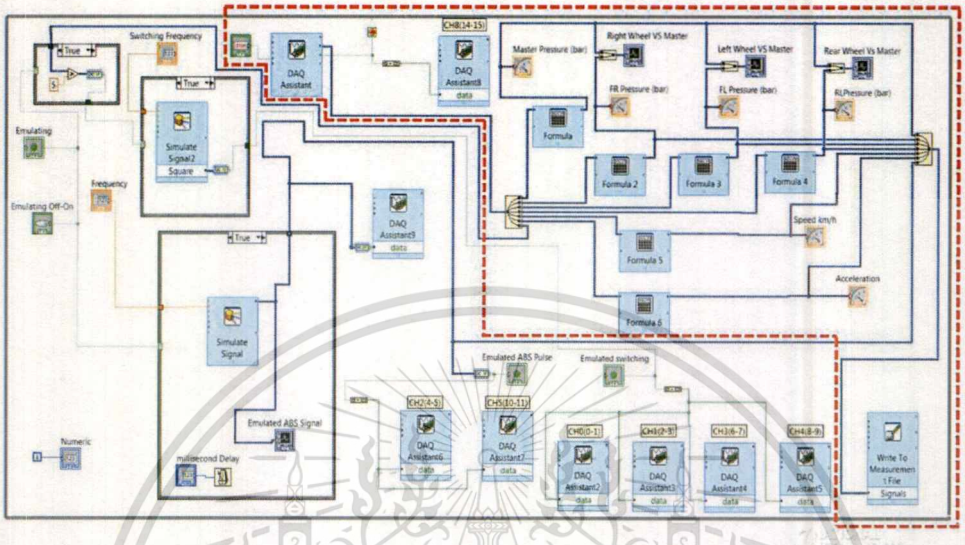

Figure 3.21 LabVIEW programming codes

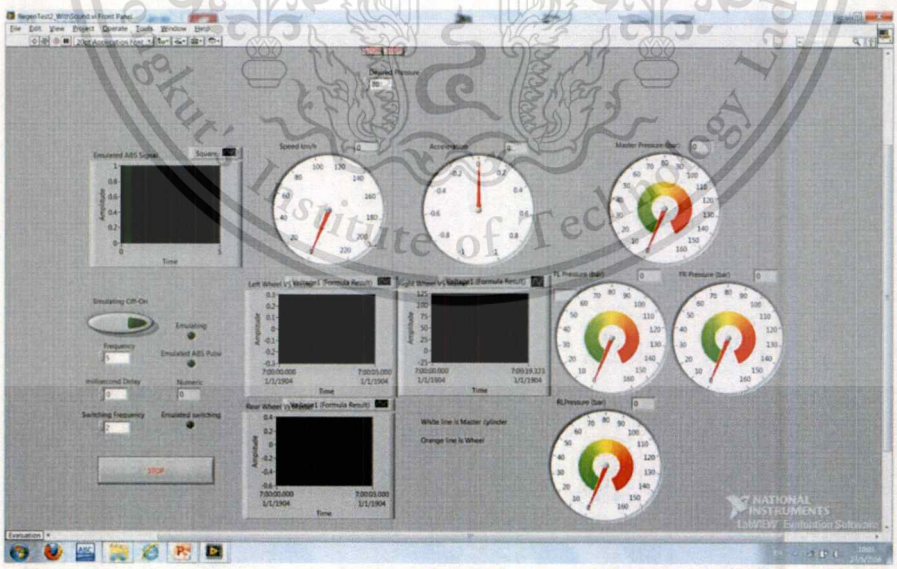

Figure 3.22 LabVIEW front panel for DAQ interface

This material is reserved for educational use only, not allowed for commercial use.
Forbidden to modify the content, and cite the document when use.

3.2.2 Results

As explained in the previous section, the proof of concept is set up to verify the proposed concept. The emulated "wheel lock-up" signal is sent into the ABS to investigate the brake pressure characteristics. In this experiment, eight conditions are set at 40% and 80% of brake pedal travel at the car speed of 20, 40, 50, 60 km/h. The result of 1st condition, 40% brake pedal position and initial speed at 20 km/h, is show in Figure 3.23. Figure 3.23a shows the emulated "wheel lock-up" signal fed to the front wheels channel of the ABS control unit.

Figure 3.23b presents the comparison of brake fluid pressures at the master cylinder, the left front brake caliper, right front brake caliper, and the left rear brake drum and vehicle velocity. The brake pressures of front left and right calipers are regulated down to zero in relation with the emulated "wheel lock-up" signal, shown in Figure 3.23a. However, the brake pressure of rear wheel drum is not reduced, but it equals to that of master cylinder since the emulated "wheel lock-up" signal is sent to only both front wheel channels of the ABS controller. From this result, it is reasonable to conclude that the pressure reduction can be performed until the brake pressure equals to zero. In addition, the brake pressure reduction of each wheel is performed independently.

Figure 3.23c shows the comparison of total braking energy and regenerative one. The ratio of the recovered energy to all braking energy of approximately 65% is reached, since the brake force at the front wheels is regulated to be zero almost all braking time and the brake force distribution ratio between front and rear axle of the experimental car from the calculation is 2:1. Therefore, the braking energy of both front wheels is not dissipated by friction brake but is recovered by regenerative brake up to 65% of all braking energy. This result can be concluded that if the regenerative brake is used instead of the front friction brakes at all braking time, the recovered energy can be achieved up to 65%.

This material is reserved for educational use only, not allowed for commercial use.
Forbidden to modify the content, and cite the document when use.

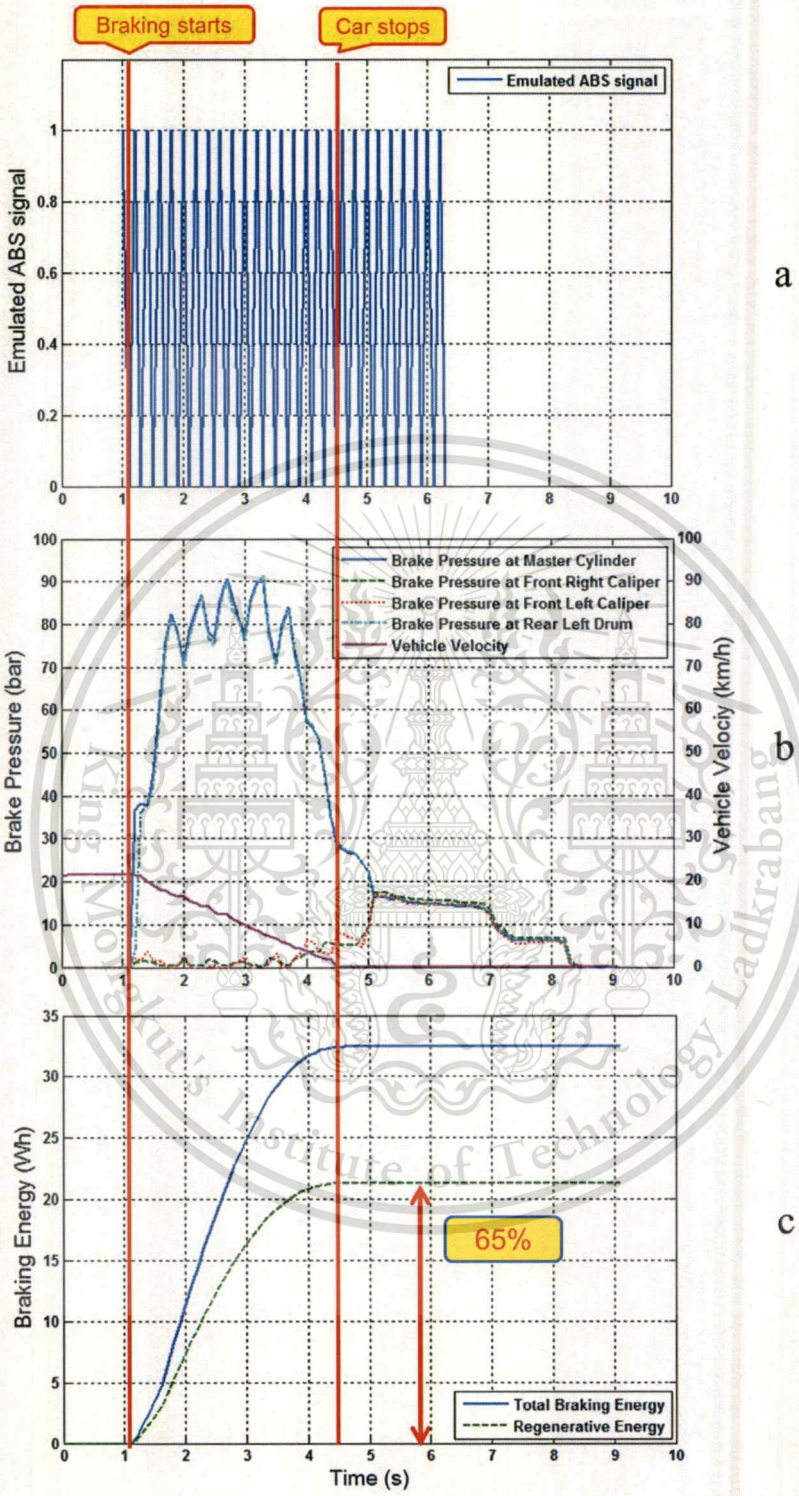

Figure 3.23 Proof of concept results

(1st condition, 40% brake pedal position and initial speed = 20 km/h)

This material is reserved for educational use only, not allowed for commercial use.
Forbidden to modify the content, and cite the document when use.

To verify the feasibility of the proposed scheme at various higher vehicle speeds, the 2nd, 3rd, and 4th condition are set at different higher initial speed. Figure 3.24 shows the result of the 2nd condition, 40% brake pedal position and 40 km/h initial speed. Figure 3.24a shows the emulated "wheel lock-up" signal, used in this condition.

In Figure 3.24b, the brake pressures of both front wheels are reduced at the vehicle speed around 30 km/h. At the same time, the brake fluid pressure at the master cylinder suddenly increases due to the ABS operation, in which the ABS decreases the brake pressures at the front wheel calipers by pumping the brake fluid from the calipers to the damping chamber, located at the master cylinder circuit. From the results of this condition, it is found that the emulated "wheel lock-up" signal is compatible with the velocity that is lower than 30 km/h. Moreover, the brake fluid pressure in the master cylinder circuit increases while the ABS reduces the brake fluid pressure. The reason is that the ABS pumps the brake fluid from the caliper circuit to the master cylinder circuit. The increase of brake pressure in the master cylinder results in the pressure sensor capturing the inaccurate brake demand. Thus, to improve the accuracy of capturing brake demand, a brake force requirement should be measured by a brake pedal position sensor instead of the pressure sensor. In addition, a brake pressure control system at master cylinder circuit should be developed for the proposed scheme to control the brake pressure at the master cylinder not to increase during the period of brake fluid pressure reduction.

Figure 3.24c shows the percentage of recovered energy, about 59%, which is lower than 1st condition because its brake force regulating has not been started since the first time of braking. In the period without the brake pressure reduction, the breaking energy is dissipated by friction brake resulting in the lower recovered energy. From the results, it can be concluded that the amount of recovered energy depends on the quantity of brake pressure reduction.

The result of the 3rd condition, 40% brake pedal position and 50 km/h initial speed is shown in Figure 3.25. The brake pressure reduction of this condition is started at 25 km/h, lower than those of 1st and 2nd, thus the recovered energy is only 38%. The result of this condition proves the conclusion explained in the previous condition. The emulated "wheel lock-up" signal is

This material is reserved for educational use only, not allowed for commercial use.
Forbidden to modify the content, and cite the document when use.

compatible with vehicle speed that is lower than 30 km/h. The less brake pressure reduction the lower recovered energy.

The results of other conditions are also in same tendency and they are displayed in appendix A. From all results, the ABS starts to reduce the brake pressure at the vehicle speed lower than 30 km/h. It can be concluded that the emulated "wheel lock-up" signal is compatible with the vehicle speed lower than 30 km/h. Since the ABS can generally regulate the brake pressure at all speeds. In addition, the emulated "wheel lock-up" signal is identical in all conditions and it is only one factor, used to control the ABS in this experiment. Therefore, if the emulated "wheel lock-up" signal is further studied and improved, the ABS will regulate the brake pressure at all velocities.

In conclusions, the results show the ABS capability of controlling the brake pressure. The feasibility of the proposed scheme is confirmed. Moreover, by the result analysis, the potential of recovered energy is up to 65% of all braking energy according to the ratio of brake force distribution between front axle and rear axle of the experimental car, which is 2:1. However, after the regenerative process, the recovered energy must be stored in the storage devices. A further study is still required to implement the process of energy storage.

King Mongkut's Institute of Technology Ladkrabang

This material is reserved for educational use only, not allowed for commercial use.
Forbidden to modify the content, and cite the document when use.

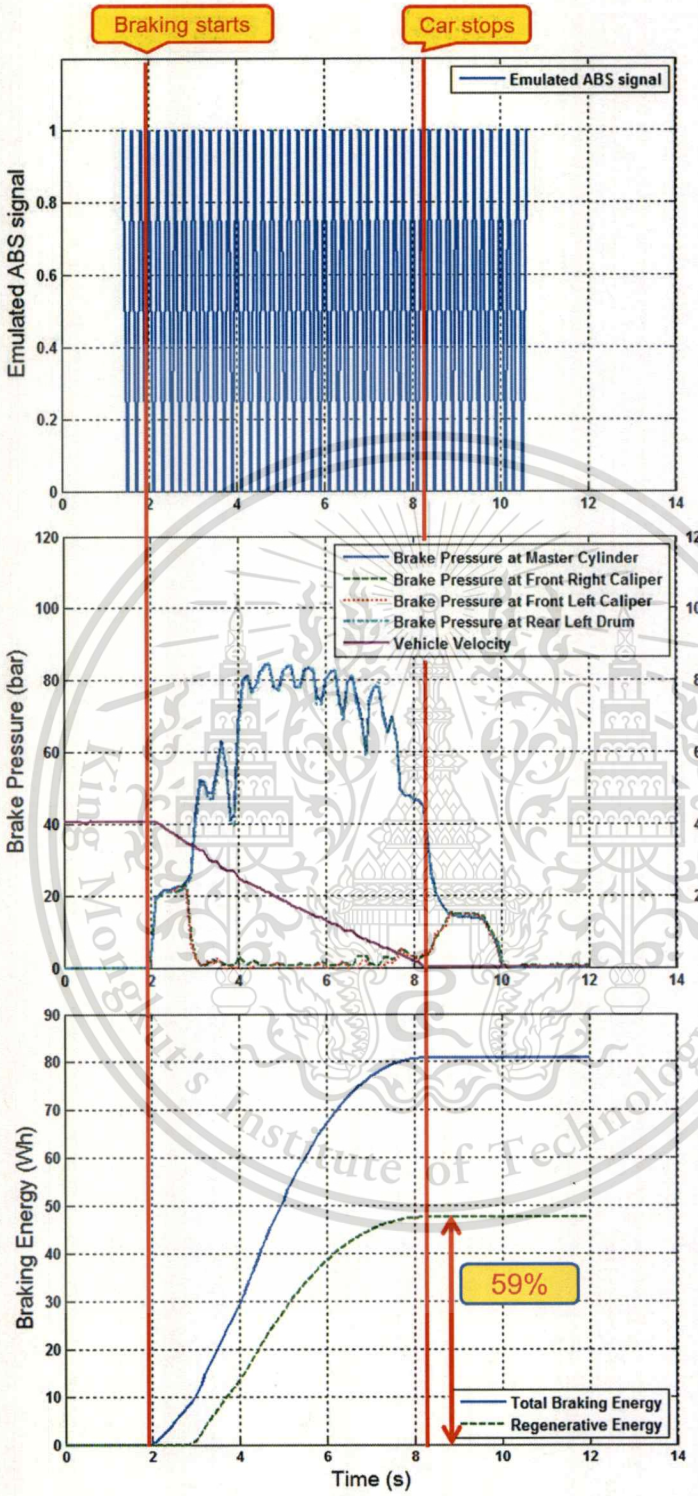

Figure 3.24 Proof of concept results

(2nd condition, 40% brake pedal position and initial speed = 40 km/h)

This material is reserved for educational use only, not allowed for commercial use.
Forbidden to modify the content, and cite the document when use.

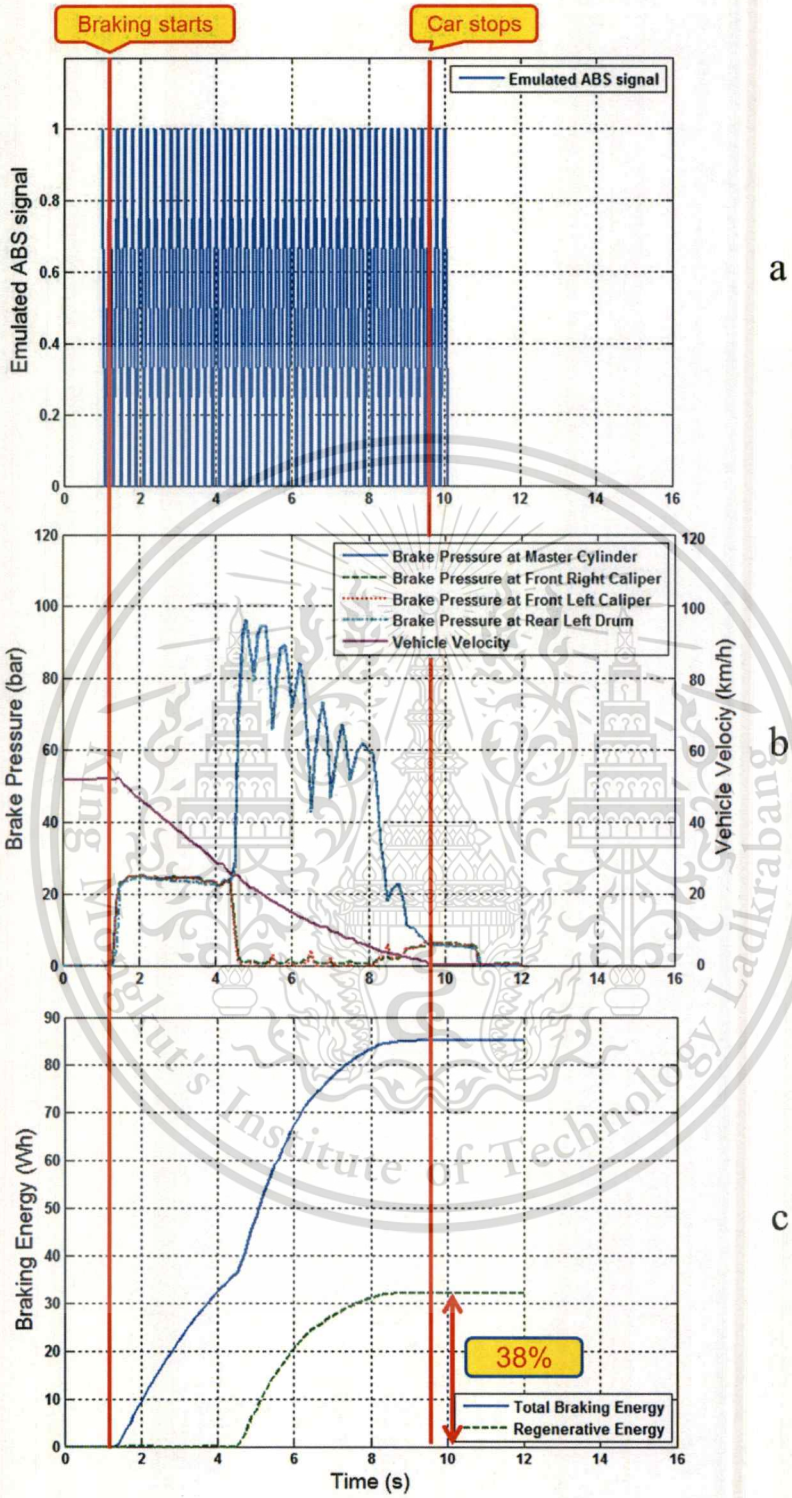

Figure 3.25 Proof of concept results

(3rd condition, 40% brake pedal position and initial speed = 50 km/h)

This material is reserved for educational use only, not allowed for commercial use.
Forbidden to modify the content, and cite the document when use.

3.3 Mathematical Modeling

In this section, the details of mathematical modeling are explained. To predict the performance of the proposed scheme, a computational analysis is adopted. The reference criteria of this analysis are recovery efficiency, safety, and ride comforted during braking. The proposed scheme is benchmarked against the ABS-equipped conventional braking scheme, the parallel scheme, and the modified parallel scheme. The mathematical modeling of this study is formulated in MATLAB/Simulink. The mathematical model mainly composes of the vehicle dynamic model, the ABS-equipped conventional braking model, and the regenerative braking model of the proposed scheme, the parallel scheme, and the modified parallel scheme. The parameters used in the simulation are shown in Table 3.2, Figure 3.26, Figure 3.27, and Figure 3.28. Table 3.2 shows vehicle parameters. Figure 3.26 is the longitudinal coefficient of friction vs. slip. Figure 3.27 displays the torque/speed characteristics of the propelling motor. Figure 3.28 displays the weight factor versus battery SOC.

Table 3.2 Vehicle parameters (* Specification data, ** Estimated data, ***Measured data)

Motor	
Peak torque*	240 Nm
Peak Power*	75 kW
Transaxle system	
Fixed gear ratio (i)*	1.303
Rear axle gear ratio (N_d)*	4.294
Body	
Vehicle mass**	1520 kg
Distance of CG from front axle**	1.25 m
Distance of CG from rear axle**	1.25 m
CG height**	0.8 m
Brake and wheel	
Brake pad friction coefficient*	0.4
Front piston diameter***	57 mm
Rear piston diameter***	29.1 mm
Front disc effective radius***	108.5 mm
Rear disc effective radius***	103.3 mm
Wheel inertia**	6.8 kg−m^2
Wheel radius (17565r15)*	0.32 m

This material is reserved for educational use only, not allowed for commercial use.
Forbidden to modify the content, and cite the document when use.

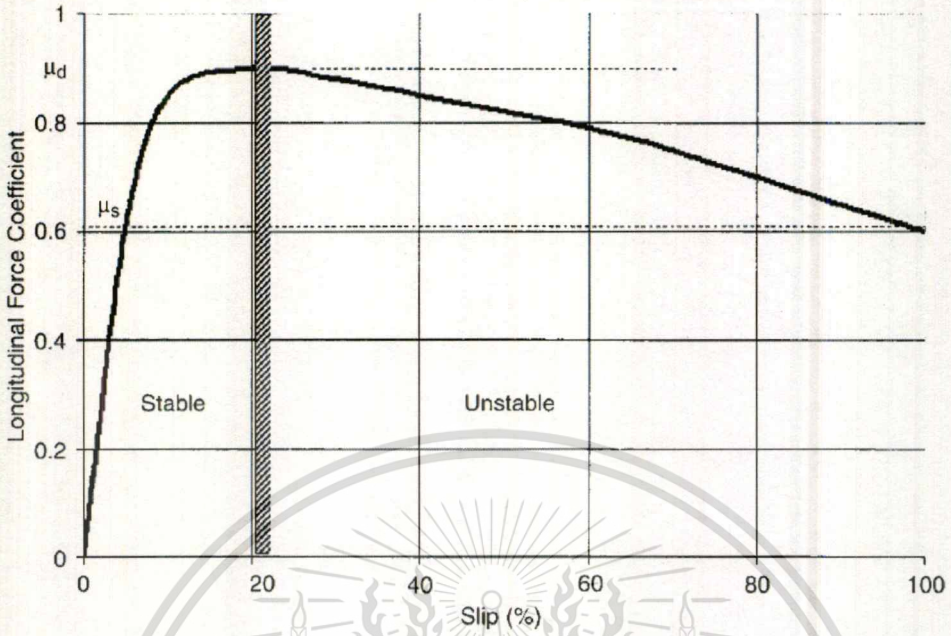

Figure 3.26 Longitudinal coefficient of friction vs. Slip (%) [SAE J2246 (1992)]

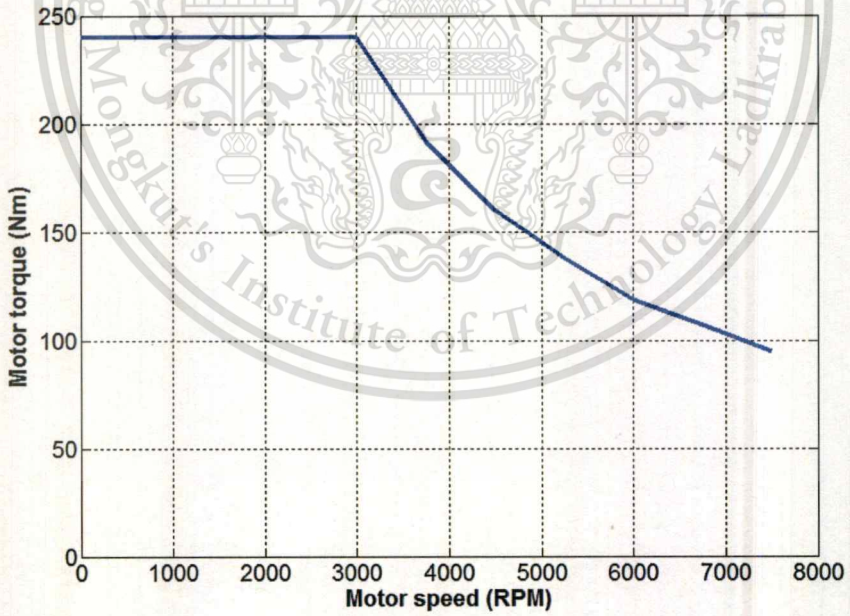

Figure 3.27 Torque/speed characteristics of the propelling motor

This material is reserved for educational use only, not allowed for commercial use.
Forbidden to modify the content, and cite the document when use.

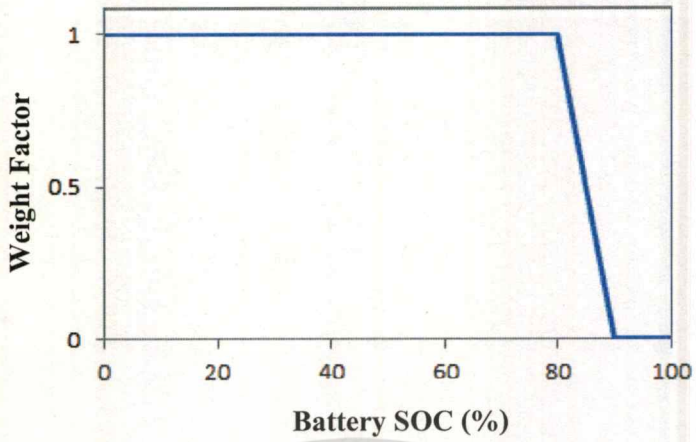

Figure 3.28 Weight Factor vs. Battery SOC (%)

3.3.1 Mathematical Model of ABS-equipped Conventional Braking Scheme

This section talks about the mathematical model of the ABS-equipped conventional braking scheme. Figure 3.29 shows the comprehensive model of the ABS-equipped conventional braking scheme. The model is started by the command of braking pedal position to estimate the amount of friction brake torque in the mechanical brake block. The signal of the mechanical brake block is sent to the ABS modulator in which the mechanical brake torque is regulated. The quantity of the regulated torque depends on the difference between the desired slip and the actual slip. In this study, the desired slip is set at 20%. This slip value maximizes the friction coefficient between tire and road surface thus minimizes the stopping distance as shown in the longitudinal coefficient of friction versus slip data illustrated in Figure 3.26. The actual slip rate is calculated by using equation 3.8 where V_{wheel} is wheel speed and $V_{vehicle}$ is vehicle speed. From this equation, the slip rate is zero percent if the wheel speed and the vehicle speed are even and the slip rate equals to 100% when the wheel is locked up. The ABS controller monitors the different value between the desired slip and the actual slip. If the monitored value is a minus value meaning that the actual slip is more than 20% and the longitudinal force coefficient decreases as shown in Figure 3.26. The ABS controller sends command to the ABS modulator to regulate the friction brake torque.

This material is reserved for educational use only, not allowed for commercial use.
Forbidden to modify the content, and cite the document when use.

After the ABS block, the friction brake torque is sent to the wheel speed block in the vehicle dynamic model. The wheel speeds are calculated by using the friction brake torque and the tire force. The tire force is also used for calculating the vehicle speed. After these calculations, the wheel speed and the vehicle speed are sent to calculate the actual slip. The actual slip is used for the ABS model, explained above and for the estimation of the friction coefficient (μ) between tire and road surface. In the mu-slip look-up table block, the friction coefficient (μ) is estimated by using the data shown in Figure 3.26. The tire force is calculated by using the friction coefficient (μ) and the vertical load. During braking, the vertical loads acted on the front and rear axle are dynamically changed by inertia effect. The calculation of the vertical load is done by using equation 3.9 and 3.10. W_f' and W_r' are vertical load of front and rear axle, respectively. m is vehicle mass. g is gravity of acceleration. a_x is longitudinal deceleration. c, d, and h are distance of the center of gravity from front axle, rear axle, and center of gravity height, in that order, as shown in Figure 3.30. The calculation of the front tire forces and the rear tire forces is performed by using equation 3.11 and 3.12, respectively. F_{bf} is front tire force and F_{br} is rear tire force. $\mu(s)$ is the friction coefficient between tire and road surface getting from the Mu-slip block and f and r indices refer to front and rear tire. As explained about the input of the wheel speed block, the front and rear wheel velocity is calculated by equation 3.13 and 3.14, respectively. I_{wheel} is the wheel moment inertia, R_t is tire radius, T_{bf} is front brake torque generated by friction brake. T_{br} is rear brake torque generated by friction brake. The vehicle velocity is calculated by using equation 3.15.

The mathematical model calculates the longitudinal load transfer of the vehicle during braking. The longitudinal load transfer represents the passenger ride comfort. Its calculation is done by using equation 3.16. The longitudinal load transfer ratio during a braking period is defined as the load transfer from the rear axle to the front axle that results from a forward longitudinal force acting at the center of gravity at a height above the road surface (forward longitudinal force possibly corresponding to the inertial force at braking) [32].

This material is reserved for educational use only, not allowed for commercial use.
Forbidden to modify the content, and cite the document when use.

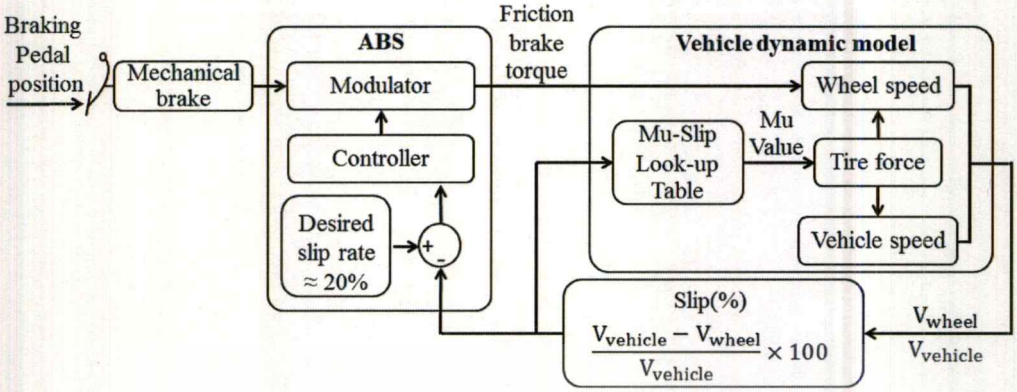

Figure 3.29 Comprehensive model of ABS-equipped conventional braking scheme

$$\text{Slip}(\%) = \frac{V_{vehicle} - V_{wheel}}{V_{vehicle}} \times 100 \tag{3.8}$$

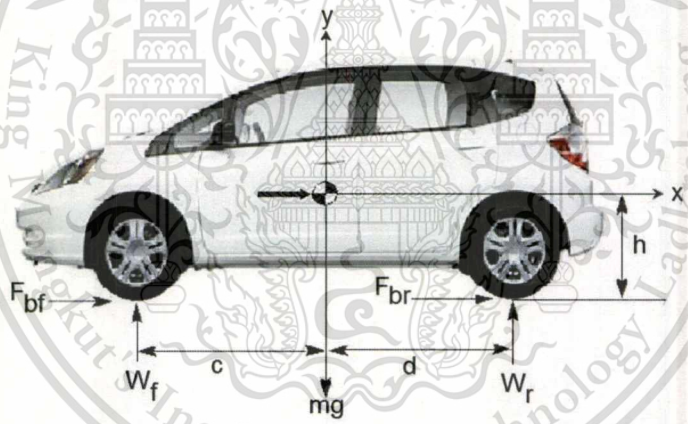

Figure 3.30 Free-body diagram of a car during braking

$$W_f' = \frac{mgd}{c+d} + \frac{ma_x h}{c+d} \tag{3.9}$$

$$W_r' = \frac{mgc}{c+d} - \frac{ma_x h}{c+d} \tag{3.10}$$

$$F_{bf} = \mu_f(s_f) \times W_f' \tag{3.11}$$

This material is reserved for educational use only, not allowed for commercial use.
Forbidden to modify the content, and cite the document when use.

$$F_{br} = \mu_r(s_r) \times W'_r \tag{3.12}$$

$$I_{wheel}\frac{d\omega}{dt} = (R_t \times F_{bf}) - T_{bf} \tag{3.13}$$

$$I_{wheel}\frac{d\omega}{dt} = (R_t \times F_{br}) - T_{br} \tag{3.14}$$

$$m\frac{dv}{dt} = -(F_{bf} + F_{br}) \tag{3.15}$$

$$\text{Longitudinal load transfer} = \frac{W'_f - W'_r}{W'_f + W'_r} \tag{3.16}$$

3.3.2 Mathematical Model of Proposed Regenerative Scheme

This section explains about the mathematical model of the proposed scheme. The comprehensive model of the proposed Scheme is shown in Figure 3.31. This model mainly composes of the model of ABS-equipped conventional brake explained in the previous section and the model of proposed scheme. The regenerative model receives the signal of master cylinder pressure to estimate the regenerative brake demand. Another input signal is the wheel speed, used for calculating the available regenerative brake torque in the motor torque characteristic block. The available regenerative brake torque force is regulated by multiplying the weight factor W.F. (SOC) block and regulating under the brake torque demand in the torque demand limitation block. The weight factor (W.F.), which is the function of battery SOC, is illustrated in Figure 3.28. The weight factor is assigned to be one from SOC = 0% to SOC = 80%, meaning the battery is fully capable for charging. In the SOC range of 80%-90%, the weight factor is linearly decreased from one to zero. From SOC = 90% onwards, the weight factor is set to be zero to protect the battery from overcharging. The torque demand limitation block regulates the regenerative brake torque not exceeding the brake demand. After that, the emulated-signal controller receives the signal of the brake demand, the regenerative brake torque, and the friction brake torque. It checks if the brake demand given by the driver is equal to the summation of front

This material is reserved for educational use only, not allowed for commercial use.
Forbidden to modify the content, and cite the document when use.

wheel frictional brake torque and front wheel regenerative torque. In the case that the condition is false, the control unit feeds an emulated "wheel lock-up" command to the block of slip rate switching. Whenever the slip rate switching block receives the emulated "wheel lock-up" command, it provides emulated wheel lock-up slip rate into ABS block to decrease braking torque of frictional braking system. By using this means, the reduced braking torque is as close as the provided regenerative one. Nonetheless, this model has both regenerative brake torque and friction brake torque acting on the front wheels. The calculation for the front wheel speed is different from that of ABS-equipped conventional brake model. The front wheel speed is calculated by equation 3.17, which is different from equation 3.14 of ABS-equipped conventional brake model. T_{regf} is regenerative braking torque at the front wheels. In addition, there is the calculation of the regenerative efficiency, which is added into this model. The regenerative efficiency is calculated by equation 3.18.

$$I_{wheel}\frac{d\omega}{dt} = (R_t \times F_{bf}) - T_{bf} - T_{regf} \tag{3.17}$$

$$\text{Regenerative efficiency} = \frac{\int_o^t T_{regf} d\theta}{\int_0^t (T_{bf} + T_{br}\, T_{regf}) d\theta} \tag{3.18}$$

This material is reserved for educational use only, not allowed for commercial use.
Forbidden to modify the content, and cite the document when use.

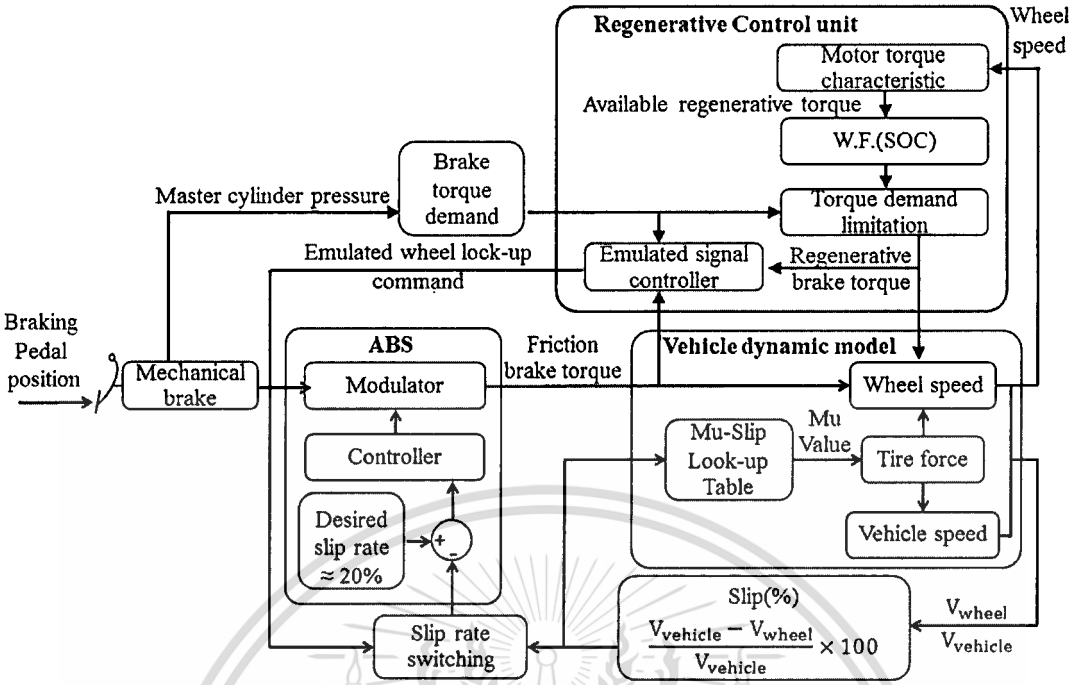

Figure 3.31 Comprehensive model of proposed regenerative scheme

3.3.3 Mathematical Model of Parallel Regenerative Scheme

This section provides details of the mathematical model of the parallel scheme. The comprehensive model of the parallel regenerative scheme is shown in Figure 3.32. This model is mainly divided into two parts, the ABS-equipped conventional brake model and the parallel scheme model. About background of the parallel scheme, its working principle is that the regenerative brake force is provided in parallel with the friction brake force. In the motor torque characteristic, the wheel speed signal is adopted to estimate the available regenerative torque from motor. The amount of regenerative brake force is regulated by the W.F. (SOC) and the brake demand as same as the model of the proposed scheme explained in the previous section. The front wheel speed of this model is calculated by using equation 3.17 as same as that of the proposed scheme model.

This material is reserved for educational use only, not allowed for commercial use.
Forbidden to modify the content, and cite the document when use.

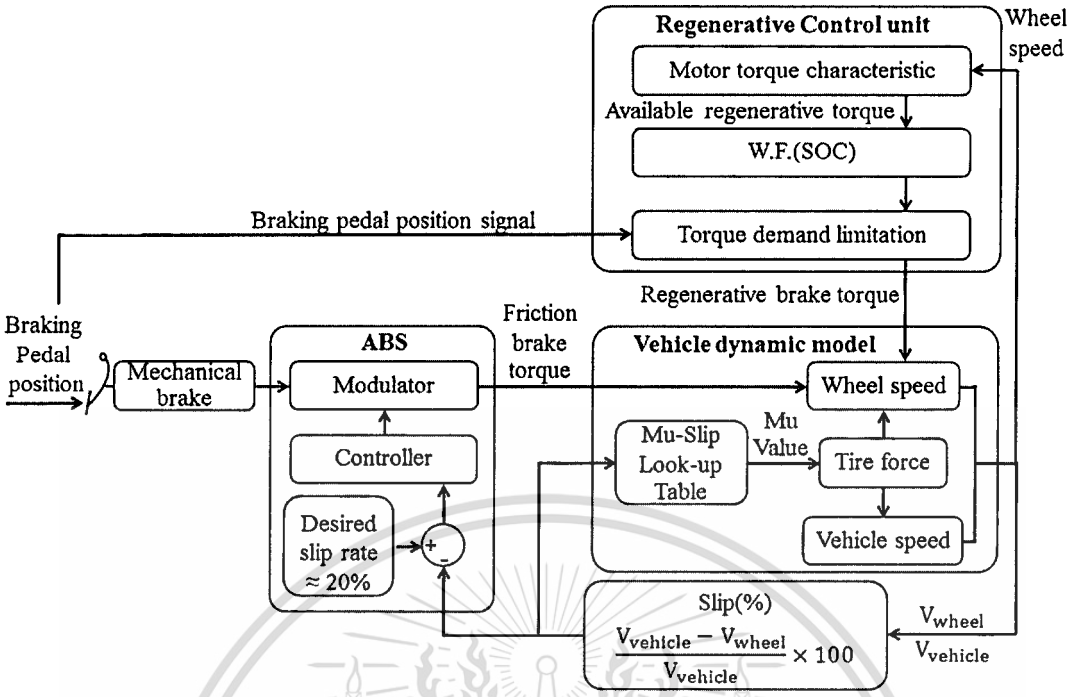

Figure 3.32 Comprehensive model of parallel regenerative scheme

3.3.4 Mathematical Model of Modified Parallel Regenerative Scheme

This section explains about the mathematical model of the modified parallel scheme. For the background of the modified parallel scheme, this scheme is developed from the parallel regenerative scheme by adding a friction brake force controller to allow only the operation of regenerative brake. The idea of this add-on feature is to control solenoid valve to pause brake fluid pressure until the required braking force of four wheels is greater than the available regenerative brake force. Therefore, this simulation model, shown in Figure 3.33, is also developed from the model of the parallel scheme. The brake torque requirement is sent to the block of torque demand limitation and solenoid valve controller. The solenoid valve controller block is responsible for controlling solenoid valve in the block of mechanical brake. It compares between the braking torque demand of four wheels and the available regenerative braking torque in order to send the command of solenoid valve control into the mechanical brake block. The condition of comparison is shown in the final condition of the flowchart in Figure 2.20.

This material is reserved for educational use only, not allowed for commercial use.
Forbidden to modify the content, and cite the document when use.

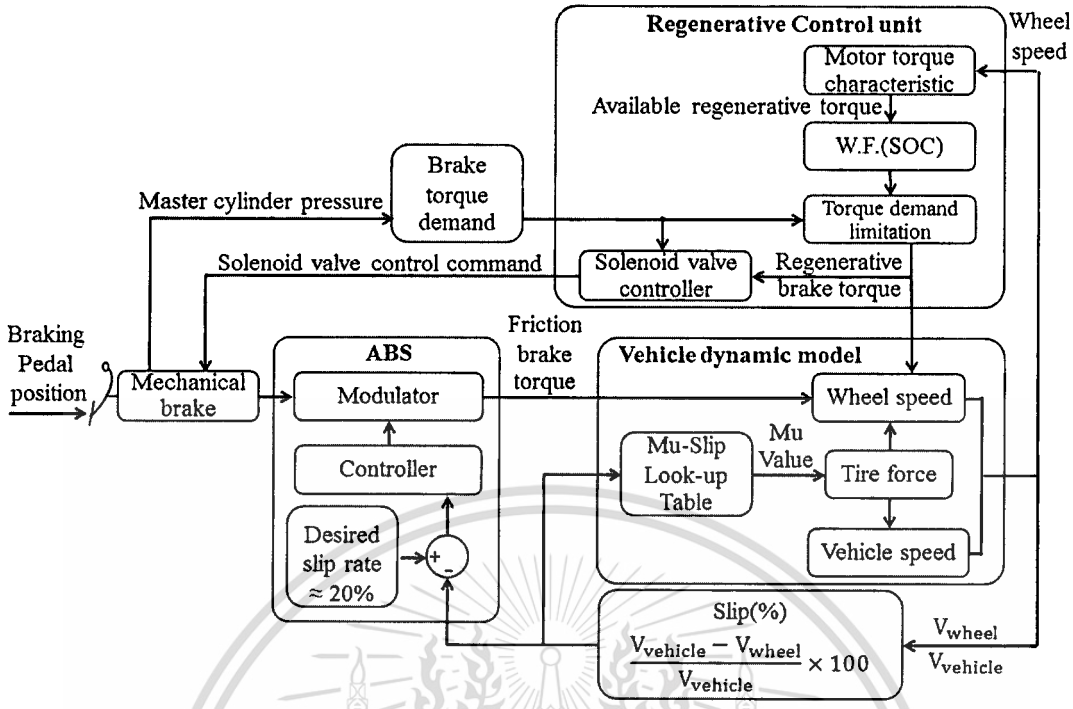

Figure 3.33 Comprehensive model of modified parallel regenerative scheme

3.4 Verification of Brake Model

This section focuses on the verification of the mathematic brake model. The main objective of this experiment is to verify the mathematical brake model. Since the brake model is the most important part of this mathematical analysis, its accuracy is verified. This experimental verification is also carried out by field test as same as the proof of concept. Test procedure is started by field tests at different conditions to record data of brake force demand and vehicle velocity. Then, the recorded data of brake force demand are fed into mathematical brake model to calculate vehicle velocity and acceleration of each condition. After that, the calculated results are compared with experimental results to verify the accuracy of simulation model. Since this mathematical model uses the most similar parameters with the experimental vehicle, if the mathematical model is correct, the calculated results should be similar to the experimental results. In this experiment, six conditions are set at 40% and 80% of brake pedal travel at car speed of 40,

This material is reserved for educational use only, not allowed for commercial use.
Forbidden to modify the content, and cite the document when use.

50, 60 km/h. Each condition is repeated 3 times as same as the proof of concept; so overall test number is 18 times as shown in Table 3.3.

Table 3.3 Test conditions for verification of brake model

Testing Number	% Brake Pedal	Testing Velocity (km/h)	Number of times
1	40%	40	1
2			2
3			3
4		50	1
5			2
6			3
7		60	1
8			2
9			3
10	80%	40	1
11			2
12			3
13		50	1
14			2
15			3
16		60	1
17			2
18			3

3.4.1 Results

In this section, the verification results of brake model are presented and discussed. For the results of the first condition, the comparison of experimental velocity and calculated one as well as the input brake pressure are shown in Figure 3.34. The first condition is 40% brake pedal and 40 km/h initial velocity. The calculated velocity and the real one are quite similar and its average error is less than 10%. This error is potentially due to the approximation of some simulation parameters. However, there are unsmooth points of real velocity in the period of 2.2 to 3 seconds. These unsmooth points are caused by the unsmooth surface of testing track. Since the slightly unsmooth testing track is the factor unable to control and the error is in the accepted range, thus the mathematical model does not consider this effect. Later, the comparison of experimental and calculated acceleration is shown in Figure 3.35. Their accelerations are same in tendency.

This material is reserved for educational use only, not allowed for commercial use.
Forbidden to modify the content, and cite the document when use.

However, the experimental acceleration has unsmooth points at the same period of unsmooth velocity since the experimental accelerations is calculated by the experimental velocity.

Figure 3.36 shows the comparison of experimental velocity and calculated velocity as well as brake pressure profile of the 2nd condition, initial velocity 50 km/h and brake pedal position 40%. The experimental and calculated acceleration of the 2nd condition is shown in Figure 3.37. The experimental vs. calculated velocity and brake fluid pressure of the 3rd condition, initial velocity 60 km/h and brake pedal position 40%, is shown in Figure 3.38. The experimental and calculated acceleration of the 3rd condition is shown in Figure 3.39. The results of other conditions are shown in appendix B. All calculation results are similar to their experimental results and there are some unsmooth points in experimental results due to the effect of unsmooth testing track. In conclusion, the mathematical brake model of this study is verified. The computational findings and experimental results are similar. Their average errors are less than 10%.

King Mongkut's Institute of Technology Ladkrabang

This material is reserved for educational use only, not allowed for commercial use.
Forbidden to modify the content, and cite the document when use.

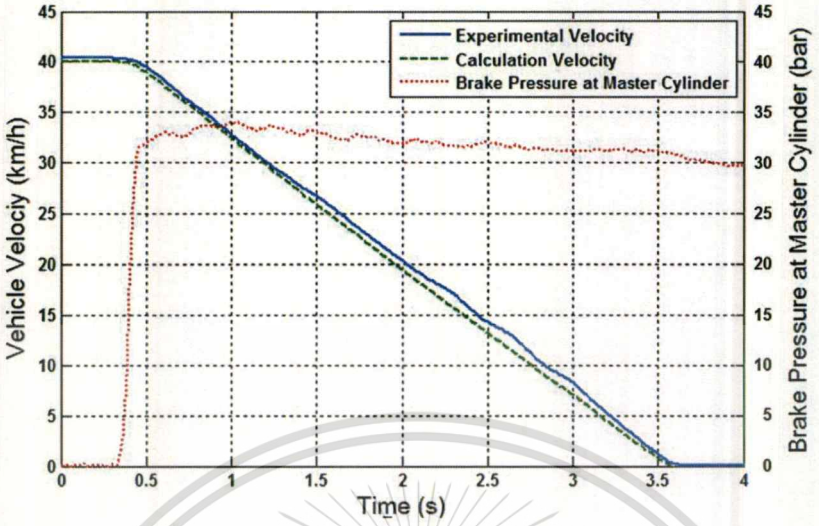

Figure 3.34 Calculation vs. experimental velocity and brake fluid pressure (1^{st} condition, 40% brake pedal position and initial speed = 40 km/h)

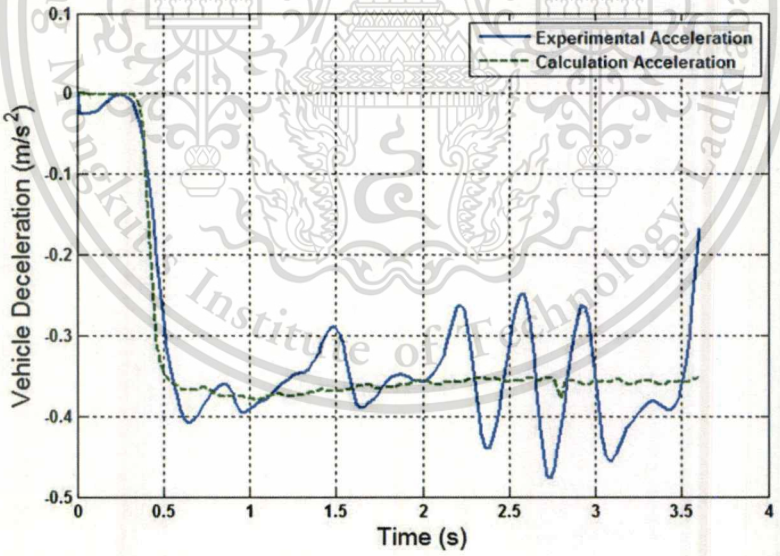

Figure 3.35 Calculation vs. experimental deceleration (1^{st} condition, 40% brake pedal position and initial speed = 40 km/h)

This material is reserved for educational use only, not allowed for commercial use.
Forbidden to modify the content, and cite the document when use.

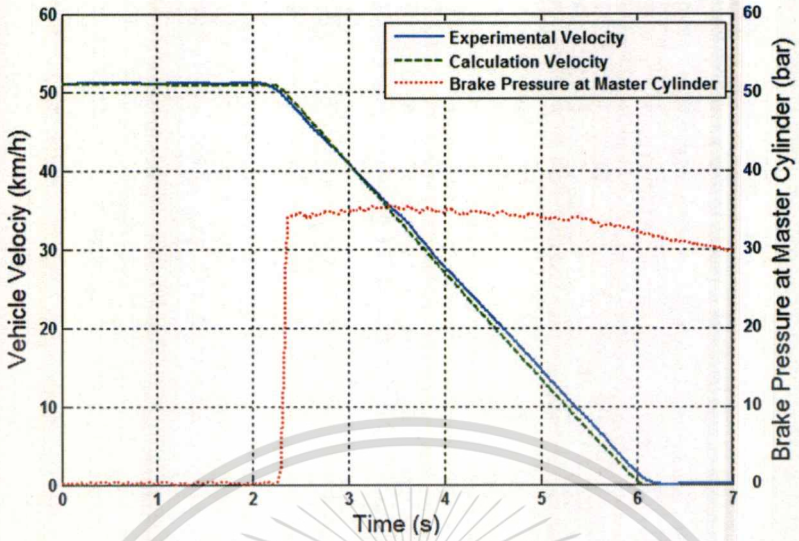

Figure 3.36 Calculation vs. experimental velocity and brake fluid pressure (2^{nd} condition, 40% brake pedal position and initial speed = 50 km/h)

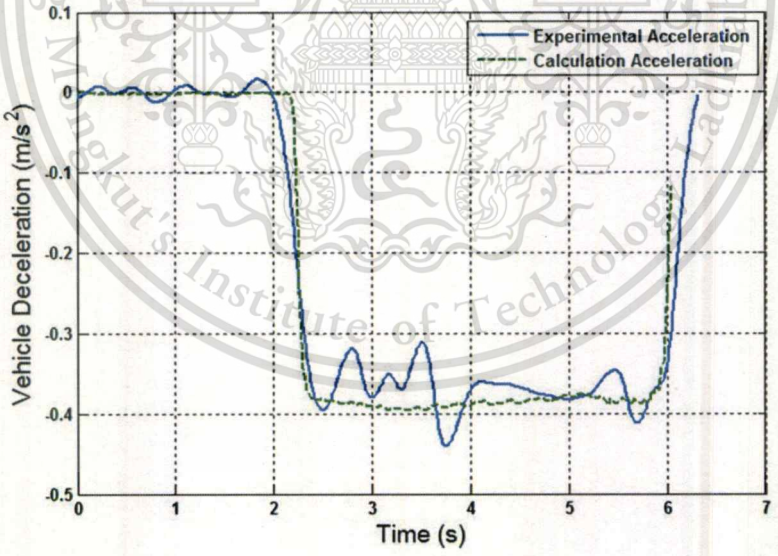

Figure 3.37 Calculation vs. experimental deceleration (2^{nd} condition, 40% brake pedal position and initial speed = 50 km/h)

This material is reserved for educational use only, not allowed for commercial use.
Forbidden to modify the content, and cite the document when use.

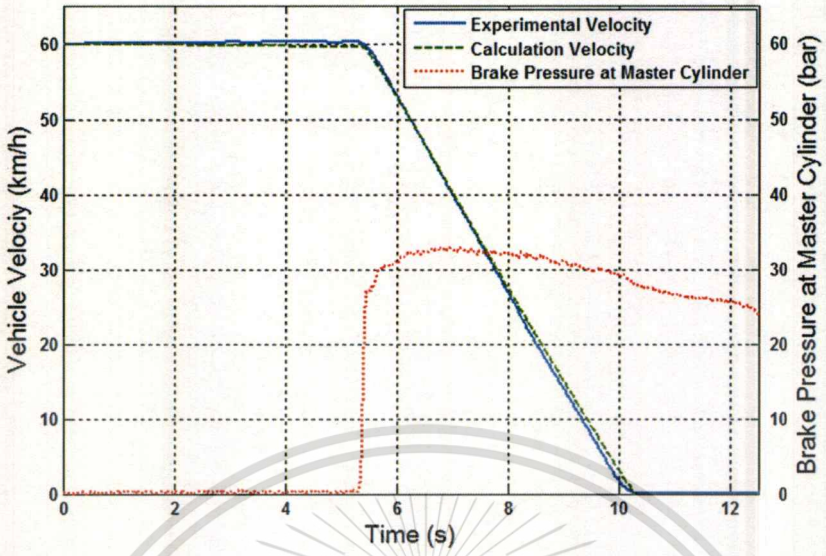

Figure 3.38 Calculation vs. experimental velocity and brake fluid pressure (3^{rd} condition, 40% brake pedal position and initial speed = 60 km/h)

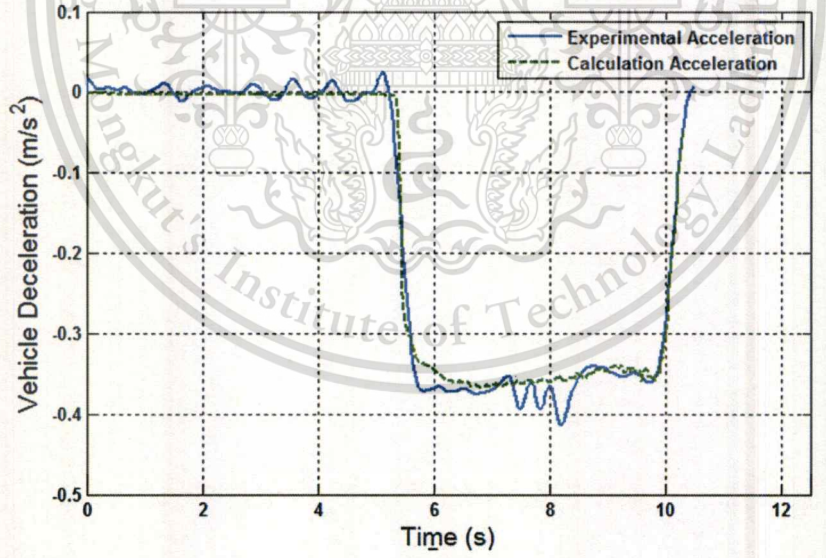

Figure 3.39 Calculation vs. experimental deceleration (3^{rd} condition, 40% brake pedal position and initial speed = 60 km/h)

This material is reserved for educational use only, not allowed for commercial use.
Forbidden to modify the content, and cite the document when use.

CHAPTER 4

SIMULATION RESULTS AND DISCUSSIONS

This chapter presents the calculation results obtained from the mathematical model explained in the previous chapter. In addition, the discussions of results are provided in this chapter. The performance of the proposed scheme is compared to those of ABS-equipped conventional brake scheme, parallel regenerative scheme, and modified parallel regenerative scheme.

4.1 Characteristics of Regenerative Braking Schemes

As explained in the previous chapter, each of regenerative schemes has its own characteristics of brake force distribution. The brake force distribution of the regenerative schemes is the process of proportioning between a regenerative brake force and a friction brake force. This section discusses about the brake force distribution of each scheme. The comparisons of brake force demand and friction brake force at the front wheels are presented. The brake force demand and the friction brake force at the front wheels are displayed in the form of brake fluid pressures at the master cylinder and at the front wheel calipers, respectively. Figure 4.1 shows the master cylinder and front caliper brake pressure contours of the proposed scheme, the ABS-equipped conventional brake scheme, the parallel scheme, and the modified parallel scheme. These results are calculated under identical conditions of brake force demand, initial velocity, and normal braking without wheel slip. The solid line is the brake pressure at the outlet of master cylinder, representing the demanded brake force. The dotted line is the brake pressure in the front brake caliper, representing the amount of friction brake force.

Figure 4.1(a) presents the brake pressure contours of the proposed scheme. From the figure, it is obvious that the friction brake pressure is less than the required brake pressure. The proposed scheme decreases the amount of friction brake force as equal as the amount of available regenerative brake force. By sending an emulated "wheel lock-up" signal to the ABS control unit,

This material is reserved for educational use only, not allowed for commercial use.
Forbidden to modify the content, and cite the document when use.

the pressure of the frictional brake is decreased, resulting in the reduced friction brake force. The amount of this reduced brake force is subsidized by that of the regenerative one. The summation of the friction brake force and the regenerative one still equals to the brake force demand.

Figure 4.1(b) shows the brake pressure contours of the ABS-equipped conventional brake scheme. The brake pressure in the front calipers is identical to the brake pressure at the master cylinder. In a normal braking situation, an ABS-equipped conventional brake does not alter the brake pressure provided to the brake force generator. Only in the case of wheel locking-up, the ABS-equipped conventional brake scheme alters the amount of brake pressure by reducing the brake pressure. Thus, the provided friction brake force of the front wheels entirely equals to the demanded brake force.

Figure 4.1(c) illustrates the brake pressure contour of the parallel regenerative scheme. The amount of friction brake force is provided as equal as that of brake force demand. Since the friction brake force of the parallel scheme is provided as same as that of the ABS-equipped conventional brake scheme, the brake pressure at the front calipers is identical to that at the master cylinder. Simultaneously, the regenerative brake force is provided in parallel with the friction brake force. Since the front wheels have two brake forces working together, its braking time is shorter than that of the ABS-equipped conventional brake.

Figure 4.1(d) provides the brake pressure contours of the modified parallel regenerative scheme. From the figure, during the period of 0-0.4 second, the brake fluid pressure in the calipers equals to zero, since the scheme regulates the brake fluid pressure to be zero by a solenoid valve. If the brake force demand is less than the available regenerative brake force, the solenoid valve will cut the brake pressure. During this period, only the regenerative brake force is provided at its full capacity. After this period, the brake force demand is greater than the available regenerative brake force. The solenoid valve allows the brake fluid to flow to the calipers, thus the brake pressure in the calipers equals to the brake pressure demand. In addition, the regenerative brake force is still provided in parallel with the friction brake force as same as the

This material is reserved for educational use only, not allowed for commercial use.
Forbidden to modify the content, and cite the document when use.

parallel scheme. Therefore, its braking time is shorter than that of the ABS-equipped conventional brake.

In conclusion, the friction brake pressure progression of each scheme is compared in this section. The friction brake force of the proposed scheme is reduced as equal as the amount of regenerative brake force. Thus, the summation of the friction brake force and the regenerative one is equal to the amount of brake force demand. With this reason, the amount of brake force generated by the proposed scheme equals to the amount of brake force generated by the ABS-equipped conventional brake scheme. Therefore, their braking performances are identical. The braking time of both parallel schemes is shorter than that of the ABS-equipped conventional brake scheme, since they have an additional regenerative brake forces provided in parallel with the friction brake forces. During a braking situation, the brake force distribution is an important factor that influences to the braking distance, longitudinal load transfer, and regenerative efficiency. In the later sections, the results of the braking distance, the longitudinal load transfer during braking, and the regenerative efficiency are presented and discussed.

This material is reserved for educational use only, not allowed for commercial use.
Forbidden to modify the content, and cite the document when use.

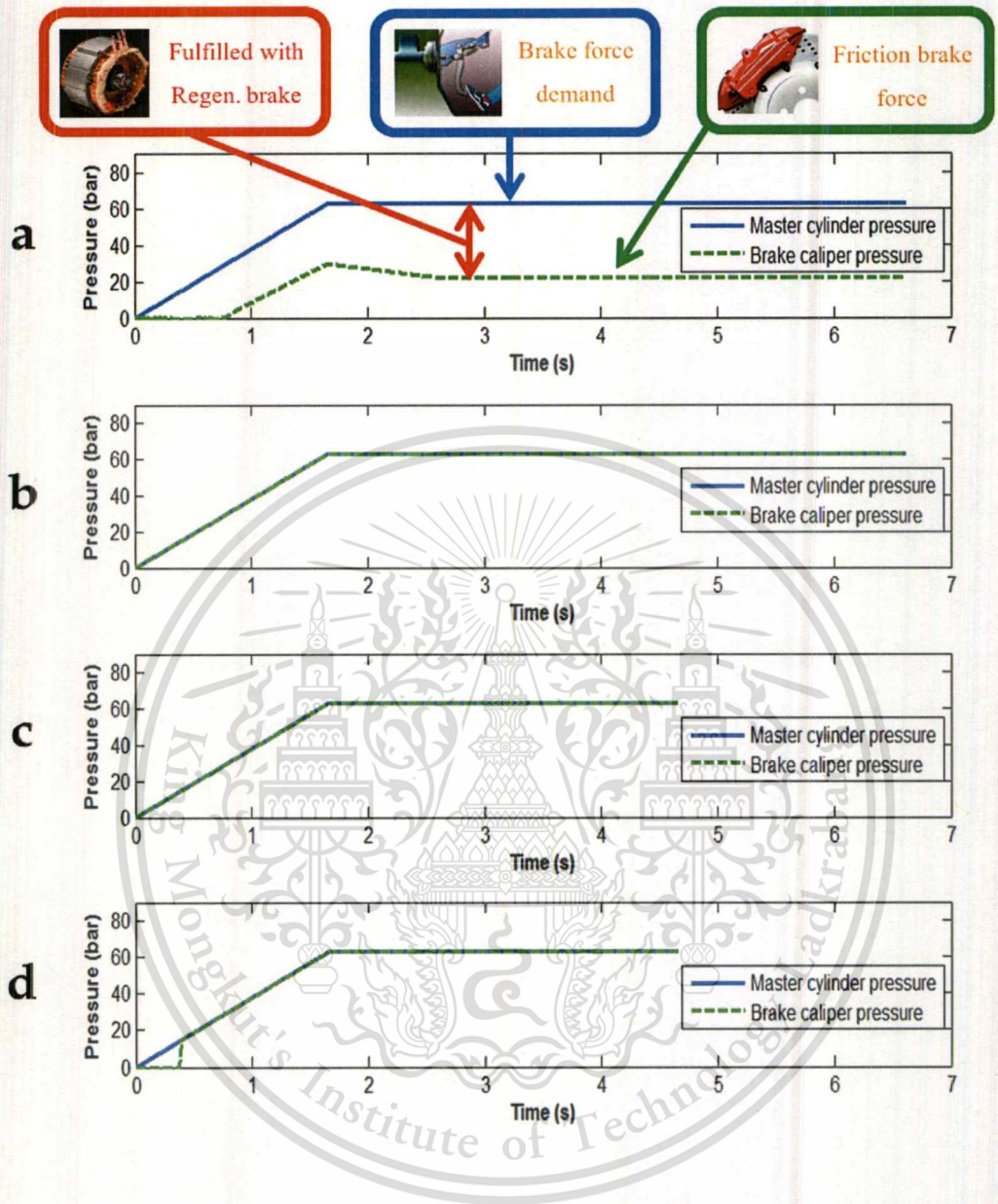

Figure 4.1 Brake pressure contour. a) Proposed regenerative scheme. b) ABS-equipped conventional scheme. c) Parallel regenerative scheme. d) Modified parallel regenerative scheme.

This material is reserved for educational use only, not allowed for commercial use.
Forbidden to modify the content, and cite the document when use.

4.2 Braking Distance

In this section, the results of braking distance are presented and discussed. A braking distance is defined as the distance traveled from the point where a vehicle starts to be applied its brakes to the point where it comes to completely stop. Figure 4.2 presents the comparison of braking distances calculated from the mathematic models of proposed scheme, ABS-equipped conventional brake scheme, parallel scheme, and modified parallel scheme. From Figure 4.2, the braking distance of the proposed scheme is identical to that of the conventional brake, since their brake force distribution of both systems are identical. Whereas, the braking distances of both parallel schemes are shorter than those of the proposed scheme and the ABS-equipped conventional brake scheme. The main reason of this shorter braking distance is the additional regenerative brake force applied at the front wheels. Nevertheless, this shorter braking distance caused by the over demand of brake force may not be safe in some road conditions. For example, on a slippery road surface, the over-demanded brake force can lead to a wheel lock and then loss of vehicle maneuverability and stability.

In summary, the braking distance mainly corresponds to the brake force distribution explained in the last section. The proposed scheme can provide the braking distance as identical as that of the ABS-equipped conventional brake scheme because of similar brake force distributions in both systems.

This material is reserved for educational use only, not allowed for commercial use.
Forbidden to modify the content, and cite the document when use.

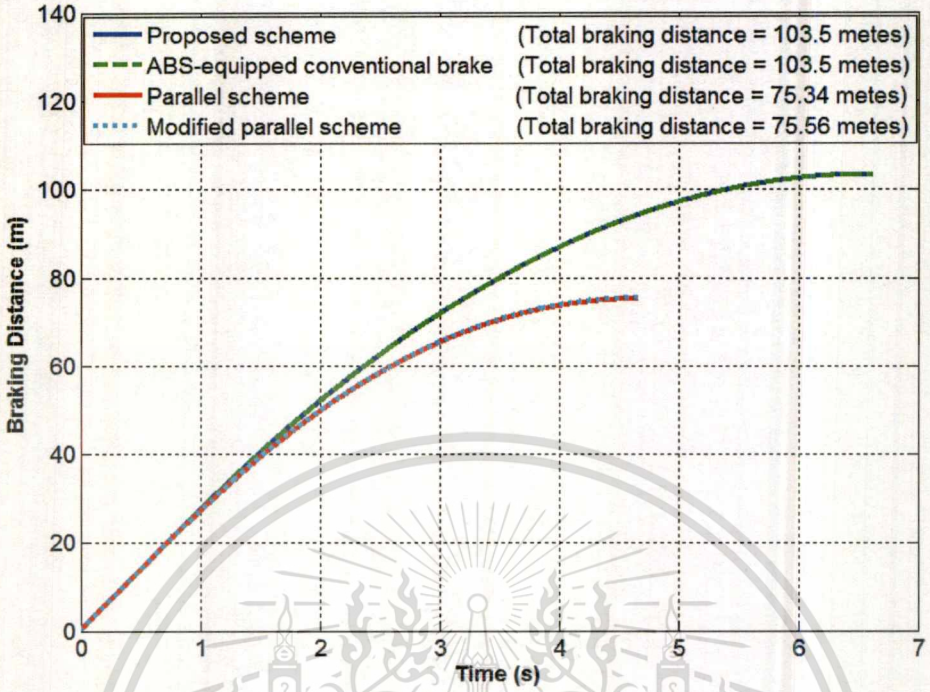

Figure 4.2 Braking distance

4.3 Regenerative Efficiency

This section presents and discusses about the regenerative efficiency. The regenerative efficiency indicates the proportion of recovered braking energy. It is calculated by the ratio between the recovered braking energy and the entire supplied braking energy. The calculation of the regenerative efficiency is explained in Section 3.3.2. The estimated efficiency of each scheme is illustrated in Figure 4.3. The final accumulative efficiency achieved by the proposed scheme is higher than those achieved by the parallel schemes. As explained in the previous section, the proposed scheme allows the operation of regenerative brake at its full capacity, since it is able to regulate the amount of friction brake force. In the case of parallel schemes, the regenerative brake forces are limited instead of the friction brake force, since the parallel schemes cannot regulate the friction brake force. The brake force limitation is done to maintain the distribution between the front and rear brake forces similar to that of the conventional braking system. The brake force

This material is reserved for educational use only, not allowed for commercial use.
Forbidden to modify the content, and cite the document when use.

distribution of the conventional braking system is set to follow the ideal brake force distribution. If a car is desired for the front and rear wheels to lock up at the same time on any road, the braking force on the front and rear axle must closely follow the ideal brake force distribution [16]. If the regenerative brake force is limited, the lower regenerative efficiency is achieved. With the reason of brake force limitation, the parallel schemes attain lower final regenerative efficiency than the proposed scheme. The behavior variation of the proposed scheme efficiency is characterized by the friction and regenerative brake force distribution. Referred to Figure 4.1a, the brake pressures of the front wheels calipers are regulated to be zero at the beginning period of braking in which the front wheels have only the operation of regenerative brakes. After this period, the friction brake cooperates with the regenerative brake at the front wheels. Therefore, the efficiency of the beginning period is higher than that of the final period. In the same way, the comparison of the parallel schemes reveals that the final efficiency of the modified parallel scheme is slightly higher than that of the parallel scheme. The explanation for this result is that the modified parallel scheme has the friction brake force regulation at the start of braking (0 to 0.4 second) as shown in Figure 4.1d. During this period, the friction brake force is cut, and only the regenerative one is operated; therefore, its maximum regenerative efficiency is reached. After this period, the amount of the regenerative brake force of this scheme is provided as same as those of the parallel scheme. Consequently, the regenerative efficiency of the modified parallel scheme is decreased. However, due to the maximum efficiency at the beginning period, the final accumulative efficiency of the modified parallel scheme is slightly higher than that of the parallel scheme.

In conclusion, the level of regenerative efficiency depends on the important factor: the brake force distribution explained in section 4.1. The more applied regenerative brake force the more regained regenerative efficiency. From the results, the proposed scheme provides the highest accumulative regenerative efficiency, since it allows the regenerative brake to operate at full capacity for all braking process.

This material is reserved for educational use only, not allowed for commercial use.
Forbidden to modify the content, and cite the document when use.

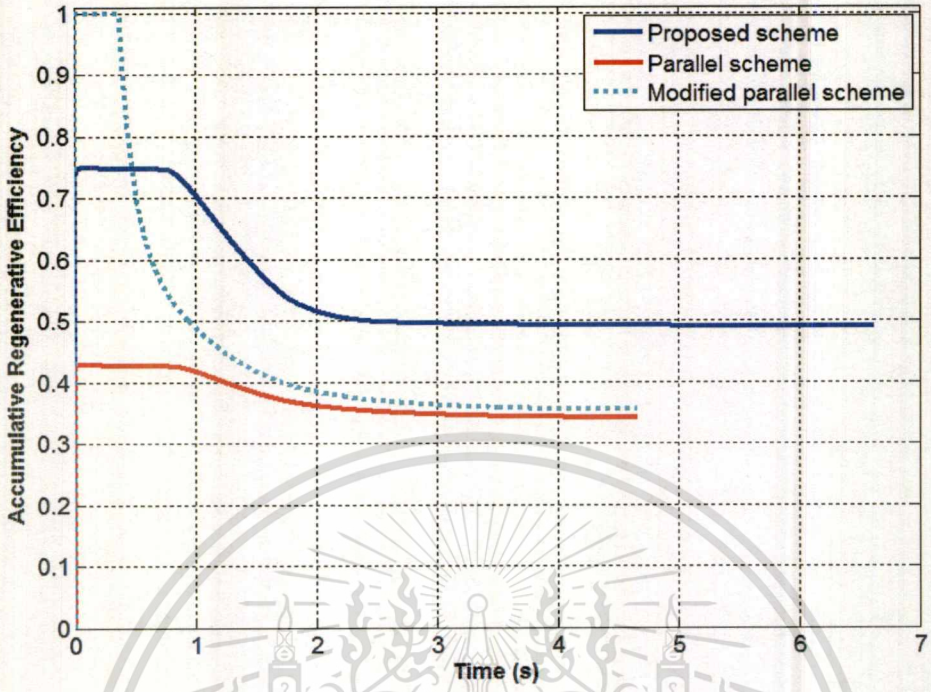

Figure 4.3 Accumulative regenerative efficiency

4.4 Longitudinal Load Transfer

This section focuses on the longitudinal load transfer during braking representing passengers ride comfort during braking. The longitudinal load transfer ratio during a braking period is defined as the load transfer from the rear axle to the front axle that results from a forward longitudinal force acting at the center of gravity at a height above the road surface (forward longitudinal force possibly corresponding to the inertial force at braking) [32]. The calculation of longitudinal load transfer is presented in Section 3.3.1. As shown in Figure 4.4, the higher load transfer ratio, which theoretically results in negative passenger ride comfort, is reached by both parallel regenerative schemes. The proposed scheme and the ABS-equipped conventional brake scheme offer the lower level of load transfer ratio meaning that they provide the better passenger ride comfort during braking. The vertical drop line of the results may indicate the variation of wheel slip while the vehicle is going to completely stop. Perhaps, the variation of wheel slip

This material is reserved for educational use only, not allowed for commercial use.
Forbidden to modify the content, and cite the document when use.

directly affects the amount of the tire force generated between tire and road surface, the inertial force, and the longitudinal load transfer, sequentially. However, this explanation is only an assumption. A further study is required to validate this assumption.

In summation, the longitudinal load transfer directly varies with the amount of generated brake force. In case that the brake force is provided more than the demanded brake force, the longitudinal load transfer is increased. Therefore, this leads to the negative passenger ride comfort. In both parallel schemes, the additional regenerative brake forces are provided in parallel with the friction brake force of the front wheels; as a result, the overall generated brake force is higher than the brake force demand. The parallel schemes show the negative passenger ride comfort. On the other hand, the proposed scheme utilizes the same brake force distribution as in the conventional braking system. Consequently, it can be assumed that, the passenger ride comfort during braking is similar to the one of the conventional braking system.

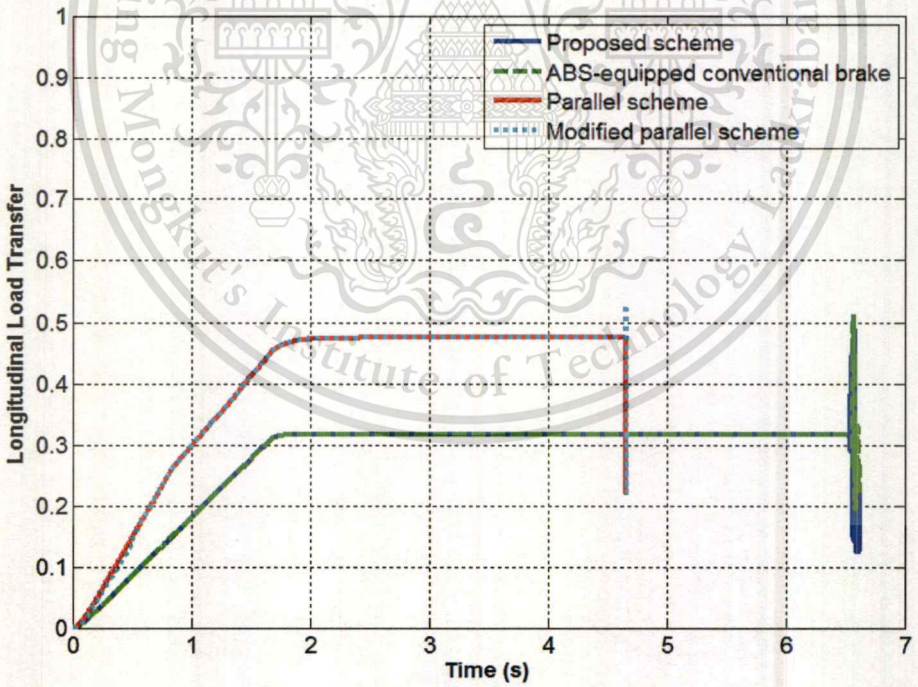

Figure 4.4 Longitudinal load transfer

This material is reserved for educational use only, not allowed for commercial use.
Forbidden to modify the content, and cite the document when use.

CHAPTER 5

CONCLUSIONS AND SUGGESTIONS

This chapter is divided into two sections. The first section presents the conclusion of this research based on the results and analysis. The other section offers the suggestion for a further study.

5.1 Conclusions

The main objective of this study is to develop the regenerative braking system for retrofitted EVs. The problem statement of this study is that the conventional braking system of the retrofitted EVs is not designed for co-performing with a regenerative braking system. Thus, a brake force management system is required. In the previous studies, there primarily are two concepts: series scheme and parallel scheme. However, there are some disadvantages in the previous schemes. The disadvantages of series scheme are that it is suitable only for a front-rear split brake layout, and it requires a great deal of modification effort. The disadvantages of parallel scheme are an insufficient energy recovery efficiency, a low level of ride comfort during braking, and a risk of wheel-locking situation.

To integrate a regenerative braking in the retrofitted EVs and solve the disadvantages of previous studies, this study proposes an innovative brake force management scheme. This scheme allows the regenerative brake to operate at its full capacity and maintains the generated brake force not exceeding the brake force demand. By utilizing a unique feature of an anti-lock braking system (ABS), the amount of friction brake force is reduced as equal as the amount of provided regenerative brake force. In this function, the ABS is controlled by the emulated "wheel lock-up" signal that is a command signal sent by the regenerative braking system. Based on this concept, the proposed scheme can be retrofitted into both cross-link and front-rear split brake layouts. In

This material is reserved for educational use only, not allowed for commercial use.
Forbidden to modify the content, and cite the document when use.

addition, this scheme requires only minor modification that leads to the reduction of modification, cost, and time.

Furthermore, the proof of concept is accomplished to verify the feasibility of the proposed scheme. This verification is done in field tests. The emulated "wheel lock-up" signal is sent into the ABS to investigate the characteristics of brake pressure. The results show the ABS capability of controlling the brake pressure. From the results, the feasibility of the proposed idea is confirmed. Moreover, by the result analysis, the potential of recovered energy is up to 65% of all braking energy according to the ratio of brake force distribution between front axle and rear axle of the experimental car, which is 2:1. However, after the regenerative process, the recovered energy must be stored in the storage devices. A further study is still required to implement the process of energy storage.

After the proof of concept is achieved, a computational analysis is adopted to predict the performance of the proposed scheme. The reference criteria are a recovery efficiency, safety, and ride comfort during braking. The proposed scheme is compared to the ABS-equipped conventional brake scheme, the parallel scheme, and the modified parallel scheme. The mathematical modeling of this study is formulated in MATLAB/Simulink. The accuracy of the mathematical model is verified by the result obtained from field tests. The computational findings and field test results are similar. Their average errors are less than 10%, which may be caused by the approximation of simulation parameters.

In the previous chapter, the performance of the proposed scheme, the parallel scheme, and the modified parallel scheme are reported and discussed. It can be concluded that the proposed scheme surpasses both parallel schemes with the following advantages:

- Higher accumulative regenerative efficiency
- Greater brake force distribution between regenerative and friction brake
- Better passengers ride comfort during braking

This material is reserved for educational use only, not allowed for commercial use.
Forbidden to modify the content, and cite the document when use.

5.2 Suggestions

Although this work is finished, it is only the first step for studying the regenerative braking system for a retrofitted electric vehicle. Following suggestions can be applied to improve this work:

- In this study, it is found that the emulated "wheel lock-up" signal is compatible with the vehicle speed that is lower than 30 km/h since the results of the proof of concept show the brake pressure reductions, which start lower than 30 km/h. However, the ABS generally can regulate the brake pressure at all speeds. A further study about the emulated "wheel lock-up" signal should be done to determine the emulated "wheel lock-up" signal that can be used for regulating the brake pressure at all speeds.
- From the proof-of-concept results, it is observed that the brake fluid pressure in the master cylinder circuit increases while the ABS reduces the brake fluid pressure. The reason is that the ABS pumps the brake fluid from the caliper circuit to the master cylinder circuit. The increase of brake pressure in the master cylinder results in the pressure sensor capturing the inaccurate brake demand. Thus, to improve the accuracy of capturing brake demand, a brake force requirement should be measured by a brake pedal position sensor instead of the pressure sensor. Moreover, a brake pressure control system at the master cylinder circuit should be developed for the proposed scheme to control the brake pressure in the master cylinder not to increase during the period of brake fluid pressure reduction.
- In a regenerative braking system, there are two brake systems working together. For friction brake system, there are many additional safety features (e.g. ABS, electronic brake force distribution (EBD), and electronic stability control (ESC)). However, the safety features for the regenerative brake system are only optional and not widespread now. Besides, this study focuses only on the integration of a regenerative braking system into retrofitted EVs. Thus, the safety features for the regenerative brake system is an interesting topic for a further study.

This material is reserved for educational use only, not allowed for commercial use.
Forbidden to modify the content, and cite the document when use.

- This study focuses on the testing condition of single braking in a straight line. To comprehensively investigate the performance of the regenerative braking system and the cooperation of the regenerative brake and the driving-safety system, the further study should be done in driving cycles or driving patterns.

This material is reserved for educational use only, not allowed for commercial use.
Forbidden to modify the content, and cite the document when use.

REFERENCES

[1] Kim D., and Kim H. 2006. "Vehicle stability control with regenerative braking and electronic brake force distribution for a four-wheels drive hybrid electric vehicle." **Proc. IMechE Part D: J. Automobile Engineering.** vol.220(6) : 683-693.

[2] Cholula S., Claudio A., and Ruiz J. 2005. "Intelligent Control of the Regenerative Braking in an Induction Motor Drive." **The 2nd International Conference on Electrical and Electronics Engineering (ICEEE) and XI Conference on Electrical Engineering (CIE 2005).** : 302-308.

[3] Triger L., Paterson J., and Drozdz P. 1993. "Hybrid Vehicle Engine Size Optimization." **SAE Paper #931793.** (August 1993)

[4] LaPlante J., Anderson C.J., and Auld J. 1995. "Development of a Hybrid Electric Vehicle for the US Marine Corps." **SAE Paper #951905.** (August 1995)

[5] Feng W., Hu Z., Xiao-jian M., Lin Y., and Bin Y. 2007. "Regenerative Braking Algorithm for a Parallel Hybrid Electric Vehicle with Continuously Variable Transmission." **The International Conference on Vehicular Electronics and Safety (ICVES 2007).**

[6] Gao Y., Chen L., and Ehsani M. 1999. "Investigation of the Effectiveness of Regenerative Braking for EV and HEV." **SAE Paper#1999-01-2910.** (August 1999)

[7] Panagiotidis M., Delagrammatikas G., and Assanis D. 2000. "Development and Use of a Regenerative Braking Model for Parallel Hybrid Electric Vehicle." **SAE Paper#2000-01-0995.** (August 2000)

[8] Jang S., Yeo H., Kim C., and Kim H. 2001. "A Study on Regenerative Braking for a Parallel Hybrid Electric Vehicle." **KSME International Journal.** vol.15(11) : 1490-1498.

[9] Yeo H., Kim D., Hwang S., and Kim H. 2004. "Regenerative Braking Algorithm for a HEV with CVT Ratio Control during Deceleration.", 04CVT-41. paper presented by Dynamic System Design & Control Lab., Sungkyunkwan University, Korea.

This material is reserved for educational use only, not allowed for commercial use.
Forbidden to modify the content, and cite the document when use.

REFERENCES (CONT.)

[10] Tur O., Ustun O., Member IEEE, and Tuncay R.N. 2007 "An Introduction to Regenerative Braking of Electric Vehicles as Anti-Lock Braking System." **The Intelligent Vehicles Symposium, 2007 IEEE.** : 944-948.

[11] Peng D., ZHANG Y., YIN C.-L., and ZHANG J.-W. 2008. "Combined Control of A Regenerative Braking and Anti-Lock Braking system For Hybrid Electric Vehicles." **International Journal of Automotive Technology.** vol.9(6) : 749-757.

[12] Gou J., Wang J., and Cao B. 2009. "Regenerative Braking Strategy for Electric Vehicles." **Proceeding of the 2009 IEEE Intelligent Vehicles Symposium.**

[13] Ahn J. K., Jung K. H., Kim D. H., Jin H. B., Kim H. S., and Hwang S. H. 2009. "Analysis of a Regenerative Braking System for Hybrid Electric Vehicles using an Electro-Mechanical Brake." **International Journal of Automotive Technology.** Vol.10 : 229-234.

[14] Zhang J. L., Yin CH. L., and Zhang J. W. 2010. "Improvement of Drivability and Fuel Economy with a Hybrid Antiskid Braking System in Hybrid Electric Vehicles." **International Journal of Automotive Technology.** Vol.11(20) : 205-213.

[15] Tehrani M., Hairi -Yazdi R., Haghpanah-Jahromi B., Esfahanian1 V., Amiri M., and Jafari R. 2011. "Design of an Anti-Lock Regenerative Braking System for a Series Hybrid Electric Vehicle." **International Journal of Automotive Engineering.** Vol.1(2) : 16-20.

[16] Ehsani M., Gao Y., Gay S.E., and Emadi A. 2003. **Modern Electric, Hybrid Electric, and Fuel Cell Vehicles – Fundamentals, Theory, and Design.** CRC Press, Ltd., Boca Raton, Florida USA.

[17] Larminie J. and Lowry J. 2003. **Electric Vehicle Technology Explained.** John Wiley and Sons, Ltd., The atrium, Southern Gate, Chichester, West Sussex, England.

[18] Westbrook M. H. 2007. **The Electric Car Development and fuel-cell cars.** Co-published by The Institution of Engineering and Technology, London U.K. and Society of Automotive Engineers, Warrendale, PA, USA.

This material is reserved for educational use only, not allowed for commercial use.
Forbidden to modify the content, and cite the document when use.

REFERENCES (CONT.)

[19] Fuhs A. E. 2009. **Hybrid Vehicles and the Future of Personal Transportation.** CRC Press, Ltd., Boca Raton, Florida, USA.

[20] DeMers. and Steven M. 2008. **Mechanical and Regenerative Braking Integration for a Hybrid Electric Vehicle.** Master's thesis, University of Waterloo.

[21] Smith D.E., Miller J.W., and Irick D.K. 2005 **Challenge X control system hardware and software development.** Technical report, University of Tennessee.

[22] Heisler H. 2002. **Advance Vehicle Technology 2nd edition** Butterworth Heinemann. Woburn, Massachusetts.

[23] Stone R. and Ball J.K. 2004. **Automotive Engineering Fundamentals.** SAE international, Warrendale, Pennsylvania.

[24] **National Instruments,** Documentation.

[25] Selim A.O., Keith J.B., Adam S., Chris M., Gary W., Graham H., Cian H., and Ross M. 2013. "Regenerative braking strategies, vehicle safety and stability control systems: critical use-case proposals." Vehicle System Dynamics. **International Journal of Vehicle Mechanics and Mobility,** 51:5, 684-699.

[26] Jazz/Fit (GE) service manual. 2009. **Honda Motor Company.**

[27] Yaris sedan/hatchback service manual. 2007. **Toyota Motor Company.**

[28] **Holykell Technology CO., Ltd.,** Documentation.

[29] **Racelogic Ltd.,** VBOX documentation.

[30] Kijpaiboon C. 2011. **LabVIEW ซอฟต์แวร์เพื่อการพัฒนาระบบการวัดและควบคุม.** SE-EDUCATION Public Company Limited, Bangkok, Thailand.

[31] Chanthanumataporn S., Lerspalungsanti S., and Pimsarn M. 2011. "Design of Regenerative Braking Systemfor an Electric Vehicle (EV) Modified from Used Car." **The Second TSME International Conference on Mechanical Engineering (2nd TSME ICoME 2011).**

[32] Pacejka, H. B. 2006. **Tire and Vehicle Dynamics.** Butterworth-Heinemann, Oxford.

This material is reserved for educational use only, not allowed for commercial use.
Forbidden to modify the content, and cite the document when use.

APPENDIX A

PROOF OF CONCEPT RESULTS

This material is reserved for educational use only, not allowed for commercial use.
Forbidden to modify the content, and cite the document when use.

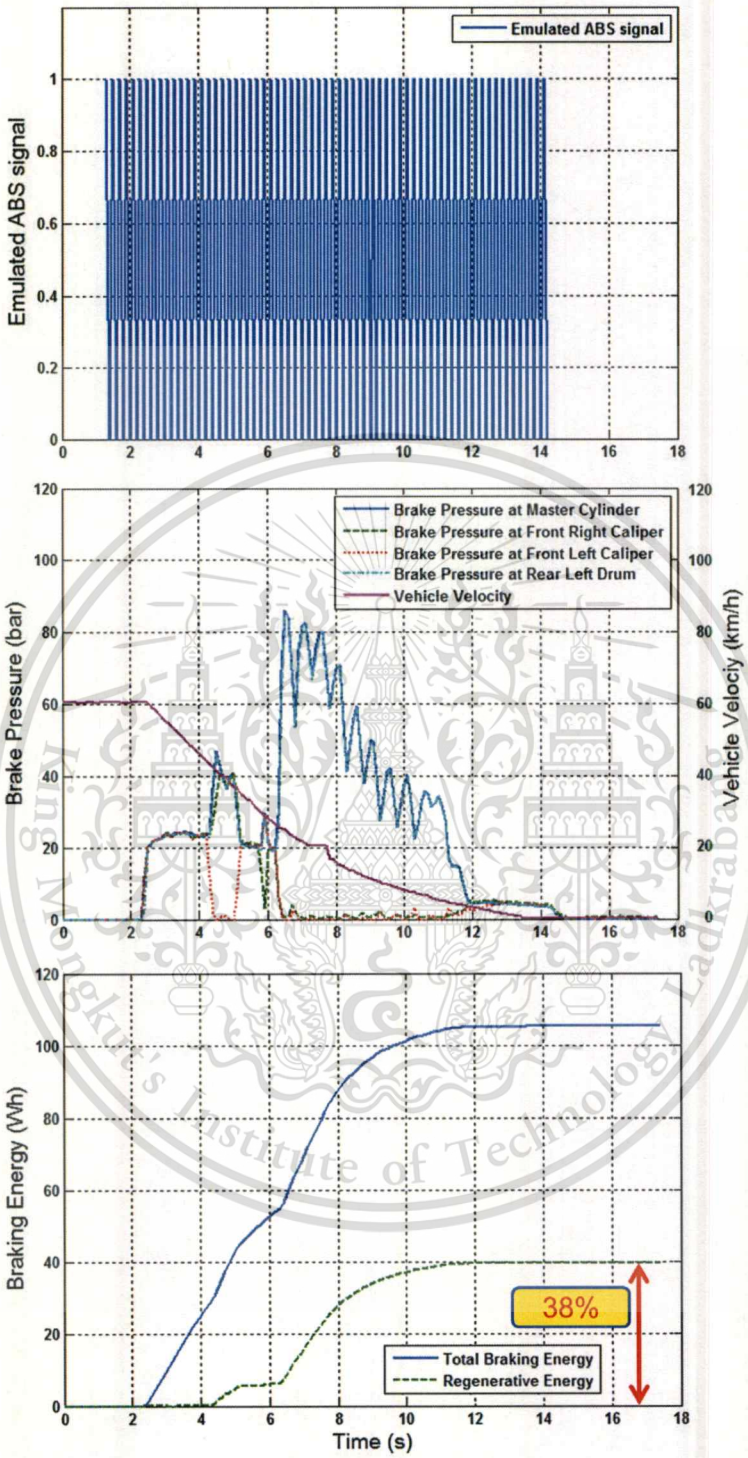

Figure A.1 Proof of concept results

(4th condition, 40% brake pedal position and initial speed = 60 km/h)

This material is reserved for educational use only, not allowed for commercial use.
Forbidden to modify the content, and cite the document when use.

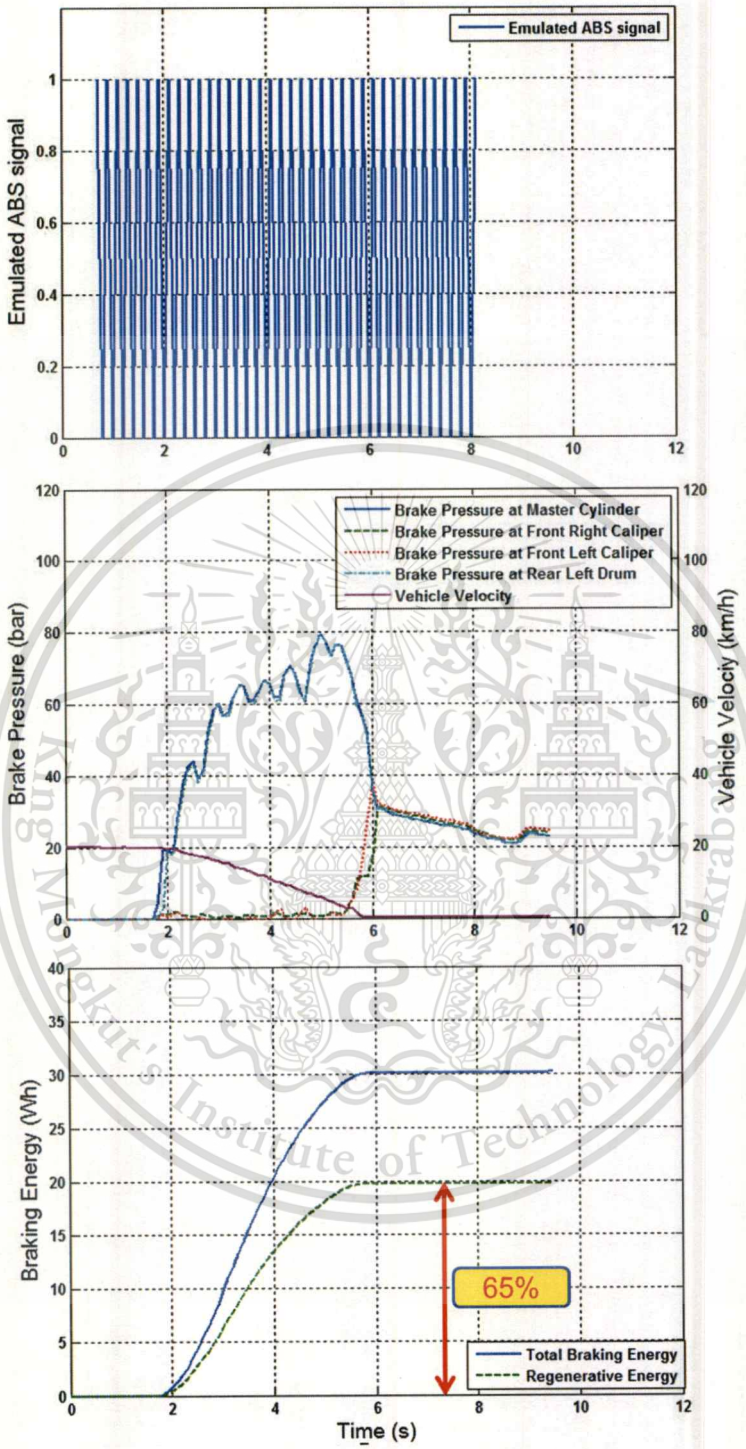

Figure A.2 Proof of concept results

(5th condition, 80% brake pedal position and initial speed = 20 km/h)

This material is reserved for educational use only, not allowed for commercial use.
Forbidden to modify the content, and cite the document when use.

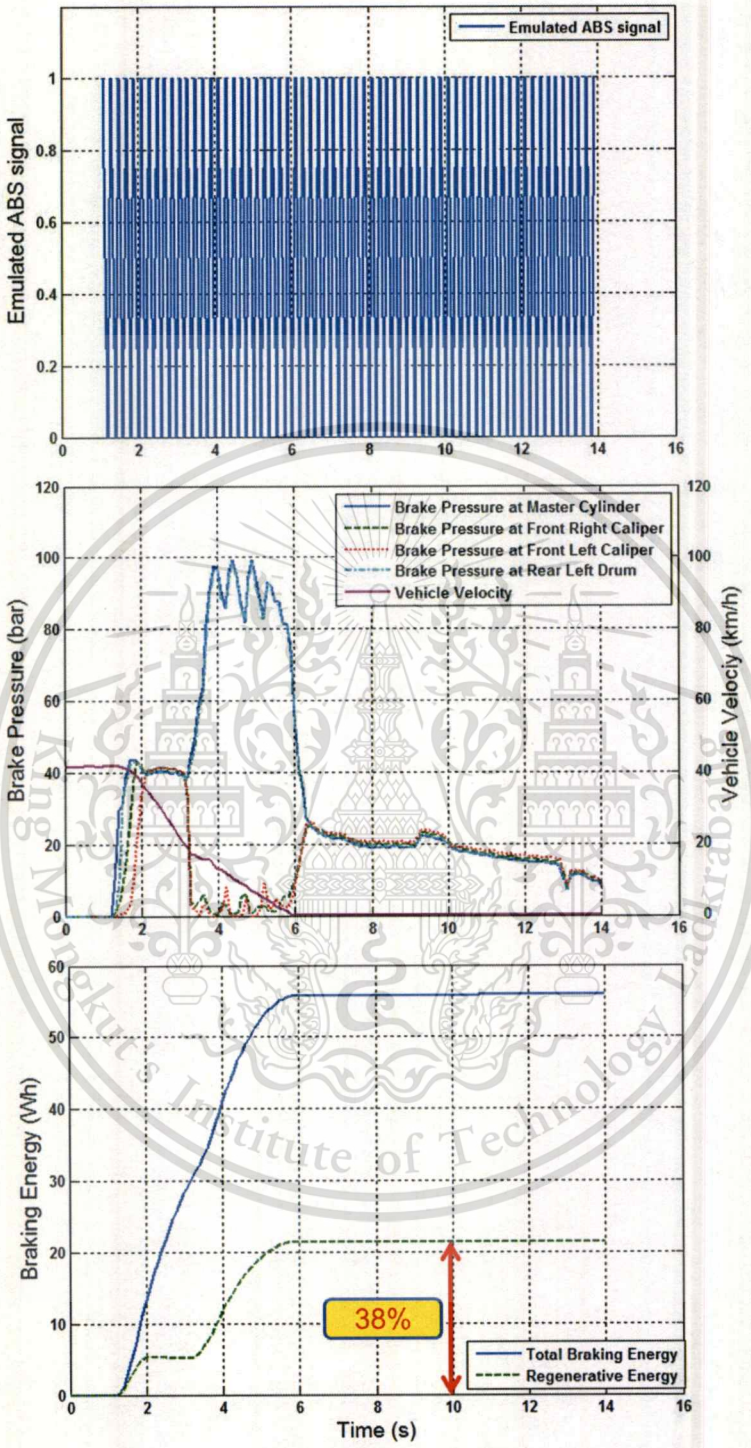

Figure A.3 Proof of concept results

(6^{th} condition, 80% brake pedal position and initial speed = 40 km/h)

This material is reserved for educational use only, not allowed for commercial use.
Forbidden to modify the content, and cite the document when use.

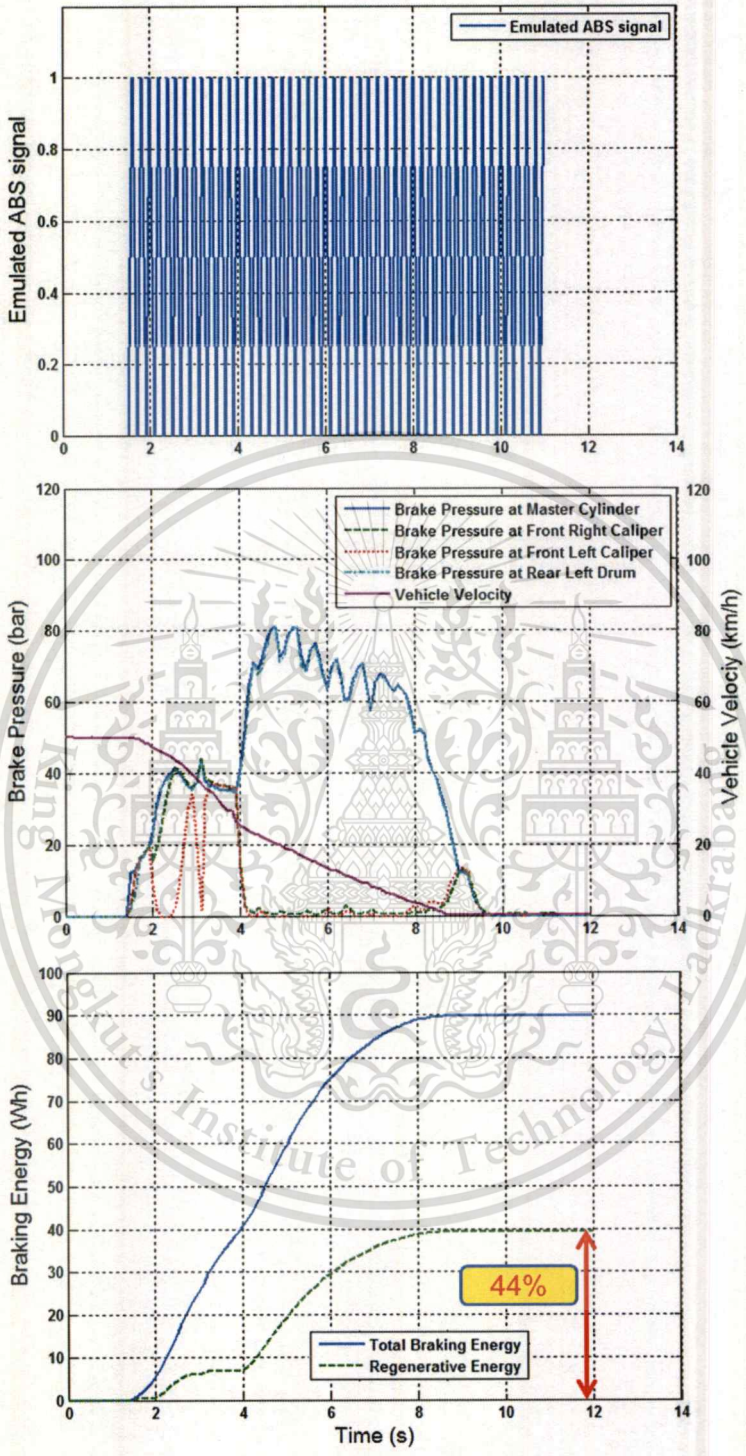

Figure A.4 Proof of concept results

(7th condition, 80% brake pedal position and initial speed = 50 km/h)

This material is reserved for educational use only, not allowed for commercial use.
Forbidden to modify the content, and cite the document when use.

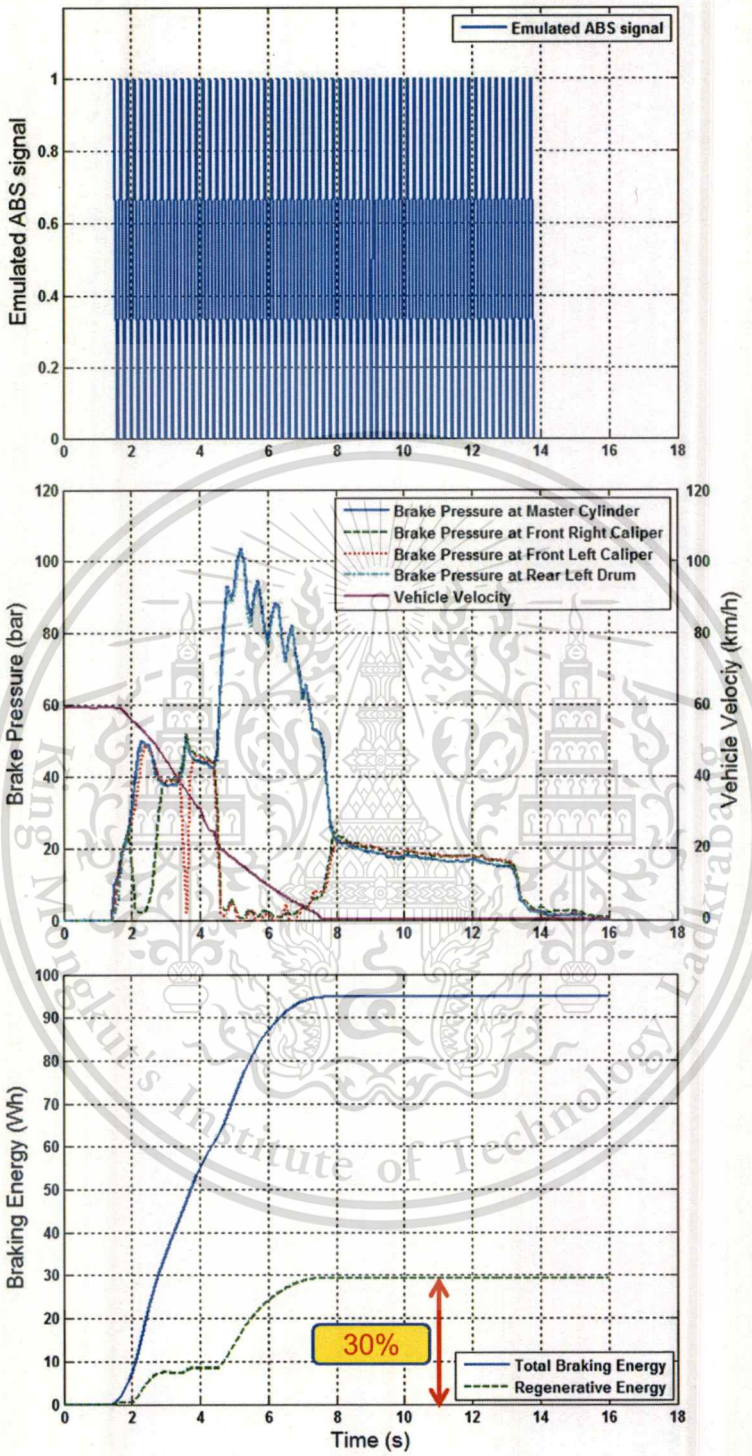

Figure A.5 Proof of concept results

(8th condition, 80% brake pedal position and initial speed = 60 km/h)

This material is reserved for educational use only, not allowed for commercial use.
Forbidden to modify the content, and cite the document when use.

APPENDIX B

SIMULATION MODEL VERIFICATION RESULTS

King Mongkut's Institute of Technology Ladkrabang

This material is reserved for educational use only, not allowed for commercial use.
Forbidden to modify the content, and cite the document when use.

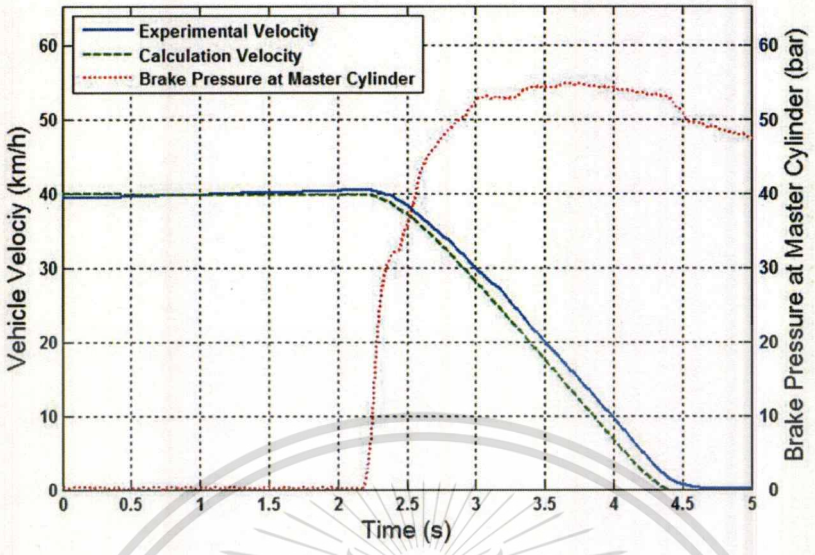

Figure B.1 Calculation vs. experimental velocity and brake fluid pressure (4^{th} condition, 80% brake pedal position and initial speed = 40 km/h)

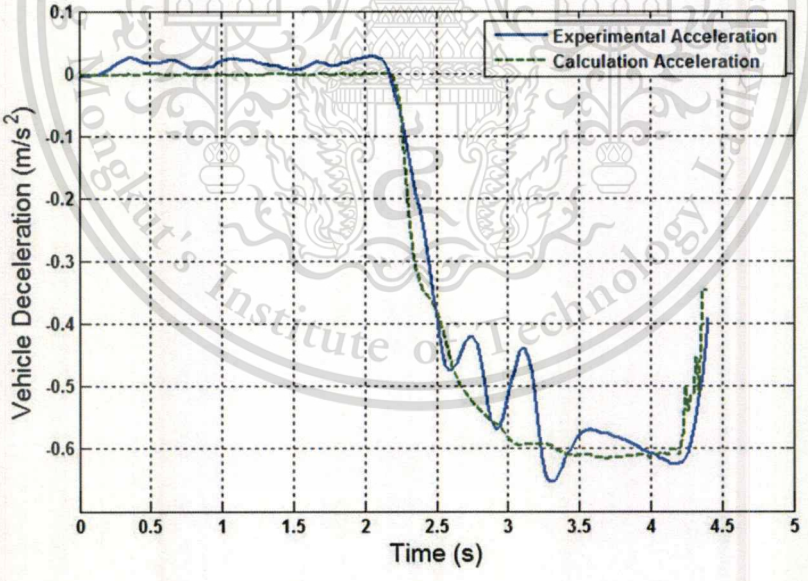

Figure B.2 Calculation vs. experimental deceleration (4^{th} condition, 80% brake pedal position and initial speed = 40 km/h)

This material is reserved for educational use only, not allowed for commercial use.
Forbidden to modify the content, and cite the document when use.

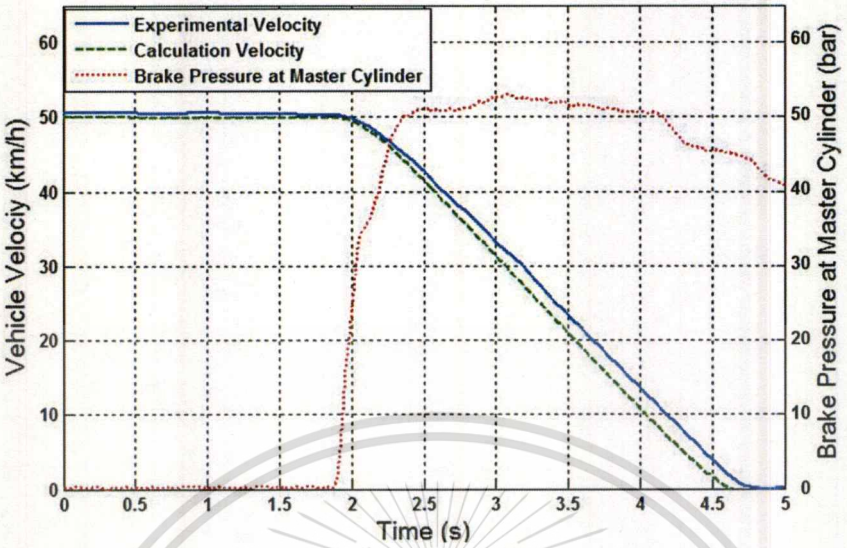

Figure B.3 Calculation vs. experimental velocity and brake fluid pressure (5^{th} condition, 80% brake pedal position and initial speed = 50 km/h)

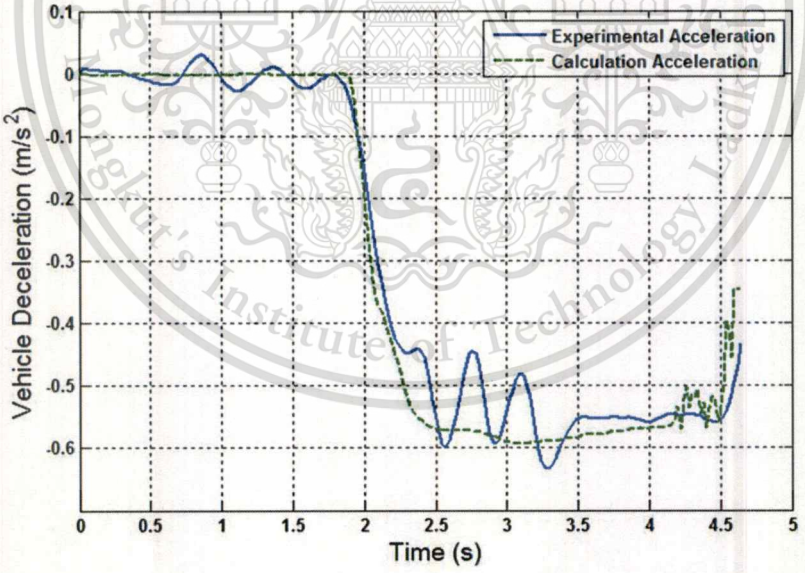

Figure B.4 Calculation vs. experimental deceleration (5^{th} condition, 80% brake pedal position and initial speed = 50 km/h)

This material is reserved for educational use only, not allowed for commercial use.
Forbidden to modify the content, and cite the document when use.

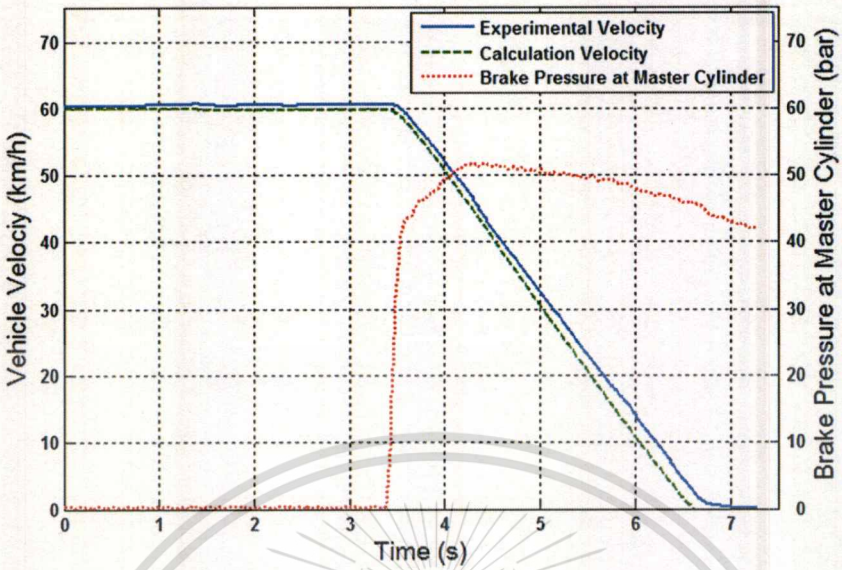

Figure B.5 Calculation vs. experimental velocity and brake fluid pressure (6^{th} condition, 80% brake pedal position and initial speed = 60 km/h)

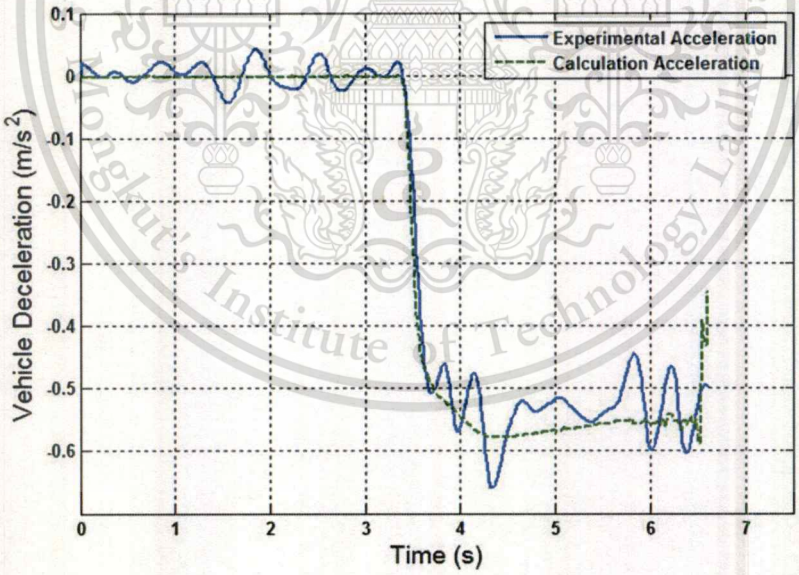

Figure B.6 Calculation vs. experimental deceleration (6^{th} condition, 80% brake pedal position and initial speed = 60 km/h)

This material is reserved for educational use only, not allowed for commercial use.
Forbidden to modify the content, and cite the document when use.

APPENDIX C

MATLAB/SIMULINK CODE

This material is reserved for educational use only, not allowed for commercial use.
Forbidden to modify the content, and cite the document when use.

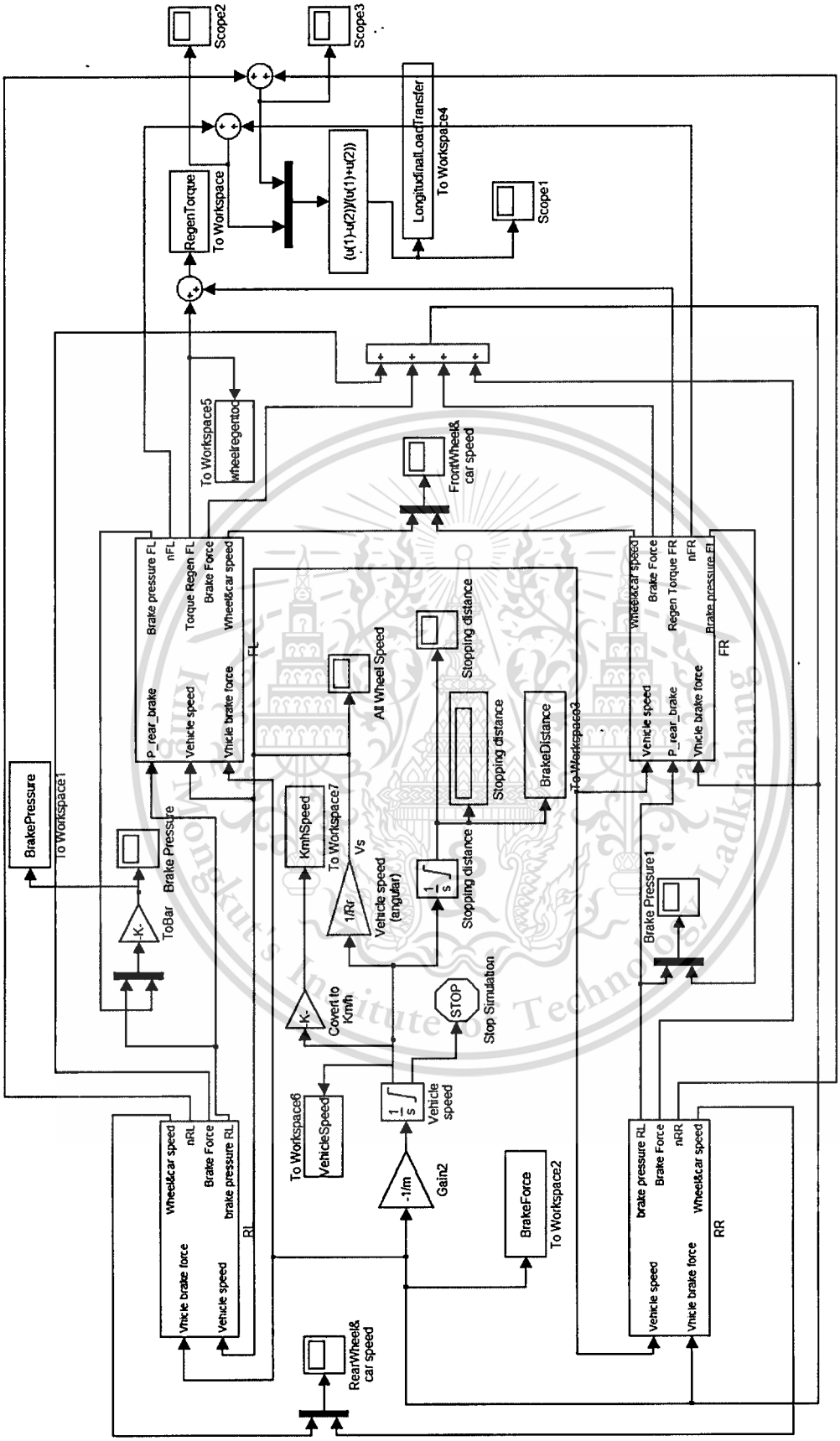

This material is reserved for educational use only, not allowed for commercial use.
Forbidden to modify the content, and cite the document when use.

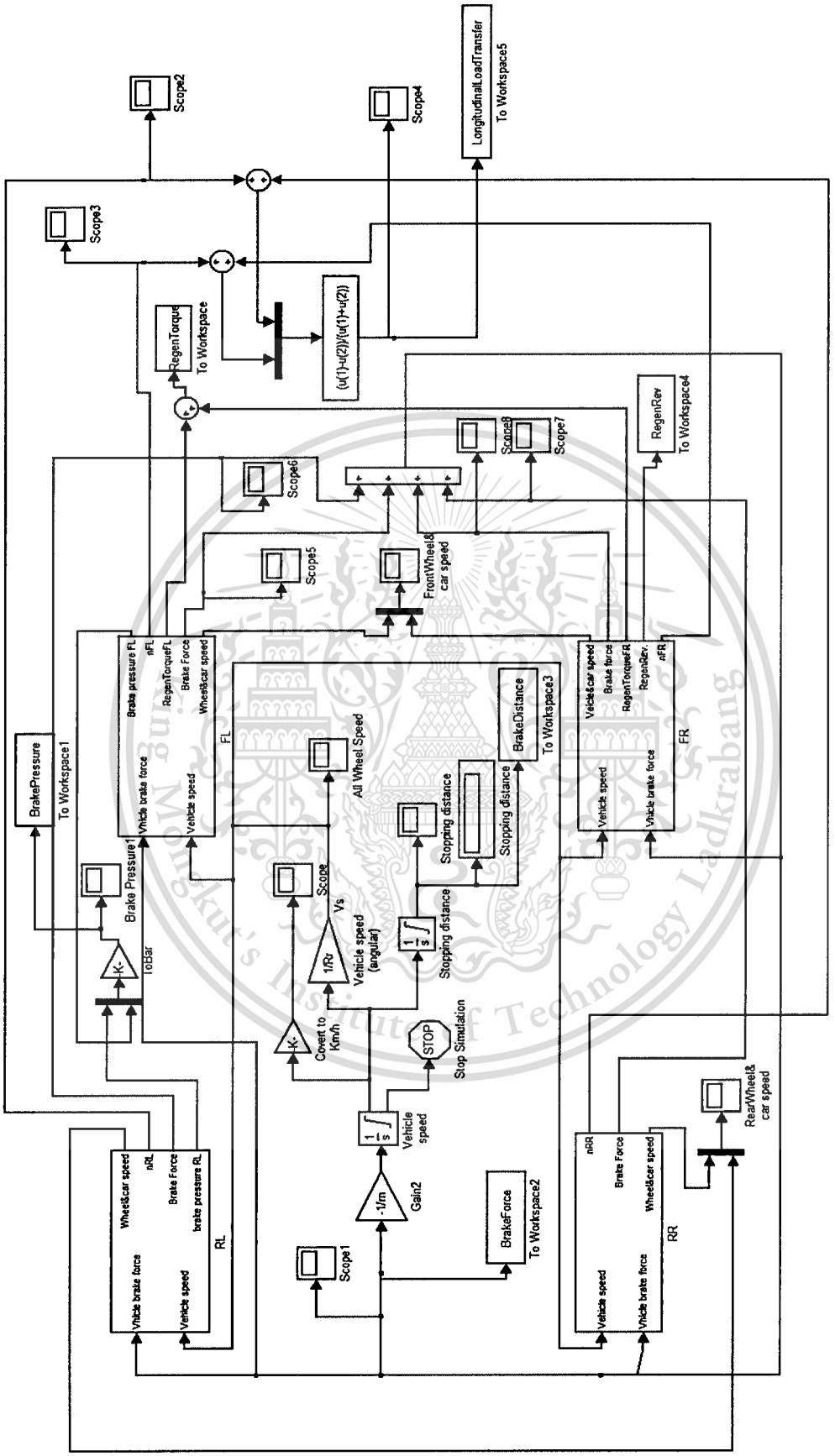

This material is reserved for educational use only, not allowed for commercial use.
Forbidden to modify the content, and cite the document when use.

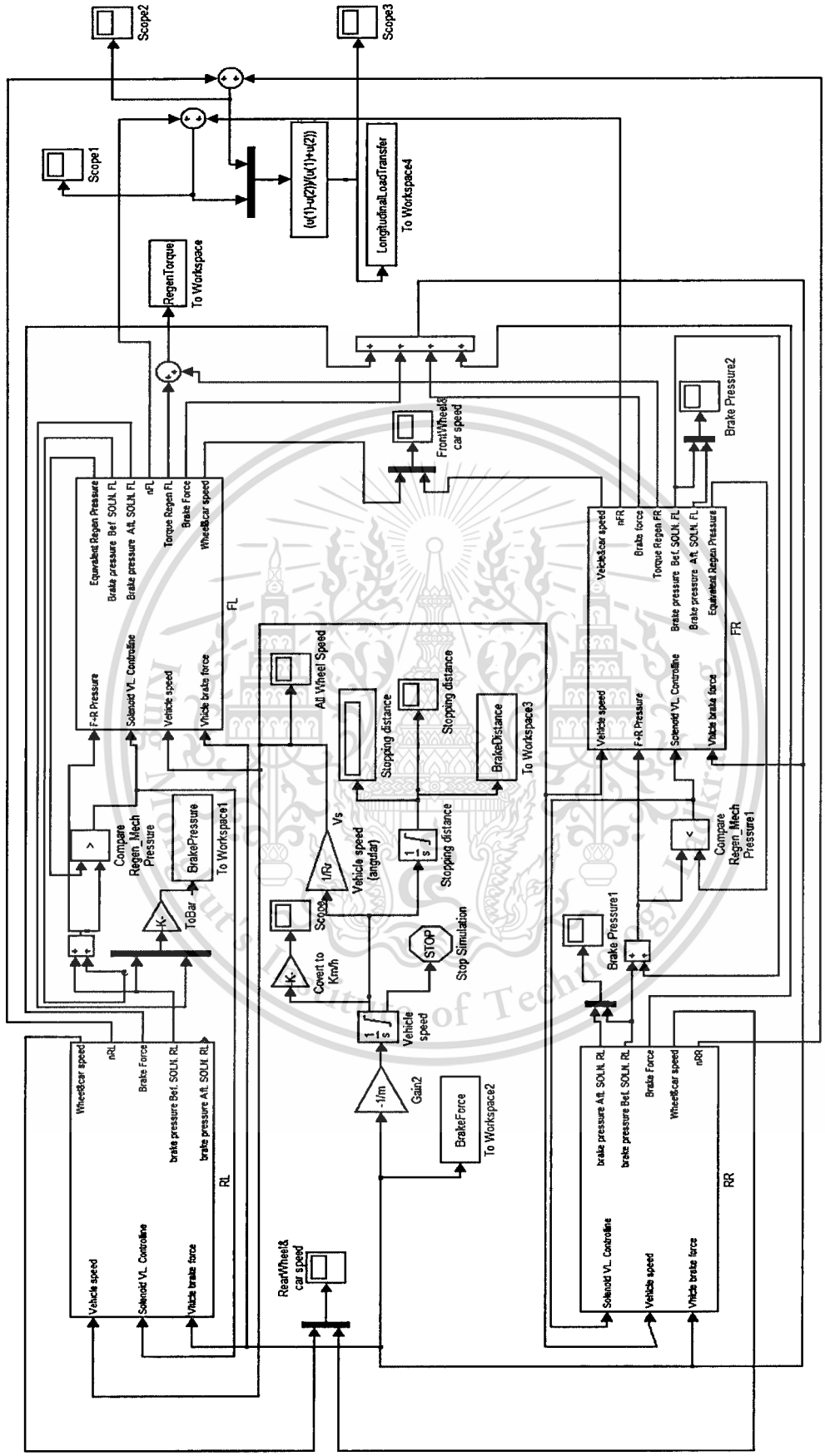

This material is reserved for educational use only, not allowed for commercial use.
Forbidden to modify the content, and cite the document when use.

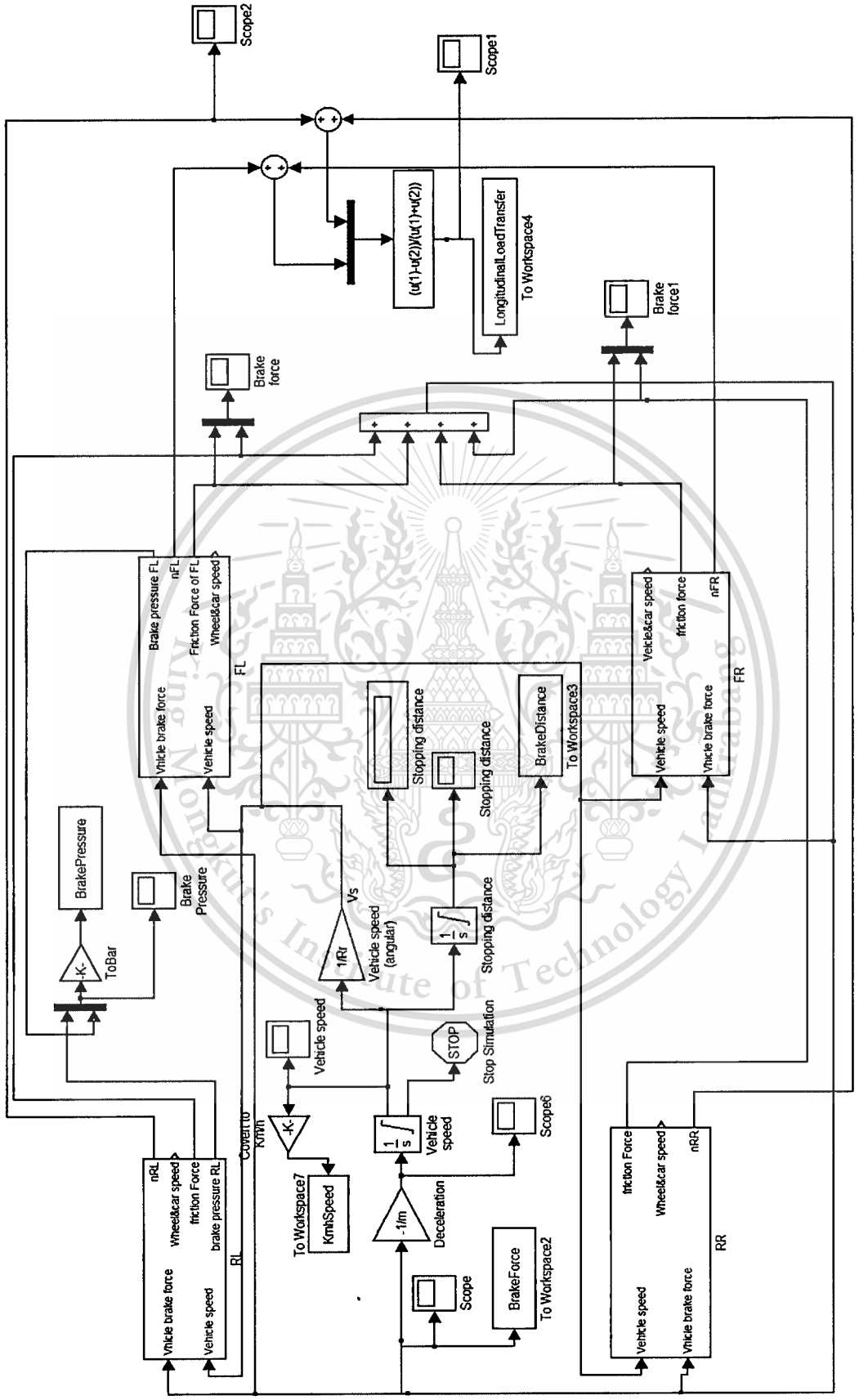

This material is reserved for educational use only, not allowed for commercial use.
Forbidden to modify the content, and cite the document when use.

APPENDIX D

LABVIEW BLOCK DIAGRAM

This material is reserved for educational use only, not allowed for commercial use.
Forbidden to modify the content, and cite the document when use.

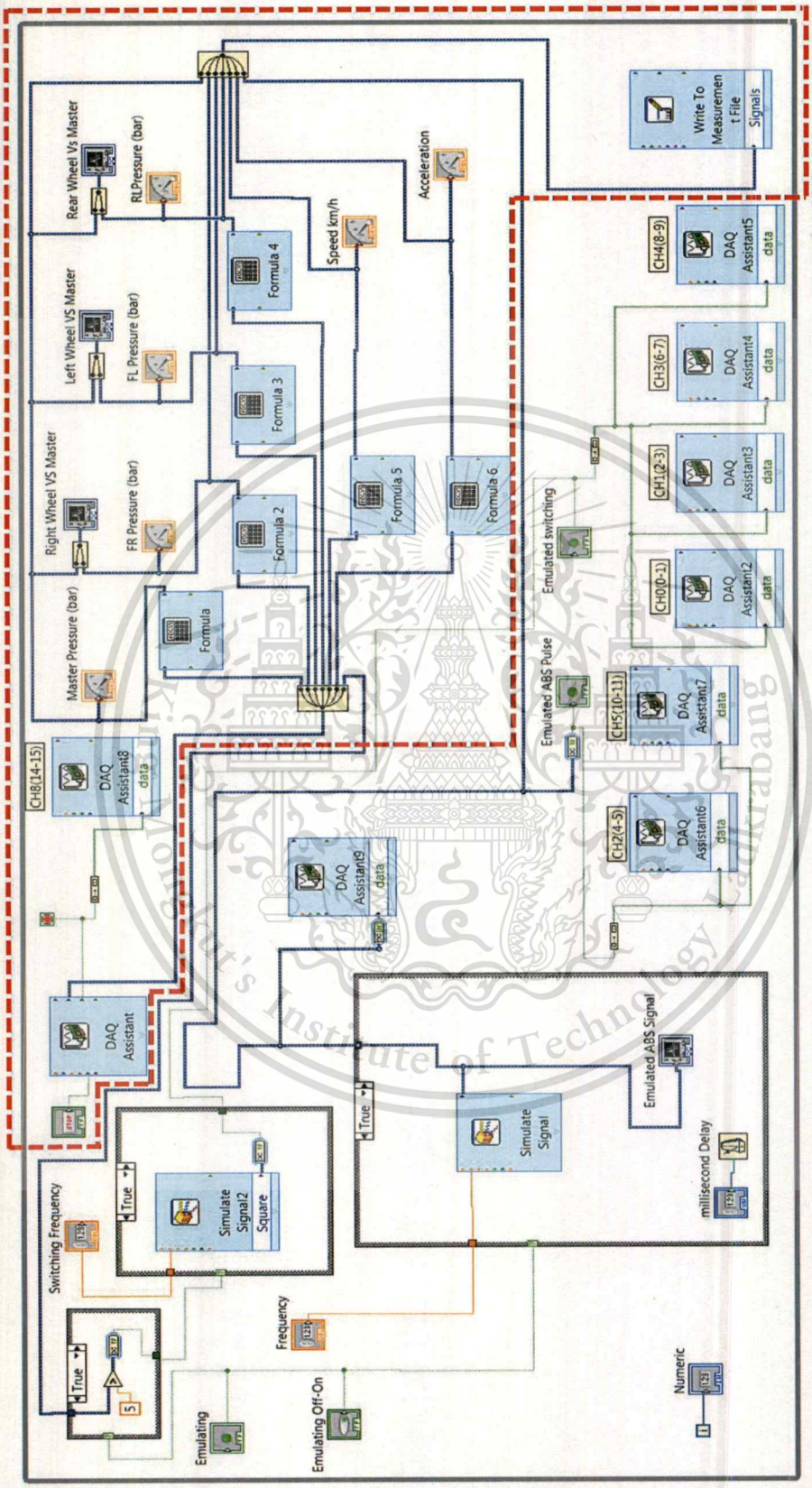

This material is reserved for educational use only, not allowed for commercial use.
Forbidden to modify the content, and cite the document when use.

APPENDIX E

PRESSURE SENSOR SPECIFICATIONS

King Mongkut's Institute of Technology Ladkrabang

This material is reserved for educational use only, not allowed for commercial use.
Forbidden to modify the content, and cite the document when use.

TECHNOLOGY

HOLYKELL®

Pressure sensor HPS300-S

Economic OEM Pressure Sensors
Model: HPS300-S
Range: -1 Bar-0-5 Bar.....1000Bar optional
Output: 1.5 mV/V...4 mV/V or3-10 mV full output
Accuracy: 0.5%F.S.
Process Mounting: 1/4"NPT;G1/2" by order
Application: Liquid and Gas pressure measuring

Pressure Type:	gauge pressure
Pressure Range:	-1 Bar...0...5 Bar.....100 Bar Optional.
Overload:	200%F.S (≤100 Bar, Ceramic types) ; 150%F.S (>100 Bar, Silicon types)
Burst Pressure:	300%F.S (≤100 Bar)
Power Supply:	10 V DC or 5～12 V DC
Output:	1.5mV/V～4 mV/V; 0～35 mV optional
Electronic Wire:	4 Wire
Accuracy: (Included Linearity Hysteresis Repeatability)	≤ ±0.5%F.S ≤ ±1%F.S Optional
Long-term Stability:	0.2%FS/year（typ. 0.3%FS/year（max.）
Zero temp. drift:	0.03%FS/℃（≤100kPa）, 0.05%FS/℃（>100kPa）
FS temp. drift:	0.03%FS/℃（≤100kPa）, 0.05%FS/℃（>100kPa）
Temperature Compensation:	-20℃~85℃
Working Temp:	-40℃～100℃
Storage Temp:	-40℃~125℃
Medium compatible:	Various media compatible with the 304/316L stainless steel
Insulation Resistance:	>10 MΩ
Electronic connection:	Fixed cable Explore Proof and water proof IP67
Process connect port:	7/16"-20UNF male1/4"NPT male, 1/2"NPT male, G1/2"... (by order)
Response time:	≤20 ms
Certificate approve:	CE Certificate.
EMC Standard:	electromagnetic radiation:EN50081-1/-2 electromagnetic susceptibility:EN50082-2
Water Proof Grade:	IP67
Remarks:	Special applications request by order

This material is reserved for educational use only, not allowed for commercial use.
Forbidden to modify the content, and cite the document when use.

APPENDIX F

RACELOGIC VBOX GPS SPECIFICATION

This material is reserved for educational use only, not allowed for commercial use.
Forbidden to modify the content, and cite the document when use.

Introduction

The VB20SL3 is a multi-purpose non-contact speed sensor. Using two advanced dual antenna GPS engines, the VB20SL3 can calculate not only the speed and direction of travel of the object upon which it is placed, but also an accurate Slip angle and Pitch and Roll angle. This data is then logged to an inserted SD card, available on a configurable CAN output and present on a USB or serial output for direct monitoring or data processing by a connected PC running VBOXTools software.
The VB20SL3 also features a built-in graphic display allowing the user to set up and configure the unit without using a PC.

The VB20SL3 is compatible with all of the existing peripherals including the Multifunction display, ADC03, TC8, FIM03, Yaw Rate Sensor and Mini Input module.

Features

- Non-contact 20Hz speed and distance measurement using GPS
- VCI CAN input for connection to external CAN systems
- Slip, Pitch and Roll Angle and True Heading measurement
- 1 x CAN bus interface (on two sockets to allow daisy-chaining)
- USB for live data, configuration, upgrading and SD data transfer
- RS232 serial interface backup for live data and configuration
- SD Card logging
- 2 x 16bit user-configurable analogue outputs
- 2 x user-configurable digital outputs
- Brake trigger input with 210KHz scan rate
- Input voltage 6V to 30V operating range
- Logging of up to 20 data channels, in addition to up to 13 standard GPS channels
- Logging and serial rates configurable between 1Hz and 20Hz

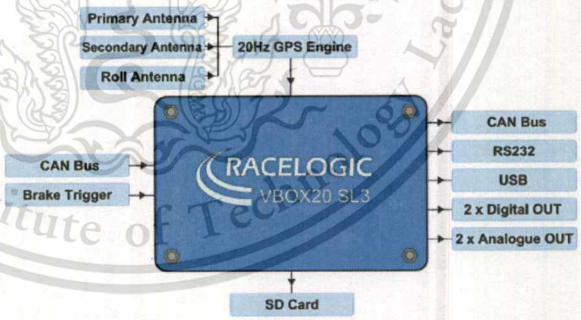

This material is reserved for educational use only, not allowed for commercial use.
Forbidden to modify the content, and cite the document when use.

Antenna Types and Placement

Whilst installation and use of the VB20SL3 is intended to be fast and simple, careful attention must be paid to placement of the antennas.

Note: It is essential that the separation of Antenna B and Antenna C from Antenna A is exactly the same as the separation values set inside the VB20SL3 via the configuration screen. If the separation is incorrect, data may not be given or may be inaccurate. The measured distance between the antennas should be the straight-line distance between the antennas regardless of the mounting angle. It is not the 2D distance between the antennas as viewed from above.

The supplied tape measure will help ensure an accurate antenna separation.

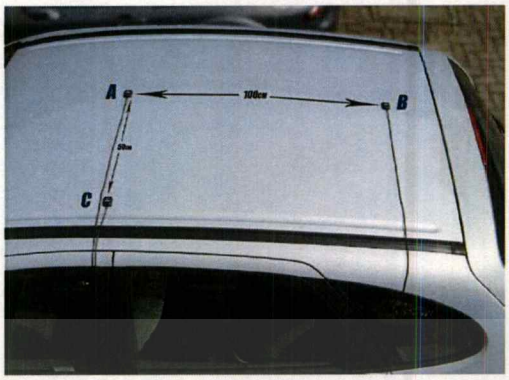

Antenna A is the *primary antenna*, from which all calculations are based. If overall slip is to be measured (at the centre of the vehicle), the primary antenna should be placed at the centre of the vehicle. Alignment of the antennas is not completely essential as the Slip Angle Sensor has the ability to calculate any offset. See the Slip Angle Offset Section.
However if you wish to measure Pitch or Roll then the alignment of the antennas must be in line with the vehicle or at 90° as accurately as possible.

The picture to the right shows a typical 3-antenna placement for the measurement of Body Slip Angle, Pitch and Roll angle. Antenna A the primary antenna is placed in the centre of the roof. Antenna B is placed behind Antenna A, allowing **True heading**, Slip angle and Pitch Angle to be measured. Antenna C is placed to the side of Antenna A allowing the measurement of Roll angle.

When measuring Slip angle Antenna B can be placed either in front or behind Antenna A. If it is placed behind Antenna A as in the picture above then the 'Swap Antenna' option needs to be enabled in the Antenna configuration options.

Digital and Analogue Outputs

The outputs on connectors OUT1 and OUT2 can be used either as frequency/pulse digital outputs or as analogue outputs that can be configured to represent any of the following parameters:

- Velocity
- Longitudinal Acceleration
- Lateral Acceleration
- Slip Angle
- Pitch Angle
- Roll Angle

For digital outputs, the scale and maximum output values can be adjusted using the VBOXTools software or via the front panel controls. For velocity, these are controlled by setting the maximum velocity and the pulses per metre. For the other parameters, the scale and maximum are controlled by setting the maximum frequency and the angle or acceleration value to which this relates. Please note that the digital outputs do not show the direction of angles and accelerations, only their magnitudes. Therefore "negative" angles or accelerations will be shown in the same way as their positive equivalents.

For analogue outputs, the values relating to the maximum voltage (+5V) and minimum voltage (0 for Velocity, –5V for all other channels) can be set, either via the front panel or using the VBOXTools software. The negative voltage capability of the analogue outputs allows the direction of angles and accelerations to be output.

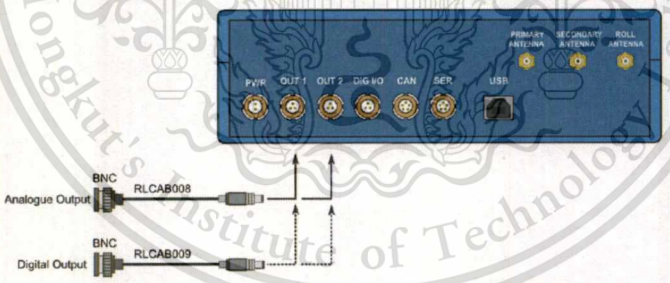

This material is reserved for educational use only, not allowed for commercial use.
Forbidden to modify the content, and cite the document when use.

APPENDIX G

DATA ACQUISITION SPECIFICATION

- **CHASSIS MODULE (NI cDAQ-9174)**
- **EMULATED "ABS" SIGNAL MODULE (NI 9485)**
- **PRESSURE SENSOR AND VBOX GPS MODULE (NI 9205)**

This material is reserved for educational use only, not allowed for commercial use.
Forbidden to modify the content, and cite the document when use.

CHASSIS MODULE (NI cDAQ-9174)

Chassis	
Number of Slots	4
Total Available Power	15 W
Input Voltage Range	9 V - 30 V
Built-In Trigger	No
Counter/Timers	
Counters	4
Resolution	32 bits
Bus Interface	
USB Specification	USB 2.0 Hi-Speed
High-Performance Data Streams	7
Types Available	Digital Output , Counter/Timer Input , Analog Output , Digital Input , Analog Input
Shock and Vibration	
Operational Shock	30 g
Random Operating Frequency Range	5 Hz - 500 Hz
Random Vibration	0.3 g
Physical Specifications	
Length	15.9 cm
Width	8.81 cm

This material is reserved for educational use only, not allowed for commercial use.
Forbidden to modify the content, and cite the document when use.

Height	5.89 cm
Weight	574 gram
Minimum Operating Temperature	-20 °C
Maximum Operating Temperature	55 °C
Maximum Altitude	5000 m
Analog inputs	
Input FIFO size	127 samples per slot
Maximum sample rate	Determined by the C Series I/O module(s)
Timing accuracy	50 ppm of sample rate
Timing resolution	12.5 ns
Number of channels supported	Determined by the C Series I/O module(s)
Analog Output	
Numbers of channels supported	
Hardware-timed task	
Onboard regeneration	16
Non-regeneration	Determined by the C Series I/O module(s)
Non-hardware-timed task	Determined by the C Series I/O module(s)
Maximum update rate	
Onboard regeneration	1.6 MS/s (multi-channel, aggregate)
Non-regeneration	Determined by the C Series I/O module(s)
Timing accuracy	50 ppm of sample rate
Timing resolution	12.5 ns
Output FIFO size	
Regeneration	8,191 samples shared among channels used
Non-regeneration	127 samples per slot
AO waveform modes	Non-periodic waveform, periodic waveform regeneration mode from onboard memory, periodic waveform regeneration from host buffer including dynamic update

This material is reserved for educational use only, not allowed for commercial use.
Forbidden to modify the content, and cite the document when use.

NI 9485

8-Channel Solid-State Relay (SSR) Digital Output Module

Specifications

The following specifications are typical for the range –40 to 70 °C unless otherwise noted.

Output Characteristics

Number of channels.....8 digital output channels
Relay type .....Normally open solid-state Relay (SSR)
Switching voltage .....60 VDC max, 30 Vrms max
Switching current, per channel1
    All channels.....0.75 A max
    Up to four channels .....1.2 A max
Switching rate (90% duty cycle)1 .....1 operation per second
Relay open time .....0.5 ms typ
Relay close time.....9.0 ms typ
On resistance.....200 mΩ max
Off state leakage .....30 µA typ
MTBF .....2,172,740 hours at 25 °C; Bellcore Issue 6, Method 1, Case 3, Limited Part Stress Method

This material is reserved for educational use only, not allowed for commercial use.
Forbidden to modify the content, and cite the document when use.

NI 9205

32-Channel, ±200 mV to ±10 V, 16-Bit Analog Input Module

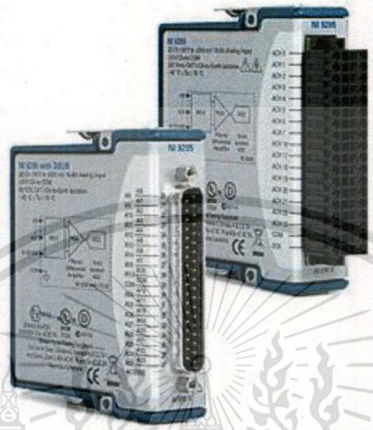

Specifications

The following specifications are typical for the range –40 to 70 °C unless otherwise noted. All voltages are relative to COM unless otherwise noted.

Analog Input Characteristics

Number of channels..... 32 single-ended or
16 differential analog input channels, 1 digital input channel, and 1 digital output channel

ADC resolution..... 16 bits

DNL.....No missing codes guaranteed

INL.....Refer to the *AI Absolute Accuracy Tables and Formulas*

MTBF ..... 775,832 hours at 25 °C; Bellcore Issue 6, Method 1, Case 3, Limited Part Stress Method

Conversion time

R Series Expansion chassis .....4.50 µs (222 kS/s)

All other chassis .....4.00 µs (250 kS/s)

This material is reserved for educational use only, not allowed for commercial use.
Forbidden to modify the content, and cite the document when use.

Input coupling.....DC
Nominal input ranges.....±10 V, ±5 V, ±1 V, ±0.2 V
Minimum overrange
(for 10 V range) 4%
Maximum working voltage for analog inputs
(signal + common mode).....Each channel must remain
within ±10.4 V of common
Input impedance (AI-to-COM)
Powered on .....>10 GΩ in parallel
with 100 pF
Powered off/overload .....4.7 kΩ min
Input bias current .....±100 pA
Crosstalk (at 100 kHz)
Adjacent channels ..... –65 dB
Non-adjacent channels .....–70 dB
Analog bandwidth..... 370 kHz
Overvoltage protection
AI channel (0 to 31) .....±30 V (one channel only)
AISENSE .....±30 V
CMRR (DC to 60 Hz)..... 100 dB

This material is reserved for educational use only, not allowed for commercial use.
Forbidden to modify the content, and cite the document when use.

APPENDIX H

IC REGULATOR LM78XX

This material is reserved for educational use only, not allowed for commercial use.
Forbidden to modify the content, and cite the document when use.

UTC LM78XX LINEAR INTEGRATED CIRCUIT

3-TERMINAL 1A POSITIVE VOLTAGE REGULATOR

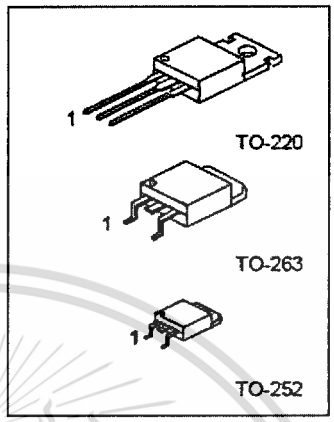

1: Input 2: GND 3: Output

DESCRIPTION

The UTC 78XX family is monolithic fixed voltage regulator integrated circuit. They are suitable for applications that required supply current up to 1 A.

FEATURES

*Output current up to 1.5 A
*Fixed output voltage of 5V, 6V, 8V, 9V, 10V, 12V, 15V ,18V and 24V available
*Thermal overload shutdown protection
*Short circuit current limiting
*Output transistor SOA protection

TEST CIRCUIT

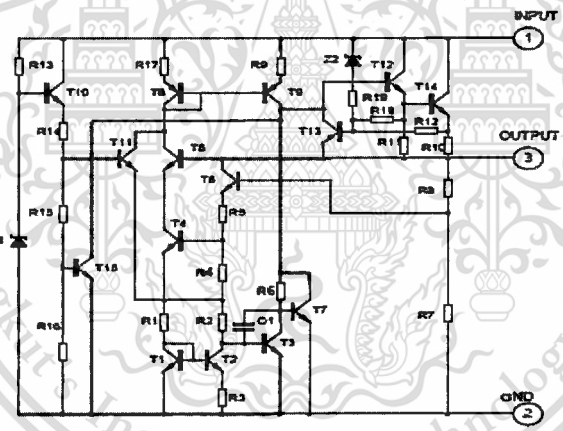

This material is reserved for educational use only, not allowed for commercial use.
Forbidden to modify the content, and cite the document when use.

UTC LM78XX LINEAR INTEGRATED CIRCUIT

ABSOLUTE MAXIMUM RATINGS

(Operating temperature range applies unless otherwise specified)

PARAMETER	SYMBOL	RATING		UNIT
Input voltage(for Vo=5~18V)			35	V
(for Vo=24V)	Vi		40	V
Output Current	Io		1	A
Power Dissipation	PD	Internally	Limited	W
Operating Junction Temperature Range	TOPR	-20	+150	°C
Storage Temperature Range	TSTG	-55	+150	°C

UTC LM7805 ELECTRICAL CHARACTERISTICS

(Vi=10V, Io=0.5A, TJ= 0°C - 125°C, C1=0.33uF, Co=0.1uF, unless otherwise specified)(Note 1)

PARAMETER	SYMBOL	TEST CONDITIONS	MIN	TYP	MAX	UNIT
Output Voltage	Vo	TJ=25°C, Io=5mA - 1.0A	4.80	5.0	5.20	V
		Vi =7.5V to 20V, Io=5mA - 1.0A,PD<15W	4.75		5.25	V
Load Regulation	ΔVo	TJ=25°C,Io=5mA - 1.5A			50	mV
		TJ=25°C,Io=0.25A - 0.75A			25	mV
Line regulation	ΔVo	Vi=7V to 25V,TJ=25°C			50	mV
		Vi=7.5V to 20V,TJ=25°C,Io=1A			50	mV
Quiescent Current	Iq	TJ=25°C, Io=<1A			8.0	mA
Quiescent Current Change	ΔIq	Vi=7.5V to 20V			1.0	mA
	ΔIq	Io=5mA - 1.0A			0.5	mA
Output Noise Voltage	VN	10Hz<=f<=100kHz		40		μV
Temperature coefficient of Vo	ΔVo/ΔT	Io=5mA		-0.6		mV/°C
Ripple Rejection	RR	Vi=8V - 18V,f=120Hz,TJ=25°C	62	80		dB
Peak Output Current	IPK	TJ=25°C		1.8		A
Short-Circuit Current	Isc	Vi=35V, TJ=25°C		250		mA
Dropout Voltage	Vd	TJ=25°C		2.0		V

UTC LM7806 ELECTRICAL CHARACTERISTICS

(Vi=11V, Io=0.5A, TJ= 0°C - 125°C, C1=0.33uF, Co=0.1uF, unless otherwise specified)(Note 1)

PARAMETER	SYMBOL	TEST CONDITIONS	MIN	TYP	MAX	UNIT
Output Voltage	Vo	TJ=25°C, Io=5mA - 1.0A	5.76	6.0	6.24	V
		Vi =8.5V to 21V, Io=5mA - 1.0A, PD<15W	5.70		6.30	V
Load Regulation	ΔVo	TJ=25°C,Io=5mA - 1.5A			60	mV
		TJ=25°C,Io=0.25A - 0.75A			30	mV
Line regulation	ΔVo	Vi=8V to 25V,TJ=25°C			60	mV
		Vi=8.5V to 21V,TJ=25°C,Io=1A			60	mV
Quiescent Current	Iq	TJ=25°C, Io=<1A			8.0	mA
Quiescent Current Change	ΔIq	Vi=8.5V to 21V			1.0	mA
	ΔIq	Io=5mA - 1.0A			0.5	mA
Output Noise Voltage	VN	10Hz<=f<=100kHz		45		μV
Temperature coefficient of Vo	ΔVo/ΔT	Io=5mA		-0.7		mV/°C
Ripple Rejection	RR	Vi=9V - 19V,f=120Hz,TJ=25°C	59	75		dB

This material is reserved for educational use only, not allowed for commercial use.

Forbidden to modify the content, and cite the document when use.

UTC LM78XX LINEAR INTEGRATED CIRCUIT

PARAMETER	SYMBOL	TEST CONDITIONS	MIN	TYP	MAX	UNIT
Peak Output Current	IPK	TJ=25°C		1.8		A
Short-Circuit Current	Isc	VI=35V, TJ=25°C		250		mA
Dropout Voltage	Vd	TJ=25°C		2.0		V

UTC LM7808 ELECTRICAL CHARACTERISTICS

(VI=14V, Io=0.5A, TJ= 0°C - 125°C, C1=0.33uF, Co=0.1uF, unless otherwise specified)(Note 1)

PARAMETER	SYMBOL	TEST CONDITIONS	MIN	TYP	MAX	UNIT
Output Voltage	Vo	TJ=25°C, Io=5mA - 1.0A	7.68	8.0	8.32	V
		VI =10.5V to 23V, Io=5mA - 1.0A, PD<15W	7.60		8.40	V
Load Regulation	ΔVo	TJ=25°C,Io=5mA - 1.5A			80	mV
		TJ=25°C,Io=0.25A - 0.75A			40	mV
Line regulation	ΔVo	VI =10.5V to 25V,TJ=25°C			80	mV
		VI =10.5V to 23V,TJ=25°C,Io=1A			80	mV
Quiescent Current	Iq	TJ=25°C, Io=<1A			8.0	mA
Quiescent Current Change	ΔIq	VI =10.5V to 23V			1.0	mA
	ΔIq	Io=5mA - 1.0A			0.5	mA
Output Noise Voltage	VN	10Hz<=f<=100kHz		58		μV
Temperature coefficient of Vo	ΔVo/ΔT	Io=5mA		-0.9		mV/°C
Ripple Rejection	RR	VI =11.5V to 21.5V, f=120Hz,TJ=25°C	56	72		dB
Peak Output Current	IPK	TJ=25°C		1.8		A
Short-Circuit Current	Isc	VI=35V, TJ=25°C		250		mA
Dropout Voltage	Vd	TJ=25°C		2.0		V

UTC LM7809 ELECTRICAL CHARACTERISTICS

(VI=15V, Io=0.5A, TJ= 0°C - 125°C, C1=0.33uF, Co=0.1uF, unless otherwise specified)(Note 1)

PARAMETER	SYMBOL	TEST CONDITIONS	MIN	TYP	MAX	UNIT
Output Voltage	Vo	TJ=25°C, Io=5mA - 1.0A	8.64	9.0	9.36	V
		VI =11.5V to 24V, Io=5mA - 1.0A,PD<15W	8.55		9.45	V
Load Regulation	ΔVo	TJ=25°C,Io=5mA - 1.5A			90	mV
		TJ=25°C,Io=0.25A - 0.75A			45	mV
Line regulation	ΔVo	VI =11.5V to 25 V, TJ=25°C, PD<15W			90	mV
		VI =11.5V to 24V,TJ=25°C, Io=<1A			90	mV
Quiescent Current	Iq	TJ=25°C, Io=<1A			8.0	mA
Quiescent Current Change	ΔIq	VI =11.5V to 24V			1.0	mA
	ΔIq	Io=5mA – 1.0A			0.5	mA
Output Noise Voltage	VN	10Hz<=f<=100kHz		58		μV
Temperature coefficient of Vo	ΔVo/ΔT	Io=5mA		-1.1		mV/°C
Ripple Rejection	RR	VI =12.5V to 22.5V, f=120Hz,TJ=25°C	56	72		dB
Peak Output Current	IPK	TJ=25°C		1.8		A
Short-Circuit Current	Isc	VI=35V, TJ=25°C		250		mA
Dropout Voltage	Vd	TJ=25°C		2.0		V

This material is reserved for educational use only, not allowed for commercial use.
Forbidden to modify the content, and cite the document when use.

UTC LM7810 ELECTRICAL CHARACTERISTICS

(VI=16V, Io=0.5A, Tj= 0°C - 125°C, C1=0.33uF, Co=0.1uF, unless otherwise specified)(Note 1)

PARAMETER	SYMBOL	TEST CONDITIONS	MIN	TYP	MAX	UNIT
Output Voltage	Vo	Tj=25°C, Io=5mA - 1.0A	9.60	10.0	10.40	V
		VI =12.5V to 25V, Io=5mA - 1.0A,PD<=15W	9.50		10.50	V
Load Regulation	ΔVo	Tj=25°C,Io=5mA - 1.5A			100	mV
		Tj=25°C,Io=0.25A - 0.75A			50	mV
Line regulation	ΔVo	VI =13V to 25V,Tj=25°C			100	mV
		VI =13V to 25V, Tj=25°C,Io<=1A			100	mV
Quiescent Current	Iq	Tj=25°C, Io=<1A			8.0	mA
Quiescent Current Change	ΔIq	VI =12.6V to 25V			1.0	mA
	ΔIq	Io=5mA - 1.0A			0.5	mA
Output Noise Voltage	VN	10Hz<=f<=100kHz		58		μV
Temperature coefficient of Vo	ΔVo/ΔT	Io=5mA		-1.1		mV/°C
Ripple Rejection	RR	VI =13V - 23V,f=120Hz,Tj=25°C	56	72		dB
Peak Output Current	IPK	Tj=25°C		1.8		A
Short-Circuit Current	Isc	VI=35V, Tj=25°C		250		mA
Dropout Voltage	Vd	Tj=25°C		2.0		V

UTC LM7812 ELECTRICAL CHARACTERISTICS

(VI=19V, Io=0.5A, Tj= 0°C - 125°C, C1=0.33uF, Co=0.1uF, unless otherwise specified)(Note 1)

PARAMETER	SYMBOL	TEST CONDITIONS	MIN	TYP	MAX	UNIT
Output Voltage	Vo	Tj=25°C, Io=5mA - 1.0A	11.52	12.0	12.48	V
		VI =14.5V to 27V, Io=5mA - 1.0A,PD<15W	11.40		12.60	V
Load Regulation	ΔVo	Tj=25°C,Io=5mA - 1.5A			120	mV
		Tj=25°C,Io=0.25A - 0.75A			60	mV
Line regulation	ΔVo	VI =14.5V to 30V,Tj=25°C			120	mV
		VI =14.6V to 27V,Tj=25°C, Io=1A			120	mV
Quiescent Current	Iq	Tj=25°C, Io=<1A			8.0	mA
Quiescent Current Change	ΔIq	VI =14.5V to 30V			1.0	mA
	ΔIq	Io=5mA - 1.0A			0.5	mA
Output Noise Voltage	VN	10Hz<=f<=100kHz		75		μV
Temperature coefficient of Vo	ΔVo/ΔT	Io=5mA		-1.5		mV/°C
Ripple Rejection	RR	VI =15V - 25V,f=120Hz,Tj=25°C	55	72		dB
Peak Output Current	IPK	Tj=25°C		1.8		A
Short-Circuit Current	Isc	VI=35V, Tj=25°C		250		mA
Dropout Voltage	Vd	Tj=25°C		2.0		V

This material is reserved for educational use only, not allowed for commercial use.

Forbidden to modify the content, and cite the document when use.

UTC LM7815 ELECTRICAL CHARACTERISTICS

(VI=23V, Io=0.5A, TJ= 0°C - 125°C, C1=0.33uF, Co=0.1uF, unless otherwise specified)(Note 1)

PARAMETER	SYMBOL	TEST CONDITIONS	MIN	TYP	MAX	UNIT
Output Voltage	Vo	TJ=25°C, Io=5mA - 1.0A	14.40	15.0	15.60	V
		VI =17.5V to 30V, Io=5mA - 1.0A,PD<15W	14.25		15.75	V
Load Regulation	ΔVo	TJ=25°C,Io=5mA - 1.5A			150	mV
		TJ=25°C,Io=0.25A - 0.75A			75	mV
Line regulation	ΔVo	VI =16.5V to 30V,TJ=25°C			150	mV
		VI =17.7V to 30V, TJ=25°C, Io =1A			150	mV
Quiescent Current	Iq	TJ=25°C, Io=<1A			8.0	mA
Quiescent Current Change	Δiq	VI =17.5V to 30V			1.0	mA
	Δiq	Io=5mA - 1.0A			0.5	mA
Output Noise Voltage	VN	10Hz<=f<=100kHz		90		μV
Temperature coefficient of Vo	ΔVo/ΔT	Io=5mA		-1.8		mV/°C
Ripple Rejection	RR	VI =18.5V to 28.5V f=120Hz,TJ=25°C	54	70		dB
Peak Output Current	IPK	TJ=25°C		1.8		A
Short-Circuit Current	Isc	VI=35V, TJ=25°C		250		mA
Dropout Voltage	Vd	TJ=25°C		2.0		V

UTC LM7818 ELECTRICAL CHARACTERISTICS

(VI=27V, Io=0.5A, TJ= 0°C - 125°C, C1=0.33uF, Co=0.1uF, unless otherwise specified)(Note 1)

PARAMETER	SYMBOL	TEST CONDITIONS	MIN	TYP	MAX	UNIT
Output Voltage	Vo	TJ=25°C, Io=5mA - 1.0A	17.28	18.0	18.72	V
		VI =21V to 33V,Io=5mA - 1.0A	17.10		18.90	V
Load Regulation	ΔVo	TJ=25°C,Io=5mA - 1.5A			180	mV
		TJ=25°C,Io=0.25A - 0.75A			90	mV
Line regulation	ΔVo	VI =21V to 33V,TJ=25°C			180	mV
		VI =21V to 33V, TJ=25°C, Io =<1A,PD<15W			180	mV
Quiescent Current	Iq	TJ=25°C, Io=<1A			8.0	mA
Quiescent Current Change	Δiq	VI =21.5V to 33V			1.0	mA
	Δiq	Io=5mA - 1.0A			0.5	mA
Output Noise Voltage	VN	10Hz<=f<=100kHz		110		μV
Temperature coefficient of Vo	ΔVo/ΔT	Io=5mA		-2.2		mV/°C
Ripple Rejection	RR	VI =22V - 32V,f=120Hz,TJ=25°C	53	69		dB
Peak Output Current	IPK	TJ=25°C		1.8		A
Short-Circuit Current	Isc	VI=35V, TJ=25°C		250		mA
Dropout Voltage	Vd	TJ=25°C		2.0		V

This material is reserved for educational use only, not allowed for commercial use.

Forbidden to modify the content, and cite the document when use.

APPENDIX I

PROCEEDINGS

- **Appendix I-1: Design of Regenerative Braking System for an Electric Vehicle (EV) Modified from Used Car**
- **Appendix I-2 : Brake Force Control Scheme for Integration of Conventional and Regenerative Braking Systems of Retrofitted Electric Vehicles**

This material is reserved for educational use only, not allowed for commercial use.
Forbidden to modify the content, and cite the document when use.

Appendix I-1: Design of Regenerative Braking System for an Electric Vehicle (EV) Modified from Used Car

This material is reserved for educational use only, not allowed for commercial use.
Forbidden to modify the content, and cite the document when use.

ETM19
The Second TSME International Conference on Mechanical Engineering
19-21 October, 2011, Krabi

Design of Regenerative Braking System for an Electric Vehicle (EV) Modified from Used Car

*Saharat Chanthanumataporn[1], Sarawut Lerspalungsanti[2] and Monsak Pimsarn[3]

[1] TAIST Toyo Tech Automotive Engineering program, International College, King Mongkut's Institute of Technology Ladkrabang, Bangkok, Thailand 10520, E-mail: ppsae4@gmail.com

[2] National Metal and Materials Technology Center (MTEC), National Science and Technology Development Agency (NSTDA), Pathumthani, Thailand, E-mail: sarawutl@mtec.or.th

[3] Department of Mechanical Engineering, King Mongkut's Institute of Technology Ladkrabang, Bangkok,10520, Thailand, E-mail: kpmonsak@kmitl.ac.th

Abstract

In general one of the main objectives of regenerative braking system is to recover as much as possible kinetic energy while braking instead of being dispersed in form of heat by only friction brake. In Electric Vehicle (EV) with regenerative braking system, most braking energy is converted to electrical form via generator switched from its motor, and stored in storage device or battery to use in vehicle's electric application or use to propel itself. Thus, the EV with regenerative braking system can extend driving range. In this study, a prototype of the EV is modified from an internal combustion engine vehicle. The regenerative algorithm and equipment, based on a conventional braking system of this EV, are presented and its functional validation is investigated by using numerical simulation. Regarding the braking torque distribution between regenerative and friction brake, the available regenerative torque from electric motor is computed depending on current vehicle velocity, the torque characteristic of the motor-generator, and the state of charge (SOC) of the Li-Ion batteries. The friction brake torque of driven wheels, front wheel, will be reduced equal to regenerative torque by reducing brake fluid pressure. To determine the regenerative system efficiency, three regenerative strategies are investigated: non-modified braking system, modified braking system with emulated ABS signal, and modified braking system with brake fluid distribution in master cylinder. In this study, the criteria for analyzing these regenerative systems are energy recovery, and braking performance represented by braking distance. The simulated results indicate that the regenerative strategy of modified braking system with emulated ABS signal is the most proper in this study.

Key words: Regenerative braking system, Electric vehicle (EV)

1. Introduction

Since the crisis of the price of fossil oil on the world market rising higher almost every time directly affects to Thailand, making most vehicle users turning the behavior to utilize low-priced alternative energy such as Gasohol, Biodiesel, Liquid Petroleum Gas (LPG) or Compressed Natural Gas (CNG). Especially, LPG and CNG are mostly popular because of their cheap prices per unit and the inexpensive

This material is reserved for educational use only, not allowed for commercial use.
Forbidden to modify the content, and cite the document when use.

budget of installation. However, the concerns about emission problem like carbon dioxide quantity or greenhouse effect still continuously take place. One of the measures of reducing traffic emission is to propel to use natural friendly vehicles for instance Battery electric vehicle (BEV). Since EV is still expensive and not widespread, the expected tendency of using the EV in Thailand should be alike the utilization LPG or CNG being alternative energy in that the conventional internal combustion engine used cars are modified to be EV.

Regenerative braking system is a significant part of EV, which is responsible for recovering potential and kinetic energy during vehicle braking and storing it into energy storage device instead of dissipating in heat form by fiction brake. The stored energy is utilized to propel vehicle [1] or to supply vehicle's electrical application. Regenerative braking system is an effective means to prolong the driving range of EV and also to improve fuel consumption rate of Hybrid Electric Vehicle (HEV), particularly for the vehicle that mainly runs in high frequent stop and go condition such as city traffic [2]. The past researches have suggested that an HEV's driving range in urban can be extended between 14 and 40% by using regenerative brake [3], [4].

In general, the regenerative braking system is collaborated with the conventional friction brake because of following reasons. The first one is that the available brake torque of motor-generator, while emergency braking occurs, is not large enough to fulfill such huge braking requirement. The second reason is that in such condition as high voltage of the energy storage component, high state of battery's charge (SOC), or high temperature to damage battery, regenerative brake cannot be operated since the reason of the damage to battery [5].

Some relevant reports of regenerative braking system that have been proposed are presented. Y.Gao et. al. [6] suggests the regenerative model and algorithm for EV and HEV focusing on vehicle stability by controlling brake force between front and rear wheels. M.Pabagiotidis et. al. [7] proposes controlling algorithm and regenerative model using specific simulation software. This algorithm relies on Look-up table to provide brake force distribution into front and rear wheels as well as generator. H.Yeo et. al. [8] proposes hydraulic braking module for regenerative braking system and algorithm for controlling regenerative braking module and continuously variable transmission (CVT). Nevertheless, all above regenerative systems are designed for front/rear split circuit braking system that cannot be applied for a passenger car with cross link circuit braking system.

The objective of this paper is to determine the most proper regenerative system for an EV modified from used car equipped with cross link circuit braking system and anti-lock brake system (ABS). In this study, a total of three strategies are proposed. The difference of each model is the method of controlling the brake fluid distribution into the regenerative and the mechanical braking system. The performance of each strategy is executed by numerical simulation. The design criteria are regenerative energy and braking performance represented by braking distance.

This material is reserved for educational use only, not allowed for commercial use.
Forbidden to modify the content, and cite the document when use.

ETM19
The Second TSME International Conference on Mechanical Engineering
19-21 October, 2011, Krabi

2. Regenerative braking strategy

The layout of internal combustion engine (ICE) vehicle and electric vehicle are shown in Figure 1 and 2 respectively. The platform of this ICE vehicle is front engine, front drive (FF) using manual transmission. Its braking system is cross link circuit or X layout with four wheel disk brakes and anti-lock brake system (ABS). The modification from engine into electric vehicle is achieved by installing motor-generator (MG) instead of engine and changing the manual transmission into fixed transmission since electric motor does not need complex-ratio transmission so as engine to maintain optimal operation on the fuel economy region. Thus, this vehicle platform is still the FF, front motor, front drive. Because regenerative torque needs medium to send this brake torque into driven wheel, the vehicle platform is factor defining that only driven wheel, front wheel in this case, can contribute regenerative braking power. Therefore, front wheels are cooperated by regenerative and friction brake force while rear wheels have only friction brake operation.

2.1 Non-modified braking system

Based on this regenerative strategy, shown in figure 2, conventional braking system is applied without modification. During braking, the mechanical braking system is operated independent of regenerative process. In this case, the pressure of brake fluid at front wheel remains as conventional. Thus, while regenerative brake operates at front wheels, the amount of front brake force is higher than normally required brake force. Nevertheless, the concern about front wheel locking is resolved by ABS that automatically reduces brake pressure if wheel locking takes place.

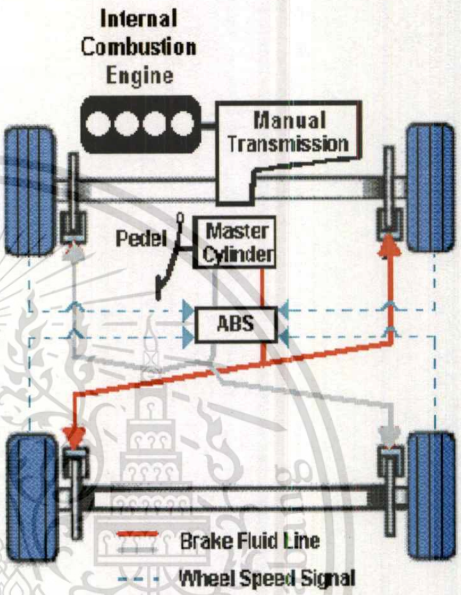

Fig. 1 Layout of the ICE vehicle and braking system

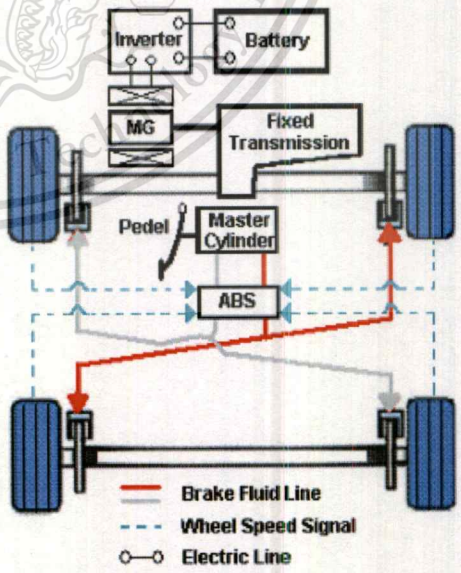

Fig. 2 Layout of the EV and braking system

This material is reserved for educational use only, not allowed for commercial use.
Forbidden to modify the content, and cite the document when use.

2.2 Modified braking system with emulated ABS signal

The objective of this system is to allow regenerative system can obtain as much energy as possible by reducing friction brake force be equal to a quantity of regenerative brake force. The layout of modified braking system with emulated ABS signal is shown in Figure 3. The modification is to trap front wheel speed signal to regenerative control unit (RCU) and then send emulated wheel speed signal to ABS control unit to simulate the wheel locking-up situation. Consequently, ABS control unit will automatically reduce brake fluid pressure at front wheel. On one hand, if sum of regenerative and front friction brake force is more than force of front wheel requirement, emulated signal is sent to reduce friction brake force. On the other hand, if friction brake force is not enough, the RCU will suddenly stop sending emulated signal to allow ABS to increase proper friction brake force. The designed algorithm of RCU can be described as followed as to distribute friction brake and regenerative brake force by using signal of motor RPM, brake fluid pressure at Master cylinder (Pm) and Caliper (Pc) and Battery SOC.

2.3 Modified braking system with brake fluid distribution in master cylinder

Mechanism of this system is to control solenoid valve to close brake fluid pressure by using solenoid valve at the outlet of master cylinder while a required brake force of four wheels is lower than the available regenerative brake force. The layout of this system is shown in figure 4. The 4 wheel brake force can be computed from outlet pressure of mater cylinder. Motor RPM and %SOC can be used to calculate the regenerative brake force.

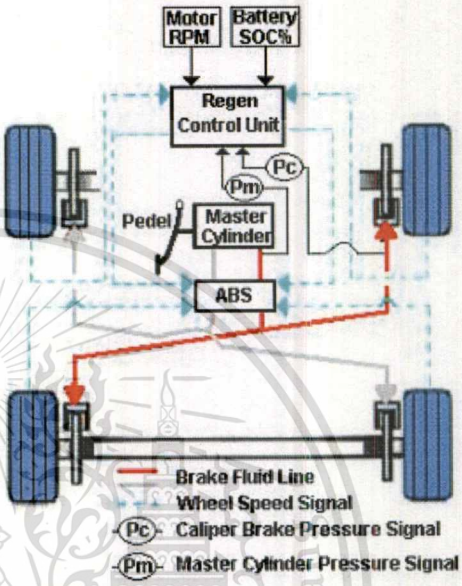

Fig. 3 Layout of regenerative system of modified braking system with emulated ABS signal

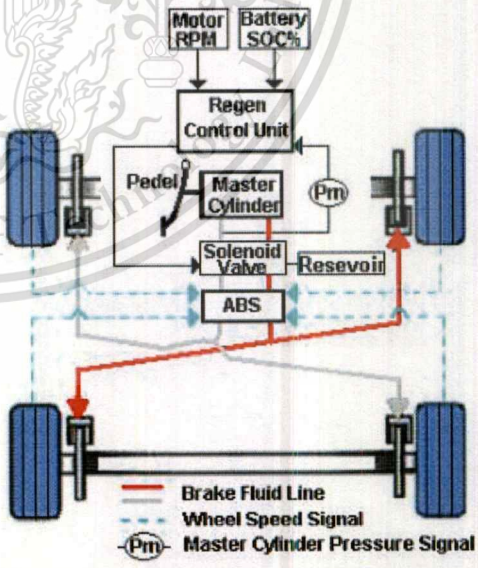

Fig. 4 Layout of regenerative system of modified braking system with brake fluid distribution in master cylinder

This material is reserved for educational use only, not allowed for commercial use.
Forbidden to modify the content, and cite the document when use.

ETM19
The Second TSME International Conference on Mechanical Engineering
19-21 October, 2011, Krabi

3. Regenerative Braking Algorithm

To manage brake force during using regenerative brake, the first thing must be achieved is to calculate magnitude of regenerative brake torque at the front wheel. This torque depends on the motor-generator torque characteristic at given RPM (T_{Reg_Motor}). gear ratio (i), and differential gear ratio (N_d). The Regenerative brake torque at front wheel (T_{Reg_FW}) can be represented as

$$T_{Reg\_FW} = T_{Reg\_Motor} \cdot i \cdot N_d \quad (1)$$

In order to easily measure and compare brake force, T_{Reg_FW} is converted to be equivalent regenerative brake pressure (ΔP) since all sensors used to measure brake force at each point are pressure sensors and in algorithm, brake force is compared by using pressure. ΔP is equal to hydraulic pressure at front caliper that should be reduced while regenerative and friction brake collaborate.

$$\Delta P = \frac{T_{Reg\_FW}}{A_{wcf} \times \mu \times 2 \times r} \quad [9] \quad (2)$$

Where A_{wcf} is the cylinder area of front caliper, μ is the friction coefficient, and r is the effective radius of brake disk.

The strategy to control regenerative system of modified braking system with emulated ABS signal is shown in figure 5. The brake assist (BA) is a mode automatically increasing hydraulic brake pressure when the pedal is suddenly pressed. If BA operates meaning that this braking is in panic situation, the brake pressure should not be reduced by all means. When the braking is not on BA mode, the RCU calculates ΔP by using equation (2) and then multiply by Weight Factor, function of battery SOC, shown in Figure 6. In this study, weight factor equals to one at SOC range of 0-80% to increase battery SOC level but at range of 80-100%, weight factor linearly decline to protect battery damage of overcharging. If ΔP^*, referred to available regenerative brake force, is larger than $P_m - P_c$, RCU sends emulated signal to ABS control unit making ABS automatically reduces friction brake force (P_c). Where P_m is master cylinder pressure referred to required brake force, P_c is caliper pressure referred to friction brake force. If ΔP^* is smaller than the difference of P_m and P_c, RCU stops sending emulated signal to increase brake friction brake force .

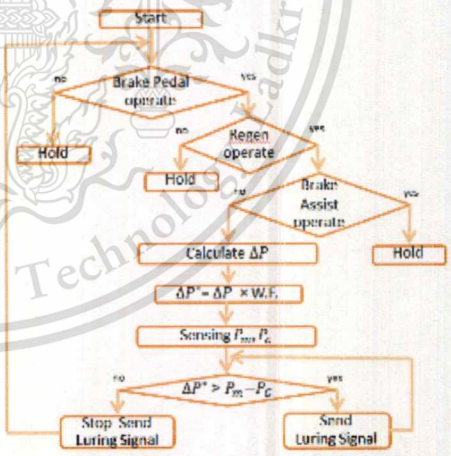

Fig. 5 Strategy flow chart of regenerative system of modified braking system with emulated ABS signal

In Figure 7, the strategy for regenerative system modified braking system with brake fluid distribution in master cylinder is presented. Most

This material is reserved for educational use only, not allowed for commercial use.
Forbidden to modify the content, and cite the document when use.

ETM19
The Second TSME International Conference on Mechanical Engineering
19-21 October, 2011, Krabi

of it is same to the first strategy but the difference is that ΔP^* and only P_m is compared to drive solenoid valve to control hydraulic brake pressure. P_m is sum total of both hydraulic pressures at master cylinder outlet. If ΔP^* is more than P_m, RCU drives solenoid to cut brake pressure. On the other hand, RCU stops driving solenoid to open hydraulic pressure normally.

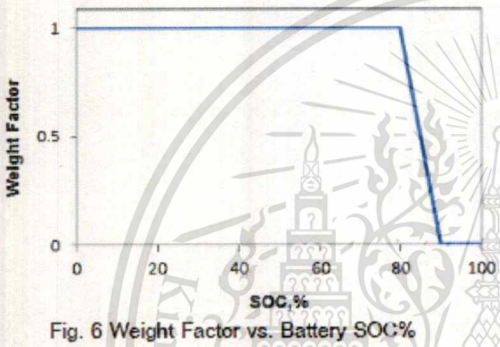

Fig. 6 Weight Factor vs. Battery SOC%

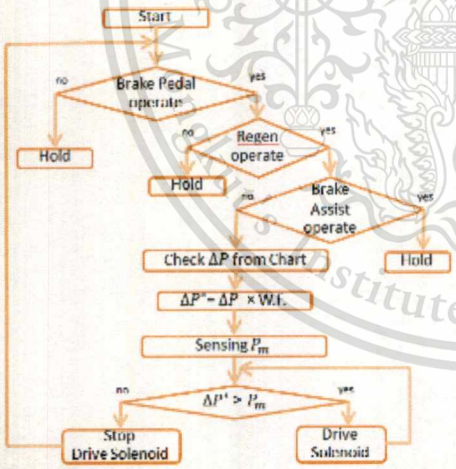

Fig. 7 Strategy flow chart of regenerative system of modified braking system with brake fluid distribution in master cylinder

4. Simulation Model

Four models are implemented by using MATLAB Simulink software and use same parameters shown in Table. 1. All models consist of model of conventional braking system with ABS and regenerative system of non-modified braking system, modified braking system with emulated ABS signal, and modified braking system with brake fluid distribution in master cylinder. The model of conventional brake with ABS is made to compare braking distance and braking pressure contour with all model of regenerative.

Table 1 Total parameter of vehicle

Motor	
Peak torque	240 Nm
Peak Power	75 kW
Transmission system	
Fixed gear ratio (i)	1.303
Rear axle gear ratio (Nd)	4.294
Vehicle	
Vehicle mass (m)	1520 kg
Frontal area (dA)	2.146 m^2
Drag coefficient (Cd)	0.35
Tire radius (Rt)	0.32 m

Simulation flowchart is shown in figure 8 in which each box is represented as component of calculation. The initial value of this simulation is brake demand and vehicle speed. Started from brake demand, brake pressure signal in hydraulic pressure box is controlled by ABS control unit box from which the result is friction brake torque. In case of regenerative operation, the controlling signal of regenerative box is send to control friction brake force. Vehicle speed can be used to calculate stopping distance of vehicle and wheel speed can be used to calculate motor torque available by using motor-torque look-up

This material is reserved for educational use only, not allowed for commercial use.
Forbidden to modify the content, and cite the document when use.

ETM19
The Second TSME International Conference on Mechanical Engineering
19-21 October, 2011, Krabi

table. The vehicle and wheel speed are also used to calculate slip rate to send to ABS control unit and find friction coefficient (Mu) between road and tire surface at Mu-slip look-up table. The friction coefficient is used to calculate vehicle speed and inertia torque of vehicle. Regenerative energy is computed from wheel RPM and generator torque in Regenerative energy box.

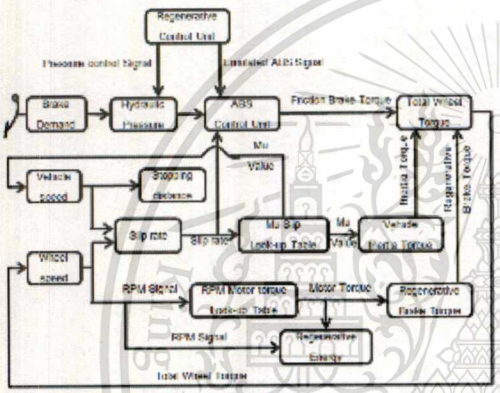

Fig. 8 Simulation Model

5. Simulation result and discussion

The percentage of braking distance is shown in Fig. 9 comparing that braking distance of conventional brake with ABS is equal to 100%. By the result, all regenerative system can reduce brake distance since they have additional brake force from regenerative braking. The lowest braking distance is of regenerative system of non-modified braking system because no strategy is used to reduce friction brake force while regenerative brake force works together. The medium braking distance is of regenerative system of modified braking system with brake fluid distribution in master cylinder since it cut brake pressure during only starting point. The greatest braking distance of three regenerative systems and nearest to conventional braking distance is of regenerative system of modified braking system with emulated ABS signal because it have the strategy to decrease friction brake force corresponding to regenerative brake force all the operation time.

Fig. 10 shows front wheel brake pressure contour of four models. The green line is brake pressure at master cylinder or demanded brake force and the blue line is brake pressure at front brake caliper. Fig. 10(a) is brake pressure of conventional brake with ABS. The brake pressure of master cylinder is equal to brake-caliper pressure meaning that ABS still has not operated. Figure 10(b) shows brake-pressure contour of regenerative system of non-modified braking system. Since, this system, front wheel have two brake forces working together but it has not used any strategy to lessen friction brake force making front wheel locking. Hence, ABS has operated to diminish friction brake force showing of blue line. Figure 10(c) is brake pressure outline of regenerative system of modified braking system with emulated ABS signal. The pressure friction brake is lower than required brake pressure corresponding to regenerative brake force owning to its strategy. Figure 10(d) provides brake pressure of regenerative system of modified braking system with brake fluid distribution in master cylinder. The strategy outcome of this system is only the period of 0-1.2 second that caliper brake pressure is equal to zero because of cutting hydraulic pressure by solenoid valve. However, the result of pressure reduction at the second of 2.8-4.3 is of ABS operation.

This material is reserved for educational use only, not allowed for commercial use.
Forbidden to modify the content, and cite the document when use.

ETM19
The Second TSME International Conference on Mechanical Engineering
19-21 October, 2011, Krabi

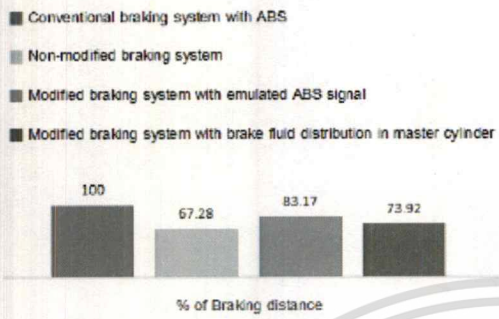

Fig. 9 Percentage of Braking distance

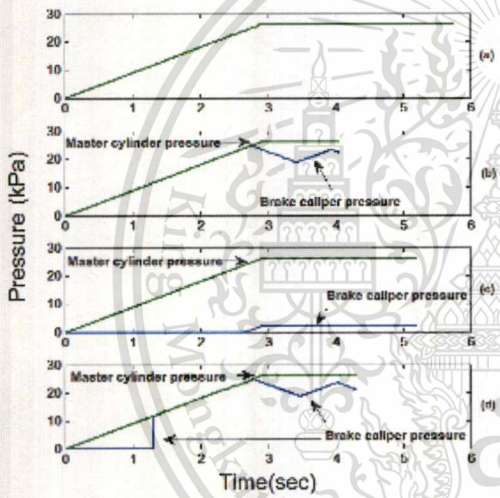

Fig. 10 Brake pressure contour

a) Conventional braking system with ABS
b) Non-modified braking system
c) Modified braking system with emulated ABS signal
d) Modified braking system with brake fluid distribution in master cylinder

Regenerative energy of each system is different depending on controlling the friction brake force, pressure at front brake caliper. The regenerative system of modified braking system with emulated ABS signal so work properly that it is the first one that can provide energy the most of any regenerative system in this study. The energy gave by regenerative system of modified braking system with brake fluid distribution in master cylinder is second order since it have pressure controlling only in starting time. The lowest provided energy is of regenerative system of non-modified braking system because of no friction brake reduction strategy.

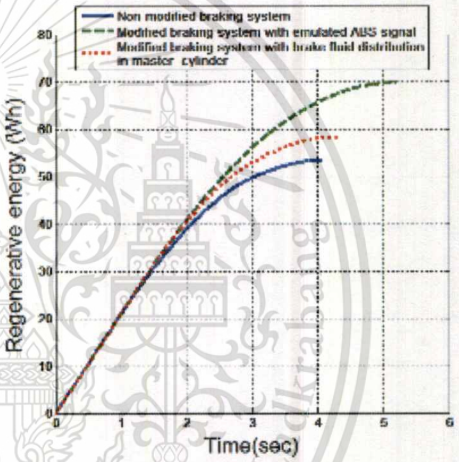

Fig. 10 Regenerative energy of each system

6. Conclusion

In this study, three candidates of regenerative braking strategies are examined by using MATLAB Simulink software. The braking situations are simulated to test design criteria of braking performance focused on braking distance and regenerative energy. The regenerative strategy of modified braking system with emulated ABS signal is the most proper in this study. Nevertheless, these criteria results must be validated in next phrase and also to investigate other criteria such as cost and feasibility.

This material is reserved for educational use only, not allowed for commercial use.
Forbidden to modify the content, and cite the document when use.

7. References

[1] Kim, D. and Kim, H. (2006). Vehicle stability control with regenerative braking and electronic brake force distribution for a four-wheels drive hybrid electric vehicle, Proc. IMechE Part D: J. Automobile Engineering, vol.220(6), June 2006, pp. 683-693.

[2] Cholula, S., Claudio, A. and Ruiz, J. (2005). Intelligent Control of the Regenerative Braking in an Induction Motor Drive, paper presented in the 2nd International Conference on Electrical and Electronics Engineering (ICEEE) and XI Conference on Electrical Engineering (CIE).

[3] Triger, L., Paterson, J. and Drozdz, P. (1993). Hybrid Vehicle Engine Size Optimization, August 1993, SAE Paper #931793.

[4] LaPlante, J., Anderson, C.J. and Auld, J. (1995). Development of a Hybrid Electric Vehicle for the US Marine Corps, August 1995, SAE Paper #951905.

[5] Feng, W., Hu, Z., Xiao-jian, M., Lin, Y. and Bin, Y. (2007) Regenerative Braking algorithm for a Parallel Hybrid Electric Vehicle with Continuously Variable Transmission, Vehicular Electronics and Safety, 2007 ICVES. Beijing IEEE, 2007: 1-4.

[6] Gao, Y., Chen, L. and Ehsani, M. (1999) Investigation of the Effectiveness of Regenerative Braking for EV and HEV, August 1999, SAE Paper 1999-01-2910.

[7] Pabagiotidis, M., Delagrammatikas, G. and Assanis, D. (2000) Development and Use of a Regenerative Braking Model for Parallel Hybrid Electric Vehicle, August 2000, SAE Paper 2000-01-0995.

[8] Yeo, H., Kim, D., Hwang, S. and Kim, H. (2004). Regenerative Braking Algorithm for a HEV with CVT Ratio Control during Deceleration, 04CVT-41, paper presented by Dynamic System Design & Control Lab. Sungkyunkwan University, Korea.

[9] Jang, S., Yeo, H., Kim, C. and Kim, H. (2001). A Study on Regenerative Braking for a Parallel Hybrid Electric Vehicle, KSME International Journal, Vol. 15(11), August 2001, pp 1490-1498, 2001

This material is reserved for educational use only, not allowed for commercial use.
Forbidden to modify the content, and cite the document when use.

Appendix I-2 : Brake Force Control Scheme for Integration of Conventional and Regenerative Braking Systems of Retrofitted Electric Vehicles

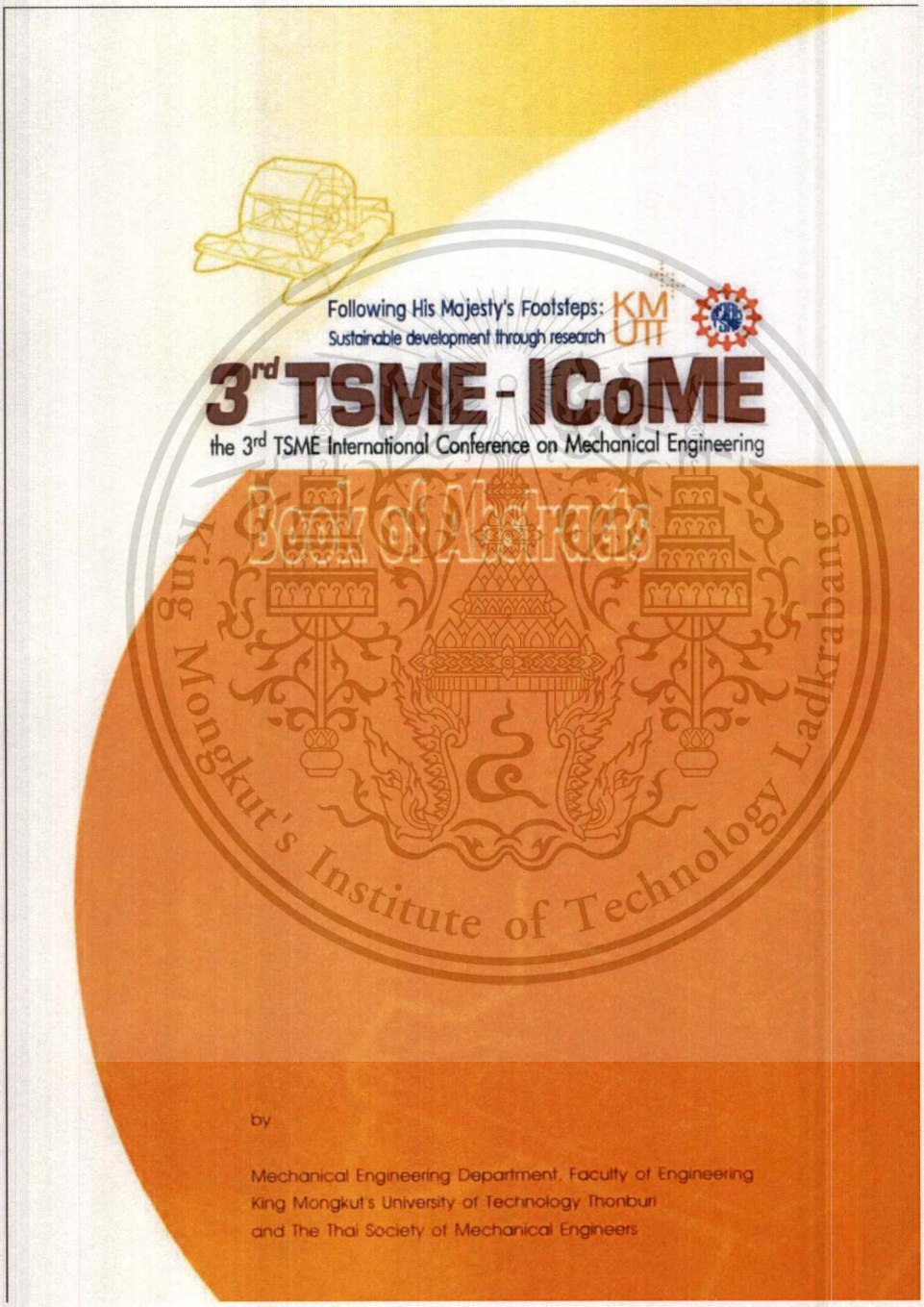

This material is reserved for educational use only, not allowed for commercial use.
Forbidden to modify the content, and cite the document when use.

Paper ID
CST 1018

The 3rd TSME International Conference on Mechanical Engineering
October 2012, Chiang Rai

Brake Force Control Scheme for Integration of Conventional and Regenerative Braking Systems of Retrofitted Electric Vehicles

Saharat Chanthanumatapom[1,*], Sarawut Lerspalungsanti[2], Sittikorn Lapapong[2], Monsak Pimsarn[3] and Masaki Yamakita[4]

[1]TAIST Tokyo Tech Automotive Engineering Program, International College, King Mongkut's Institute of Technology Ladkrabang, Chalongkrung Rd., Ladkrabang, Bangkok 10520, Thailand
[2]National Metal and Materials Technology Center (MTEC), 114 Thailand Science Park, Paholyothin Rd., Klong 1, Klong Luang, Pathumthani 12120, Thailand
[3]Department of Mechanical Engineering, King Mongkut's Institute of Technology Ladkrabang, Chalongkrung Rd., Ladkrabang, Bangkok 10520, Thailand
[4]Department of Mechanical and Control Engineering, Tokyo Institute of Technology, 2-12-1-W8-20 O-okayama, Meguro-ku, Tokyo 152-8552, Japan
*Corresponding Author: saharatch@hotmail.com, Telephone Number +66-3454-2213

Abstract

This paper proposes a new brake force control scheme for retrofitted Electric Vehicles (EVs). This scheme allows a conventional anti-lock braking system and a regenerative braking system to be seamlessly integrated with minor modification of the original system and yet provides the braking performance identical to the original braking system. The main idea of this scheme is to maintain the overall braking force to be as close as the brake demand given by a driver by utilizing a unique feature of an anti-lock braking system (ABS). To achieve this during a brake situation, an emulated "Lock" signal is sent to the ABS control unit to decrease the mechanical brake force down until the amount of reduced force is equal to the available regenerative one. Besides, the performance of this retrofitted braking system is evaluated by simulations based on four design aspects, which are energy efficiency, passenger comfort, braking distance, and practicality.

Keywords: Brake force control, Regenerative brake, Electric vehicle, Anti-lock braking system (ABS)

1. Introduction

As currently known, the global warming has increasingly become an important worldwide issue. It is believed that its cause is the increase of concentrations of greenhouse gases in the Earth's atmosphere. Examples of the greenhouse gases are carbon dioxide, nitrous oxide, etc. From the examples, one can obviously determine that one of the primary sources of these greenhouse gas emissions is the burning of fossil fuels, particularly automobile emissions. Thus, one way to mitigate this global-warming issue is to reduce the amount of the greenhouse gases emitted to the atmosphere. Changes of use from Combustion-Engine (CE) vehicles to electrical ones may be one of the possible solutions to help alleviating this issue, since an Electric Vehicle (EV) virtually has zero emission. Nonetheless, in some countries, especially developing countries, the use of EVs is still not widespread and not affordable due to its high cost. Therefore, there is an idea to study the retrofit of a combustion-engine production car to be an electric one.

Typically, a production EV is manufactured with a braking system that not only provides a braking force but also can recover some energy during braking, and this system is called a regenerative braking system. In this system, a propelling motor of an EV can function as an electrical generator converting braking energy into electrical one that can be stored in an energy storage device or used in electrical applications. To modify a CE production car to a retrofitted electric one, the add-on regenerative braking system should well cooperate with the original braking system. The main reasons that the frictional brake cannot be completely discarded from the retrofitted EV are that the solo regenerative brake cannot provide adequate braking power during an emergency braking situation, and the regenerative brake cannot be operated under some circumstances, for instance, the cases of high battery temperature and/or battery's high state of charge (SOC) [1].

There have been various modification schemes proposed. Most schemes are suitable for

This material is reserved for educational use only, not allowed for commercial use.
Forbidden to modify the content, and cite the document when use.

Paper ID
CST 1018

The 3rd TSME International Conference on Mechanical Engineering
October 2012, Chiang Rai

a car with a front-rear split circuit braking system. Examples are the work of Gao *et al.*[2] that presents the regenerative braking system for controlling the front and rear braking forces of EVs and hybrid EVs and the work of Pabagiotidis *et al.* [3] that proposes the regenerative braking algorithm for allocating the braking forces based on a look-up table. Further, Feng *et al.*[1], Jang *et. al.*[4], and Yeo *et. al.*[5] introduce hydraulic brake modules used in their regenerative braking systems that can solely be applied to the front-rear split circuits. However, braking systems of modern sub-compact and compact production cars are the cross-link circuit type; thus, the previously proposed schemes are not compatible with them. Besides, these schemes require major modification of the braking systems and high-cost equipment. Most of the braking components must be replaced with specifically designed parts. Another scheme is the parallel regenerative braking system that can be integrated with all types of braking circuits. Nonetheless, its efficiency is relatively low, and it generates non-conventional brake force distribution, resulting in negative driving comfort. Consequently, this paper proposes a new brake force control strategy and a new modification scheme that allows a regenerative braking system to be seamlessly integrated into all types of conventional friction braking systems in retrofitted EVs with slight modification of the braking systems. This scheme makes use of a feature of a standard Anti-lock Braking System (ABS) to provide a brake force distribution identical to that of the conventional braking system. Furthermore, the performance of the proposed method is investigated by simulations based on four design criteria: regenerative energy efficiency, ride comfort, braking distance, and feasibility.

The remainder of the paper is organized as follows: Section 2 introduces the new modification scheme of the braking system called the universal hydraulic module for a regenerative braking system. The new concept of brake force control strategy is presented in Section 3. Section 4 briefly gives an introduction to parallel regenerative braking system used as a benchmark to the proposed system. Simulation results and discussions are given in Section 5. Conclusions then summarize the key points of this paper.

2. Universal Hydraulic Module for Regenerative Braking System

The diagram of a conventional braking system called the cross-link circuit type is shown in Fig. 1. This braking system is typically used in modern passenger cars. To modify this system to be a regenerative braking one used in a retrofitted EV, the schematic in Fig. 2 is proposed. In a retrofitted EV, an engine is replaced by a propelling motor that can perform as a generator. An additional regenerative braking control unit is required in this scheme to manage proper braking forces among the conventional and regenerative braking systems. A pressure sensor is installed to acquire the hydraulic pressure in the master cylinder, and the other two are used to obtain the pressures in both front brake calipers. The signals from the pressure sensors are then given to the regenerative braking control unit, and so are those of the motor's angular speed and battery's state of charge (SOC). In addition, the signals transmitted from the front wheel-speed sensors are rerouted to the regenerative braking control unit instead of the ABS control unit.

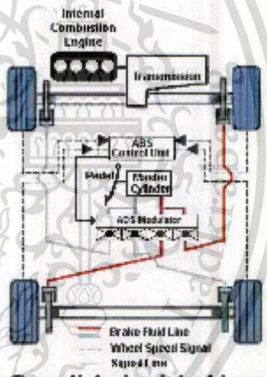

Fig. 1 Cross-link circuit braking system

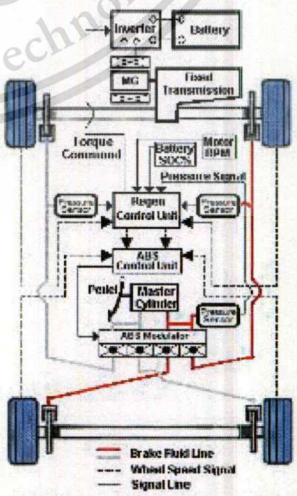

Fig. 2 Universal hydraulic module for regenerative braking system

This material is reserved for educational use only, not allowed for commercial use.
Forbidden to modify the content, and cite the document when use.

Paper ID
CST 1018

The 3rd TSME International Conference on Mechanical Engineering
October 2012, Chiang Rai

3. Proposed Regenerative Braking Strategy

In a standard braking system of a modern passenger car, there commonly are an ABS and its control unit that regulates braking forces. The ABS inherits a unique feature that can automatically release the brake pressure while the wheels are being locked up during braking. Hence, the brake force control scheme proposed in this work utilizes this feature of the ABS. To recover some energy during braking, an additional regenerative brake control unit sends an emulated "Wheel Lock-up" signal to the ABS control unit to lower the pressure of the frictional brake system, resulting in the reduced brake force. The amount of this reduced brake force is then subsidized by that of the regenerative one. Fig. 3 summarizes this novel concept of the brake force control scheme.

The scheme starts working once the brake pedal is activated. The regenerative braking control unit is going to measure the pressure in the master cylinder to determine the brake demand requested by a driver. Besides, the pressures in the front brake calipers are obtained. The pressures in the master cylinder and brake calipers are respectively converted to the demanded torque (T_{Demand}) and the front wheel frictional brake torque ($T_{Friction\_FW}$) by using Eq. 1 and Eq. 2:

$$T_{Demand} = P_{master} \times A_{wcf} \times \mu \times 2 \times r \qquad (1)$$

$$T_{Friction\_FW} = P_{caliper\_FW} \times A_{wcf} \times \mu \times 2 \times r \qquad (2)$$

where P_{master} is the brake pressure in the master cylinder, $P_{caliper}$ is the pressure in the brake caliper, A_{wcf} is the cylinder area of front caliper, μ is the friction coefficient, and r is the effective radius of brake disk.

Concurrently with the process described above, the control unit reads the motor's angular speed and the battery's state of charge to calculate the available regenerative motor brake torque (T_{Reg_Avb}) by using the following equation:

$$T_{Reg\_Avb} = T(RPM) \times W(SOC) \qquad (3)$$

Where, T(RPM) is the current motor torque estimated from the motor characteristic curve and the motor's angular speed. The weight factor (W), which is the function of battery SOC, is illustrated in Fig. 4. The weight factor is assigned to be one from SOC = 0% to SOC = 80%, meaning the battery is fully capable of charging. In the SOC range of 80%-90%, the weight factor is linearly decreased from one to zero. From SOC = 90% onwards, the weight factor is set to be zero to protect the battery from overcharging.

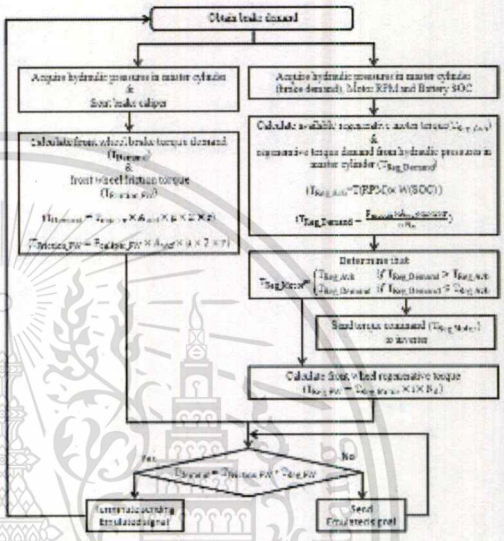

Fig. 3 Flowchart of proposed regenerative braking strategy

Fig. 4 Weight Factor vs. Battery SOC

Using Eq. 4, the pressure in the master cylinder is converted to the regenerative torque demand (T_{Reg_Demand}).

$$T_{Reg\_Demand} = \frac{P_{master} \times A_{wcf} \times \mu \times 2 \times r}{i \times N_d} \qquad (4)$$

Where, i is the gear ratio and N_d is the differential gear ratio. In the case that the regenerative torque demand is less than the available regenerative motor torque, it is necessary to regulate the motor torque not to exceed the demand. Thus, the condition in Eq. 5 is defined:

$$T_{Reg\_Motor} = \begin{cases} T_{Reg\_Avb} \; if \; T_{Reg\_Demand} > T_{Reg\_Avb} \\ T_{Reg\_Demand} \; if \; T_{Reg\_Demand} \leq T_{Reg\_Avb} \end{cases} \qquad (5)$$

This material is reserved for educational use only, not allowed for commercial use.
Forbidden to modify the content, and cite the document when use.

As a command, this torque is also sent to the inverter. Based on this torque, the gear ratio (i), and the differential gear ratio (N_d), the front wheel regenerative torque is calculated by using Eq. 6.

$$T_{Reg\_FW} = T_{Reg\_Motor} \times i \times N_d \qquad (6)$$

After obtaining all of the necessary parameters, the regenerative brake control unit checks if the demanded torque given by the driver is equal to the summation of the front wheel frictional brake torque and the front wheel regenerative torque. In the case that the condition is false, the control unit feeds an emulated "Wheel Lock-up" signal to the ABS control unit to decrease the braking force of the frictional braking system such that the reduced braking force is as close as to that provided by the regenerative system.

4. Parallel Regenerative Braking Scheme

Parallel regenerative braking scheme is one of the conventional systems, which requires no modification on the conventional braking system, meaning that it has no intelligent friction brake force control policy. Based on this regenerative scheme, the regenerative brake force generated by the motor is provided in parallel with friction brake force at front wheel. The procedure of the parallel regenerative scheme is to control the amount of the regenerative brake force corresponding to brake pedal traveling until the brake force limitation is reached. In the mean time, the friction brake force is applied according to braking demand similarly to those of the conventional brake. As a result, the total brake force at front wheel is over-demanded. Consequently, the low energy efficiency is an inherent drawback because of the regenerative brake force limitation. One of its disadvantages is the higher longitudinal deceleration during braking situation due to the longitudinal load transfer which leads to a negative passenger ride comfort.

5. Simulation Results and Discussions

In order to compare the performance of proposed scheme with that of conventional braking system and parallel scheme, all three schemes are modeled and investigated using simulation software, MATLAB Simulink. The simulation model is composed of the dynamic model of vehicle as well as the braking system equipped with the ABS system. The parameters used in the simulation are shown in Table 1.

Table 1 Simulation parameters

Motor	
Peak torque	240 Nm
Peak Power	75 kW
Transmission system	
Fixed gear ratio (i)	1.303
Rear axle gear ratio (N_d)	4.294
Vehicle	
Vehicle mass	1520 kg
Tire radius	0.32 m
Brake pad friction coefficient	0.4
Front piston diameter	57 mm
Rear piston diameter	29.1 mm
Front disc effective radius	108.5 mm
Rear disc effective radius	103.3 mm

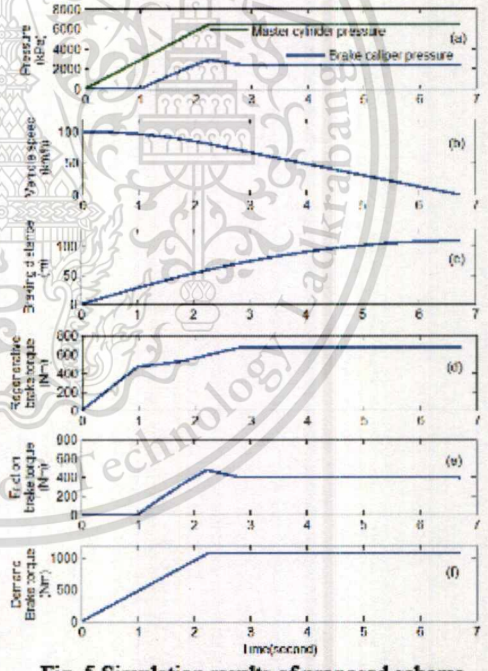

Fig. 5 Simulation results of proposed scheme

The simulation results during the braking situation of the proposed scheme are illustrated in Fig. 5. Fig. 5a presents the brake pressure in the outlet of the master cylinder and brake caliper. Master cylinder pressure is represented as brake requirement of driver and brake caliper pressure stands for amount of front friction brake force during cooperating with regenerative brake. Fig. 5b shows vehicle speed from 100 to zero km/h in

This material is reserved for educational use only, not allowed for commercial use.
Forbidden to modify the content, and cite the document when use.

Paper ID
CST 1018

The 3rd TSME International Conference on Mechanical Engineering
October 2012, Chiang Rai

around 6.7 second. Fig. 5c shows accumulative braking distance. Fig. 5d, Fig. 5e and Fig. 5f show the regenerative brake torque, front wheels friction brake torque and brake torque required by driver respectively. From the brake torque results as shown in Fig. 5d, Fig. 5d and Fig. 5f at period of 0 to 1 second, only regenerative torque is performed corresponding to brake torque demand. After that period, regenerative brake collaborates with friction brake and summation of both equal to braking torque requirement.

Fig. 6 illustrates simulation results of conventional braking system based on similar condition of brake force command. As a result, both of proposed regenerative system and conventional braking system provide same characteristic of vehicle speed and braking distance. Consequently, it can be expected that the similar passenger ride comfort is achieved as one of the conventional braking system.

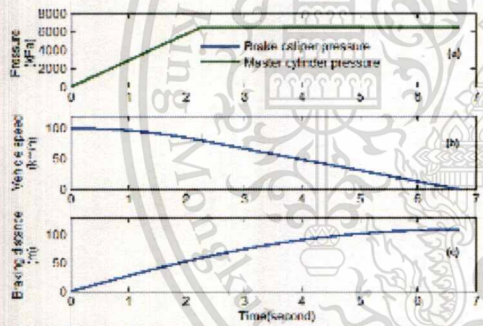

Fig. 6 Simulation results of conventional brake

Fig. 7 show simulation results of parallel scheme. In Fig. 7a, brake pressure of this scheme is shown. The pressure in the outlet of master cylinder and brake caliper is on the same line, since there is no friction brake force control. The resulted brake pressure of zero at the first half second is caused by the free gap range of brake pedal. This scheme develops regenerative brake force from the time when the brake pedal is depressed in the free gap range. In another word, only regenerative brake force is provided at the first haft second. Fig. 7b and 7c show vehicle speed and braking distance respectively. Fig. 7d show regenerative brake torque corresponding to its scheme in which regenerative braking torque develops according to the brake demand until it reaches brake torque limitation. Fig. 7e presents friction brake torque in compliance with the brake pressure as presented in Fig. 7a. As illustrated in Fig. 7f, the brake torque demand is shown in comparison to the overall brake torque acting on front wheel. At the period of the first haft second, front wheel brake torque is same as bake torque requirement but after passing the free gap, front wheel brake torque is over demand.

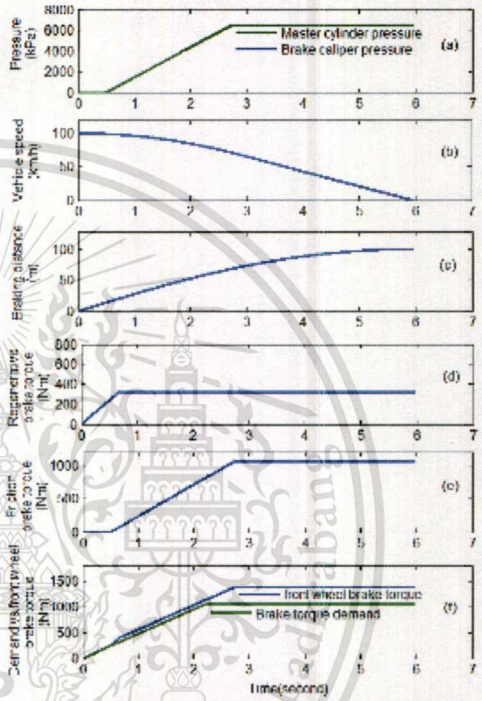

Fig. 7 Simulation results of parallel scheme

As a result of simulation illustrated in Fig. 8, the level of the accumulative regenerative efficiency is depending on the reduction of mechanical brake force. Consequently, the regenerative braking system without friction brake force control, parallel scheme, shows the lower accumulative regenerative efficiency than those of the proposed scheme. Due to the controlled brake force reduction at front wheels during the entire braking process, the regenerative braking system with emulated "Wheel locking up" ABS signal reaches the higher accumulative efficiency.

The longitudinal load transfer ratio during braking period is defined as a vertical load which is transferred from rear tire to front tire due to deceleration and inertial effects in the longitudinal direction. As shown in Fig. 9, the higher load transfer ratio, which theoretically effects negative passenger ride comfort, is reached by the regenerative parallel scheme. A

This material is reserved for educational use only, not allowed for commercial use.
Forbidden to modify the content, and cite the document when use.

lower level of load transfer ratio and corresponding higher comfort, which is similar to one of conventional vehicle, is reached by the proposed regenerative braking strategy.

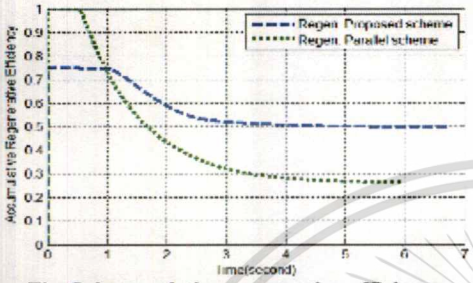

Fig. 8 Accumulative regenerative efficiency

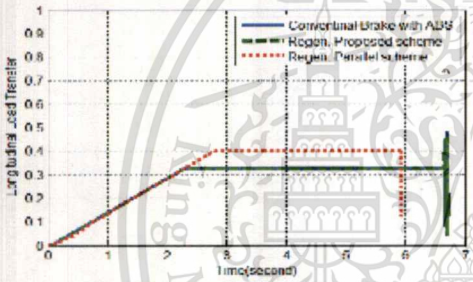

Fig. 9 Longitudinal load transfer

A comparison of the braking distance of conventional braking system, the regenerative braking system of proposed scheme and parallel scheme are shown in Fig. 10. The increase of the braking distance of the conventional brake is similar to one of the proposed regenerative scheme, since brake force distribution of both is same. For parallel scheme regenerative, its braking distance is smaller than one of the conventional brake and proposed scheme due the higher brake force at front wheel. Nevertheless, the shorter braking distance caused by the over demand of brake force can lead to the wheel locking up in slippery road surface.

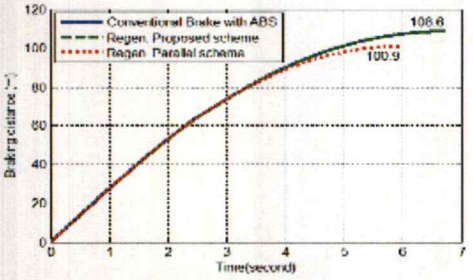

Fig. 10 Braking distance

6. Conclusions

In this study, the proposed brake force control scheme for a retrofitted electric vehicle is described. Its performance and validity are examined and compared with those of the conventional braking system and the regenerative parallel scheme using the simulation software, MATLAB Simulink. The emergency braking situations are simulated to validate the design criteria of braking performance focusing on the regenerative efficiency, the passenger comfort, the braking distance as well as the practicality. The proposed regenerative scheme is the most proper in this study. The reasons are firstly it offers higher efficiency. Secondly, this scheme provides same longitudinal load transfer as conventional brake, which is lower than the one of the parallel scheme, leading to higher passenger comfort. The simulated braking distance of proposed scheme is equal to that of the conventional braking system which passes the ECE 13H regulation. In terms of practicality, a minimum of modification is required. Thus, the application of the proposed regenerative braking scheme as a retrofit solution for an EV is reasonable

References

[1] Feng, W., Hu, Z., Xiao-jian, M., Lin, Y. and Bin, Z. (2007) Regenerative Braking algorithm for a Parallel Hybrid Electric Vehicle with Continuously Variable Transmission, Vehicular Electronics and Safety, 2007 ICVES. Beijing IEEE, 2007: 1-4.

[2] Gao, Y., Chen, L. and Ehsani, M. (1999) Investigation of the Effectiveness of Regenerative Braking for EV and HEV, August 1999, SAE Paper 1999-01-2910.

[3] Pabagiotidis, M., Delagrammatikas, G. and Assanis, D. (2000) Development and Use of a Regenerative Braking Model for Parallel Hybrid Electric Vehicle, August 2000, SAE Paper 2000-01-0995.

[4] Jang, S., Yeo, H., Kim, C. and Kim, H. (2001). A Study on Regenerative Braking for a Parallel Hybrid Electric Vehicle, KSME International Journal, Vol. 15(11), August 2001, pp 1490-1498, 2001

[5] Yeo, H., Kim, D., Hwang, S. and Kim, H. (2004). Regenerative Braking Algorithm for a HEV with CVT Ratio Control during Deceleration, 04CVT-41, paper presented by Dynamic System Design & Control Lab. Sungkyunkwan University, Korea.

This material is reserved for educational use only, not allowed for commercial use.
Forbidden to modify the content, and cite the document when use.

BIOGRAPHY

Name: Mr. Saharat Chanthanumataporn

Date of Birth: November 27, 1986

Place of Birth: Bangkok, Thailand

Education:

2006-2009	B.Eng. in Mechanical Engineering, Faculty of Engineer and Industrial Technology, Silpakorn University, Thailand
2010-2013	M.Eng. in Automotive Engineering (International program), International College, King Mongkut's Institute of Technology Ladkrabang (KMITL), Thailand

Honor and Scholarships:

2010-2012	TAIST-Tokyo Tech scholarship, the Master's Degree in Automotive Engineering funded by National Science and Technology Development Agency (NSTDA), Thailand
2011-2013	TGIST scholarship, Master's Research funded by National Science and Technology Development Agency (NSTDA), Thailand

Publications:

1. Chanthanumataporn S., Lerspalungsanti S., and Pimsarn M. 2011. *"Design of Regenerative Braking System for an Electric Vehicle (EV) Modified from Used Car."* The 2nd TSME International Conference on Mechanical Engineering, Krabi, Thailand.

2. Chanthanumataporn S., Lerspalungsanti S., Lapapong S., Pimsarn M., and Yamakita M. 2012. *"Brake Force Control Scheme for Integration of Conventional and Regenerative Braking Systems of Retrofitted Electric Vehicles."* The 3rd TSME International Conference on Mechanical Engineering, Chiang Rai, Thailand.

This material is reserved for educational use only, not allowed for commercial use.
Forbidden to modify the content, and cite the document when use.